1968

The Effect of Test Cell Glass Cylinder Diameter on Gaseous Insulation Dielectric Strength

Thomas J. Lanoue

THE EFFECT OF TEST CELL GLASS CYLINDER DIAMETER ON GASEOUS INSULATION DIELECTRIC STRENGTH

BY

THOMAS J. LANOUE

A thesis submitted
in partial fulfillment of the requirements for the
degree Master of Science, Department of
Electrical Engineering, South
Dakota State University

1968

THE EFFECT OF TEST CELL GLASS CYLINDER DIAMETER ON GASEOUS INSULATION DIELECTRIC STRENGTH

This thesis is approved as a creditable and independent investigation by a candidate for the degree, Master of Science, and is acceptable as meeting the thesis requirements for this degree, but without implying that the conclusions reached by the candidate are necessarily the conclusions of the major department.

Thesis Adviser — Date

Head, Electrical Engineering Department — Date

ACKNOWLEDGMENT

The author gratefully thanks Professor L. C. Whitman for his many helpful suggestions and generous assistance in directing and editing this thesis. Also the helpful suggestions of M. L. Manning are acknowledged. Credit is given to Westinghouse Electric Corporation, Muncie, Indiana, in particular to Saul Bennon and Harold R. Moore for their cooperation in furnishing materials for the field plots and in furnishing the typist for this thesis.

TABLE OF CONTENTS

Page

LIST OF FIGURES

LIST OF TABLES

INTRODUCTION

A. Brief History of Selection of a Tentative Standard Test Cell and Test Methods.

Dielectric properties of gases have been used in the design of electrical insulating systems for many years. In the early years air and nitrogen were found to satisfy most practical insulating applications. The dielectric strength of these gases were evaluated by various investigators using a number of different types of electrode systems and test cells. Therefore, when data from different investigators were compared, difficulty arose because of the different test conditions.[1] Due to this inconsistency of test methods the Electrical Tests Subcommittee N of ASTM Committee D-27 on Electrical Insulating Liquids and Gases undertook the development of a standard test cell for the evaluation of dielectric strength of gases. The objective of the Gaseous Dielectric Section of the subcommittee was to develop a test cell and a proposed test method which could be adapted as a standard for testing the dielectric strength of gases. In 1961 the beginning of a series of round-robin tests on three existing test cells for the determination of dielectric strength of gases was conducted by Section VI of the Electrical Tests Subcommittee N of ASTM Committee D-27 on Electrical Insulating Liquids and Gases.[2] Eleven different laboratories participated in the round-robin test. One of these laboratories was at South Dakota State University, directed by M. L. Manning. These tests were the initial step in the development of an ASTM cell for testing the dielectric strength of gases.[1,2] The test cells were contributed by the Du Pont Co., General Chemical Corp., and Westinghouse Electric Corp. The cells did differ in detailed construction from the proposed

standard cell, but the main features were almost alike. The proposed cell was to be designed so that it could be used to evaluate the insulating characteristics of gases in terms of factors such as electric field conditions, temperature and pressure dependence, electrode material and radiation effects and so on. The cell was to be designed so that the theoretical and practical aspects of the gases could be evaluated for actual applications. The material aspect of the insulating gas was more important to the ASTM Group in the development of a test cell. The ASTM test cell was to be used to rank the existing gases according to their dielectric strength and to screen and evaluate new gases. A 3/4 inch sphere to plane electrode system was selected because of the type of electric field produced by them. These electrodes were selected in order to avoid an extremely non-uniform field condition. This way corona and subsequent deterioration of the gas and other materials may be minimized. The sphere to plane configuration was selected instead of a sphere to sphere, because it simplifies the alignment problem. The plane was to serve as an electrostatic shield to the sphere, so that the effect of the cell wall or surrounding hardware on the breakdown voltage is reduced. The bottom electrode was not replaced because the breakdown voltage was assumed to be relatively insensitive to the plane. Since the breakdown voltage is linearly proportional to the spacing between the electrodes, a 0.1 inch gap was selected because this gap distance is much smaller than the sphere diameter. The cells were made of as many standard components as possible so that they could be easily replaced if needed.[2]

B. Test Methods and Results on the Tentative Standard Test Cell.

The three test cells were compared by running tests on nitrogen

and sulfur hexafluoride, which were the most commonly used gases and the easiest to obtain at the time the tests were run. Each laboratory obtained five rapidly applied 60 cycle (500 volts/sec.) breakdowns at a 0.1 inch gap spacing for both gases. Comparison of results from each cell showed that variability of breakdown was greater for SF_6 than for N_2. Variability of results were encountered in all laboratories although in some of the tests the variation was implausibly high compared to the bulk of the data. Test results differed between laboratories.[2] These differences may be due to different operators, equipment, and geography. Also these differences may be due to varying sources of gases and the presence or absence of irradiation sources. Unknown causes may exist which may not be present when other measurements in the set were made. All laboratories observed the same average breakdown voltages for nitrogen in each cell.[2]

C. Discussion of Results of Round-Robin Tests of 1961.

After testing both gases in all three test cells the data obtained was examined and discussed by various research engineers. Mr. E. R. Thomas, the manager of the Meter and Test Department of the Consolidated Edison Co., felt that a high degree of repeatability is required when making dielectric strength measurements to determine the dielectric strength of air compared to determining the same for liquids. Mr. J. S. Kresge, a senior development engineer at the General Electric Co., suggested that any attempt at expanding the function of the ASTM cell to yield more than the uniform field dielectric strength of gases would lead to complications far outweighing the value of the results obtained. Mr. Kresge also stated that it would be useless to attempt to obtain

non-uniform field data with a small cell at relatively low voltage because previous data obtained for various gases show that such data cannot be extrapolated to spacings of practical importance. Dr. G. M. L. Sommerman from the research laboratory of the Westinghouse Electric Corp., commented on the difference in results of the cells. The Du-Pont cell had a 1 percent lower breakdown than the other two cells. Dr. Sommerman suggested that the difference could probably be explained on the basis that the sphere diameter and ground plane are smaller than those of the other two cells. Dr. Sommerman believed that the differences were not due to the fact that the cells degraded with use because there was no significant indication. He could not see any correlation with irradiation. He was also surprised to see that the results for nitrogen before and after sulfur hexafluoride was tested came out exceedingly well when using the same test cell. Since in previous work done by the Westinghouse Corp., effects on nitrogen test had been encountered after using the cell for sulfur hexafluoride. Mr. G. L. Shambert, Jr., the superintendent of quality control at the Allis Chalmer Mfg. Co., admitted that the mere fact that statistical methods were applied to the results does not guarantee that the conclusions reached are physically sound. He also stated that the results indicate a high degree of probability that there was degration of the test cells with time, which is in disagreement with Dr. Sommerman. Mr. Shambert also concluded that it would be impossible in the round-robin test to separate out an effect due to radiation. Dr. T. W. Liao, the senior research engineer at the General Electric Co., summarized the discussion of the round-robin test. He mentioned that there would be no reason to

limit gaseous research to the presently proposed application of the ASTM cell. He stated that individual users must make their own tests with electrode shapes closely approximating the intended applications.

From the above discussion by various research engineers on the round-robin tests results the Seavy test cell (Contributed by the General Chemical Corp.) was selected as the proposed ASTM cell. One of the main reasons for selecting this cell was due to the deviation of test results produced by the Du Pont cell as compared to those produced by the other two cells.[1,2,3]

D. Reasons for Selecting Thesis Topic

This thesis topic was selected by the author and Professor L. C. Whitman while investigating the characteristics of C_4F_8, an electronegative gas, relative to the characteristics of air. Since the dielectric strength of air for gap spacings ranging from 0 to 2 inches for a 1 inch sphere to plane electrode system are not well documented in the literature, tests were run to obtain the dielectric strength characteristics of air at these gap spacings in a 2 inch diameter Seavy test cell. After rechecking the dielectric strength characteristics of air with the same electrode configuration in a 4 inch diameter test cell, designed by L. C. Whitman, the dielectric strength of air at gap spacings above one inch were found to differ by a significant amount for rapidly applied 60 cycle tests. This was one of the reasons the author decided to investigate the effect of test cell glass cylinder size on gaseous insulation dielectric strength. Also the proposed standards mentioned during the round-robin test for selecting a standard ASTM test cell did not mention the range of gap spacings that could be used with the proposed cell. Since the results of the

round-robin test were for a gap spacing of 0.1 inch and for one size test cell, the effect of the glass cylinder, the clamps of the cell, and the volume of gas in the cell would not be noticed on the breakdown of the gases.

E. Areas of Investigation

1. To determine the effect of test cell glass cylinder diameter on gaseous insulation dielectric strength for uniform and non-uniform fields through experimental results and field plots.

2. To obtain an upper limit for gap spacing in different size test cells for uniform and non-uniform fields.

3. To determine the effect of frequent change of gas in cell during test.

4. To determine extraneous effects, such as cell clamps.

5. To suggest the size in which a test cell should be to obtain good results in gaseous insulation dielectric strength tests.

These areas will be investigated by the author through the highest attainable accuracy that can be achieved with the precision of the test equipment available.

BASIC THEORY

A. Fundamental Theory of Gaseous Insulation Breakdown

The general theory of electrical breakdown and the resulting conduction of electricity in gases was introduced by J. S. Townsend and his co-workers, between 1900 and 1920.[4] In the following years L. B. Loeb and other investigators have improved and extended Townsend's theories to apply to various practical applications. Today, Townsend is still recognized for laying the ground work for the understanding of gaseous insulation breakdown. The following sections describe some of the basic fundamentals of the conduction of electricity in gases. For a more comprehensive study, the reader is referred to the bibliographies of the references cited in these sections.

1. Pre-spark Volt-Ampere Characteristics

The basic volt-ampere characteristic for all gaseous devices with various electrode systems is shown in the following Figure:

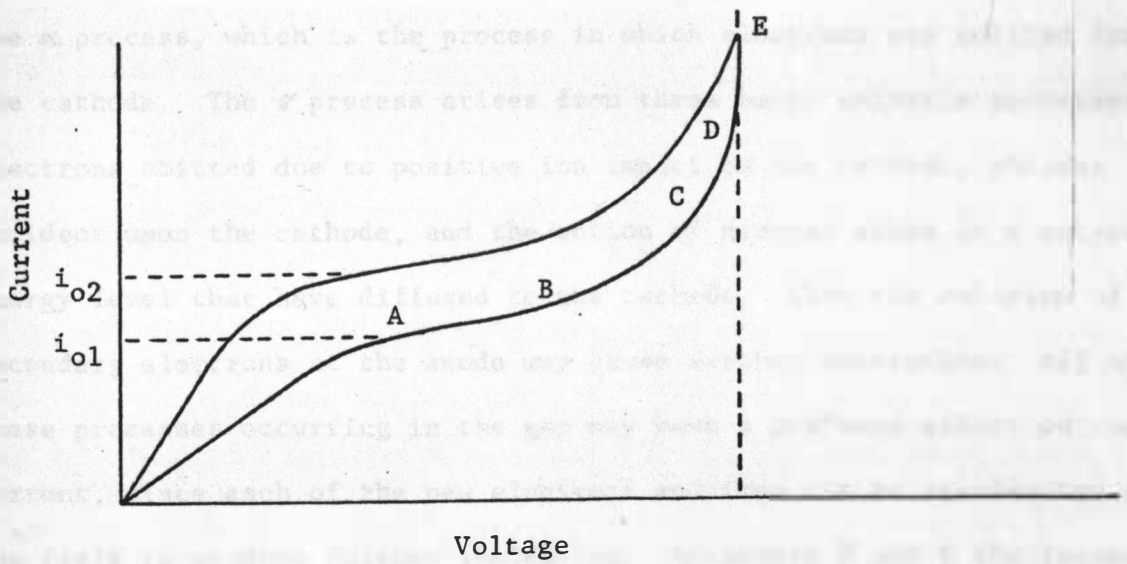

Fig. 1. Pre-spark volt-ampere characteristics.[5]

For very low voltages the only ions present in any gas are those originating from natural sources of ionization, such as photons of light and cosmic radiation, as well as β and γ rays arising from the natural radio-activity in the earth's surface.[4,5] The portion of the volt-ampere characteristic, between 0 and A, is spacecharge limited by the number of ions present in any gas due to the natural sources of ionization. At point A all of the free ions in the gas are being utilized. At point B the applied electric field is large enough to cause inelastic collisions of some of the ions and electrons with molecules. When an electron of sufficient energy collides with a molecule, it may eject from the molecule another electron and leave behind a positive ion. This process is sometimes called Townsend's α process, which continues for all higher applied voltages to the electrodes. At point C other ionization processes begin to create new ions in the gas. One of the processes is the formation of ion pairs by positive ions making inelastic collisions in the gas. This process is termed the β-process. Another process of initiating ion pairs is termed the α process, which is the process in which electrons are emitted from the cathode. The γ process arises from three basic emission processes: electrons emitted due to positive ion impact on the cathode, photons incident upon the cathode, and the action of neutral atoms in a metastable energy level that have diffused to the cathode. Also the emission of secondary electrons at the anode may cause further ionization. All of these processes occurring in the gap may have a profound effect on the current, since each of the new electrons and ions can be accelerated in the field to produce further ionization. At points D and E the increase in electric field causes many more inelastic collisions between electrons

and neutral gas molecules resulting in a higher electric current. Also at these points some of the excited molecules return to their ground state releasing a photon which may in turn, release a photoelectron from the cathode. This process is called the Θ-process. The photon released may also collide with a gas atom causing it to be excited to the ionization level. This process is called the ξ-process. At point E electron-pairs are being formed very rapidly causing the current to increase rapidly. The results of this rapid rise in electron-ion pairs is an avalanche, which leads to a spark between the electrodes.[4,5]

2. Pre-Spark Phenomena

At point B of Figure 1 the ion pairs produced by natural ionization sources acquire an increase in energy, due to the high electric field, causing inelastic ionizing collisions. The result is charge carrier amplification.

To determine the degree of amplification in the gas, assume that electrons per second per unit area in the immediate vicinity of the cathode are being accelerated toward the anode. Let x be the displacement toward the anode. Then

$$d\sigma = \sigma \alpha \, dx \qquad (1)$$

where $d\sigma$ is the number of ion pairs formed per second by electrons making ionizing collisions with gas molecules in a volume of unit cross-section with depth dx and α is a coefficient (Townsend's first coefficient) of proportionality with dimensions of electrons/meter/primary electron. If a steady-state condition with a constant source, σ_o, of electrons near the cathode is assumed, the total number of electrons per square meter at any point between the cathode and the anode is obtained by solving Equation (1).

$$\sigma(x) = \sigma_o \varepsilon^{\alpha x} \tag{2}$$

For the steady-state condition Equation (2) suggests an avalanche of electrons whose density starts near the cathode and increases exponentially to the anode. If a strong ionizing source is used to irradiate the gas such as x-rays, then Equation (1) is modified to

$$d\sigma = (\alpha\sigma + N_o)\,dx \tag{3}$$

where N_o is the ion pairs per unit volume per second being generated throughout the volume of gas between the electrodes. The steady-state electron concentration with irradiation at any point is then

$$\sigma(x) = (N_o/\alpha)(\varepsilon^{\alpha x} - 1) \tag{4}$$

The corresponding current density is

$$J(x) = (eN_o/\alpha)(\varepsilon^{\alpha x} - 1) \tag{5}$$

The Townsend coefficient α varies directly with pressure because the electron molecule collision frequency is directly proportional to pressure. The coefficient is also a function of the average energy acquired by an electron, where the average energy is directly proportional to the electric field strength, E, and the mean free path, λ. However the mean free path is inversely proportional to the pressure; therefore the Townsend coefficient is written as

$$\alpha = Pf(E/P) \tag{6}$$

When the electric field or applied voltage to the electrodes is increased to points C and D of Figure 1, the γ-processes must be considered. Now the density of electrons available per second in the immediate vicinity of the cathode is σ_o', not σ_o which was due to the α process only. The difference between σ_o' and σ_o is the rate at which electrons are supplied by the γ-processes. This difference is proportional to the total number of positive ions formed in a volume of unit

cross-sectional area. Since the density of positive ions at any point between the electrodes is equal to the density of the electrons, then Equation (2) can be modified to

$$\sigma^{+} = \sigma = \sigma_{o}' \varepsilon^{\alpha x} \tag{7}$$

Integrating Equation (7) over the gap length between the electrodes, the total number of positive ions produced in a volume of unit sectional area is

$$\int_{o}^{d} \alpha \sigma_{o}' \varepsilon^{\alpha x} dx = \sigma_{o}' (\varepsilon^{\alpha d} - 1) \tag{8}$$

The number of electrons supplied by the γ-process is proportional to the total number of positive ions found in a certain volume near the cathode per second and also to the probability, γ, that a fraction of these positive ions will contribute to electron emission at the cathode. It is also proportional to the probability χ that a fraction of those electrons emitted at the cathode will not diffuse back to the cathode. After considering these factors, the effective number of electrons emitted per unit area at the cathode is

$$\gamma \chi \sigma_{o}' (\varepsilon^{\alpha d} - 1) = \sigma_{o}' - \sigma_{o} \tag{9}$$

Therefore the surface density of electrons available at the cathode is

$$\sigma_{o}' = \sigma_{o} / [1 - \gamma \chi (\varepsilon^{\alpha d} - 1)] \tag{10}$$

and the current density at any point is

$$J(x) = e \sigma_{o}' \varepsilon^{\alpha x}$$

$$= (e \sigma_{o} \varepsilon^{\alpha x}) / [1 - \gamma \chi (\varepsilon^{\alpha d} - 1)] \tag{11}$$

The current density at the anode, J_b, is obtained by setting x = d in Equation (11). The loss of electrons due to back diffusion is usually small; therefore x is often assumed unity. The probability function, γ, is obtained from data taken on the specific cathode material and gas composition.[4,5]

3. Spark Breakdown

A spark occurs when the current density in the most sensitive volume of the gas rises very sharply. This sharp rise occurs approximately when the denominator of Equation (11) approaches zero. Then,

$$\gamma\chi(\varepsilon^{\alpha_b d} - 1) = 1 \tag{12}$$

where α_b is the particular value of α which satisfies the condition for a spark. If x = 1 and since $\varepsilon^{\alpha_b d} \gg 1$, then the condition for the spark breakdown of a gas is

$$1/\gamma = \varepsilon^{\alpha_b d} \tag{13}$$

where

$$\alpha_b = Pf(V_b/Pd) \tag{14}$$

P is pressure of the gas, d is the gap spacing between the electrodes, and V_b is the spark voltage.[4]

The conditions for breakdown therefore vary directly with V_b and inversely with pressure and interelectrode spacing for parallel plane electrodes. The spark potential, V_b, is a function of Pd as can be seen from Equations (13) and (14). This relationship between V_b and Pd is known as Paschen's Law which was discovered by Paschen in 1889.[6] The sparking potential varies directly with spacing or with pressure for values of Pd $>$ 5.7 (mmHg x mm). For lower values of Pd, the sparking potential increases rapidly. The product Pd represents the number of molecules to be encountered by an ion or electron in crossing the gap.[6]

4. The Events in an Electric Spark

The sequence of events of an electric spark is shown in Figure 2. In Figure 2(a) a few free electrons present in the gas start an avalanche. During the growth of the avalanche the more mobile electrons drift to the head of the avalanche leaving a positive ion streamer behind as shown in Figure 2(b). Due to diffusion the positive ion streamer is essentially spherical and conical.[4,6,7] The average radial diffusion distance, R, can be calculated from the Raether-Jaffi equation,

$$R = \sqrt{4Dt}$$

where t is the time of advance of the avalanche and D is the positive ion diffusion coefficient.[6]

In 1929 Loeb had suggested and shown that spark breakdowns may occur in less time than the electrons would require to drift across the gap.[6] This implies that some other source of ionization was forming electron-ion pairs in advance of the avalanche. The unknown ionizing sources were discovered by Loeb to be due to highly excited atoms in the molecules of the gas which revert to their ground state producing photons of energy. These photons liberated produce photoionization in the gas, causing the original avalanche to advance more rapidly across the gap. These photons are illustrated by the wiggly lines in Figure 2(c). In addition, electron-ion pairs formed well in advance of the avalanche may establish additional avalanches that aid in bridging the interelectrode gap in a relatively short time. Also photoelectrons are produced by photons at the cathode as shown in Figure 2(c).

As the positive ion streamer advances to the cathode, a plasma is left behind that reaches the anode. Since there is comparatively little

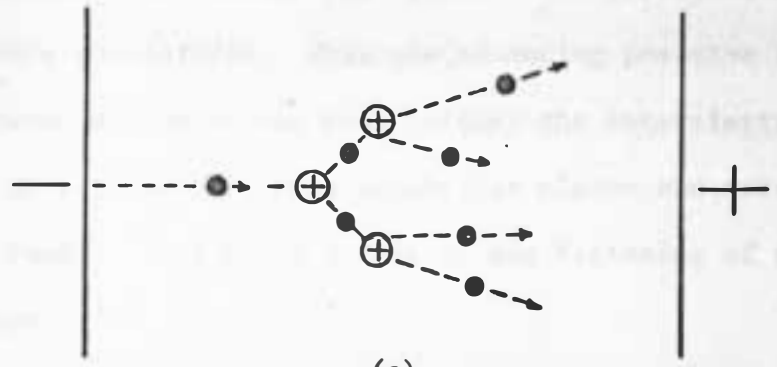

(a)

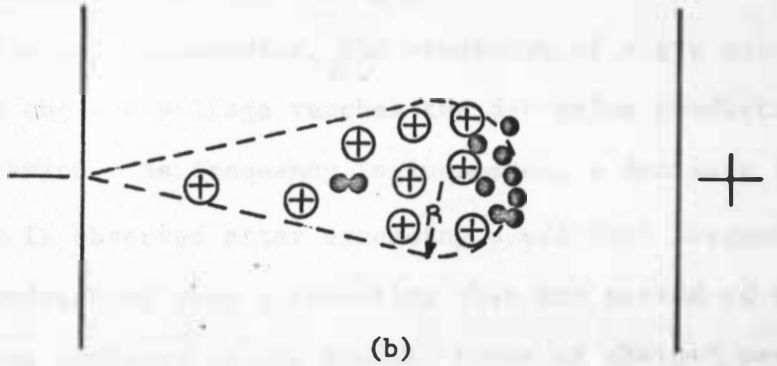

(b)

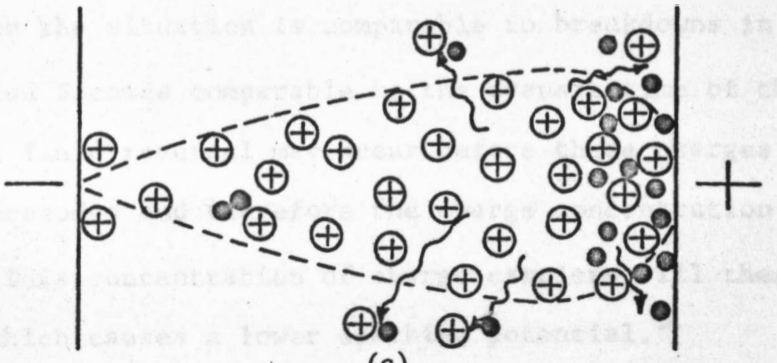

(c)

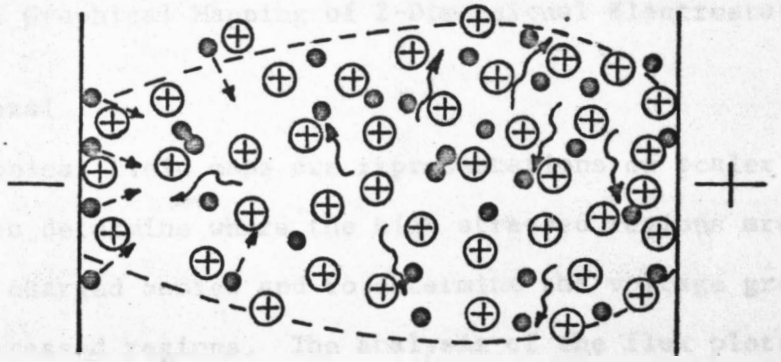

(d)

Fig. 2. The Mechanism of the Electric Spark. Positive ⊕ Negative ● [4]

voltage drop across the plasma, the result is an effective movement of the anode toward the cathode. When the advancing positive ion streamer reaches the cathode, the plasma then bridges the interelectrode space. Then a surge of cathode electrons enters the plasma and travels as a pulse to the anode. This pulse initiates the beginning of the spark between the gap.[4,7,8]

5. Breakdown Under Alternating Fields

At low a-c frequencies, the breakdown of a gas occurs when the peak value of the a-c voltage reaches the d-c value predicted by the Townsend criterion. As frequency is increased, a decrease in the sparking potential is observed after exceeding a critical frequency. This behavior is understood when considering that the period of the applied voltage is long compared to the transit times of charged particles in the gap. Then the situation is comparable to breakdowns in d-c voltages. When the period becomes comparable to the transit time of the charge carriers, the field reversal may occur before these charges are collected at the electrodes and therefore the charge concentration may increase in the gap. This concentration of charge carriers will then cause field distortion, which causes a lower sparking potential.[5]

B. Theory of Graphical Mapping of 2-Dimensional Electrostatic Fields

1. General

Graphical field maps are representations of scaler and vector fields used to determine where the high stressed regions are around electrically charged bodies and to determine the voltage gradients in these high stressed regions. The analysis of the flux plots gives the engineer a physical concept, which helps to determine the correct electrode configuration to make electrical stresses a minimum.[9]

Graphical field maps are often used to provide solutions to field problems whose analytical solutions might present almost insurmountable difficulties unless automatic computers are used. Although it is theoretically possible to find the field distribution around any configuration of conductors by means of Laplace's equation, such an approach may be impractical and field plotting must be used.

2. Two Dimensional Field Mapping

The conventional type of two dimensional field plot, known as an orthogonal plot, can be defined as a plot lying wholly within one plane and consisting of two individual but complementary systems of lines. The first systems (the flux function) intersects the second system everywhere at right angles to form a series of geometric elements known as curvilinear squares or rectangles. The first system of lines represents and coincides in direction with the lines of electric field intensity (the dielectric flux) while the second or complementary system of lines represents the lines of equal field intensity in the first system (the electrostatic equipotentials).[10]

The fundamental properties of two dimensional field mapping are the following:

1. Field and potential intersect at right angles.
2. The edge of a conductor is an equipotential line.
3. The flux lines meet a conducting edge normally.
4. In a uniform field the potential varies linearly with distance.
5. A flux tube is parallel to the field and the electric flux is constant over any cross section of a flux tube.
6. A tube of flux originates on a positive charge and ends on a negative charge.[11]

Two dimensional graphical field mapping will be introduced by a simple example. Consider two conductors one and two separated by air as shown in Figure 3. The conductors are assumed to be infinitely long to the left and to the right and normal to the page. The potential between the electrodes is 40 volts with conductor one positive and conductor two negative at 0 volts. The first step is to estimate the equipotential lines between the electrodes. The field left of point b and to the right of c is uniform, so the equipotential lines will be spaced equally apart in these regions. The equipotential lines are drawn in 10 volt steps in the uniform regions in Figure 3. The equipotential lines between b and c are tentatively drawn with reference to the equipotential lines in the uniform regions. The next step is to draw the field lines in the uniform regions. In these regions the field lines are drawn from conductor one to conductor two. These field lines will be spaced by the same spacing as the equipotential lines are spaced. In this manner the region is divided into squares. Each of these squares is the end surface of a rectangular volume with a depth, d. The squares bounded by the same field lines represent the side of a rectangular flux tube extending from the positive conductor to the negative conductor.

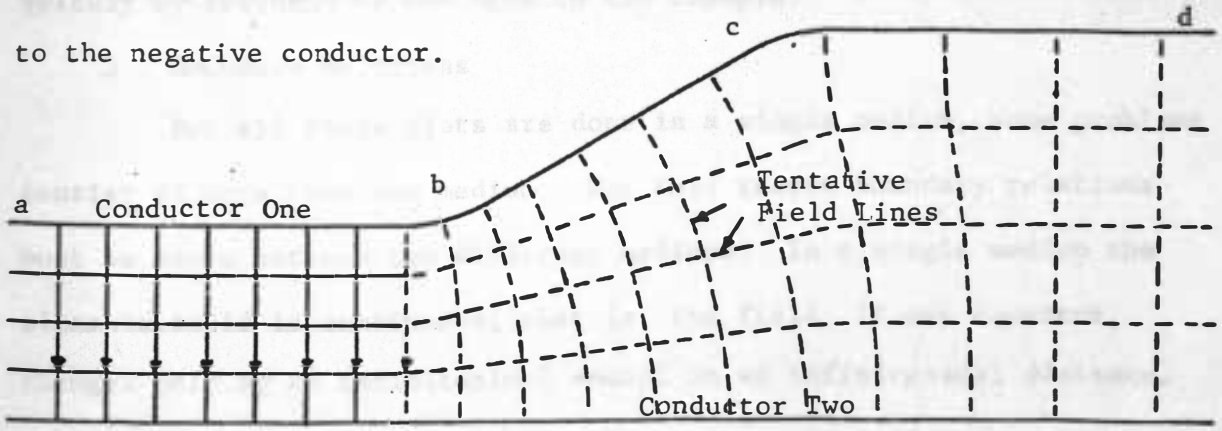

Fig. 3. Tentative Field Plot Between Two Conductors.

Next the field lines in region b to c are drawn as close as possible to be orthogonal to the tentative equipotential lines in this region. This first sketch of the field lines is only approximate; therefore, the field lines and the equipotential lines must be repeatedly drawn until the lines are orthogonal and the areas between the lines form curvilinear squares.[11,12,13]

A curvilinear square is an area that tends to yield true squares as it is subdivided into smaller and smaller areas by successive halving of the equipotential interval and the flux per tube.[11,13]

Another way and a much easier way of obtaining a field plot is by semi-graphical mapping. This mapping is done by obtaining the equipotential lines through a method of analogy. In the analogous method, the current, and potential patterns established on a conducting sheet are analogous to corresponding flux and potential functions of the actual fields being studied.[10] The conducting sheet can consist of electrical conducting paper with attached energized electrodes or an electrolytic trough. Then with the use of a high impedance DC voltmeter, the equipotential lines can be obtained. After obtaining the equipotential lines, the fields lines can be drawn very easily and quickly by freehand as was done in the example.

3. Boundary Relations

Not all field plots are done in a single medium, some problems consist of more than one medium. For this reason boundary relations must be known between two different mediums. In a single medium the electric field is continuous, that is, the field, if not constant, changes only by an infinitesimal amount in an infinitesimal distance.

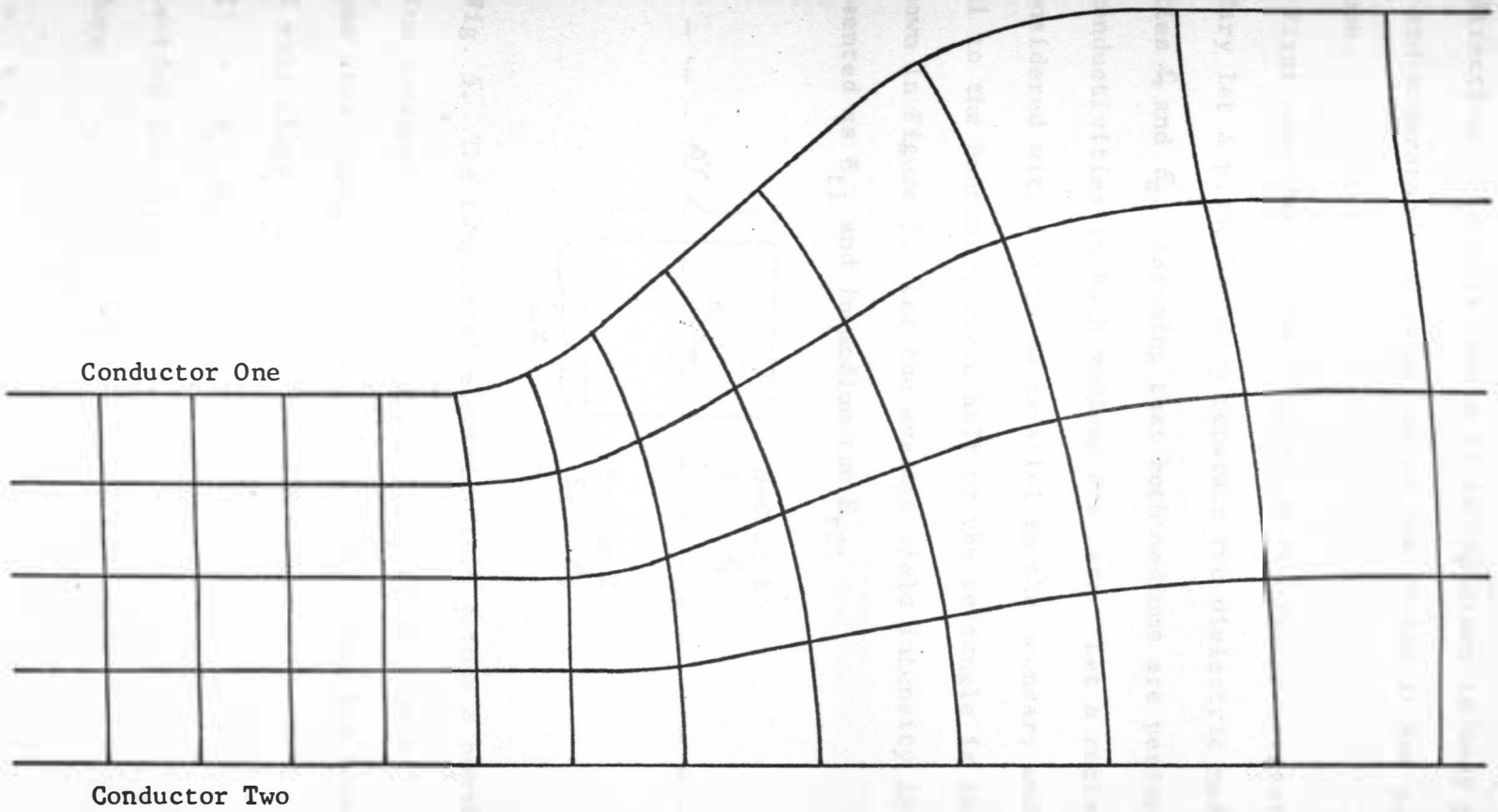

Fig. 4. Completed Field Plot of Figure 3.

However, at the boundary, the field changes abruptly both in magnitude and direction. For this reason it is important in many problems to know and understand the relations of the fields at the boundary of two mediums.

First considering the relation of the fields tangent to the boundary let a plane boundary separate two dielectric mediums of permittivities ε_1 and ε_2. Assuming that both mediums are perfect insulators, the conductivities in both mediums are zero. Let a rectangular path be considered with length ΔX parallel to the boundary and of length ΔY normal to the boundary, where half of the rectangle is in each medium as shown in Figure 5. Let the average field intensity in medium one be represented as E_{t1} and in medium two E_{t2}.

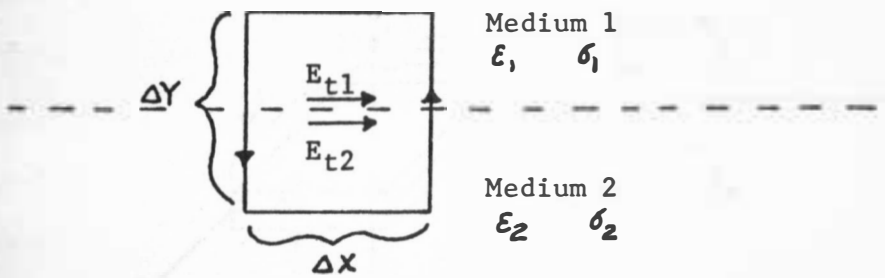

Fig. 5. The tangential electric field across a boundary.

The line integral of E around the path shown in Figure 5, which is the work per unit charge required to transport a positive test charge around this closed path, is

$$E_{t1}\Delta X - E_{t2}\Delta X = 0 \qquad (15)$$

upon letting ΔY approach zero.

Therefore

$$E_{t1} = E_{t2} \qquad (16)$$

which means that the tangential components of the electric field are the same on both sides of a boundary between two dielectrics.

If medium one would have been a conductor, then $\sigma_1 \neq 0$ and the field E_{t1} must be zero under static conditions; therefore, equation 16 would reduce to

$$E_{t2} = 0 \tag{17}$$

this means that the tangential electric field at a dielectric-conductor boundary is zero.

In order to find the relation between the fields normal to a boundary, let two dielectric mediums of permittivities ε_1 and ε_2 be separated by an XY plane as shown in Figure 6.

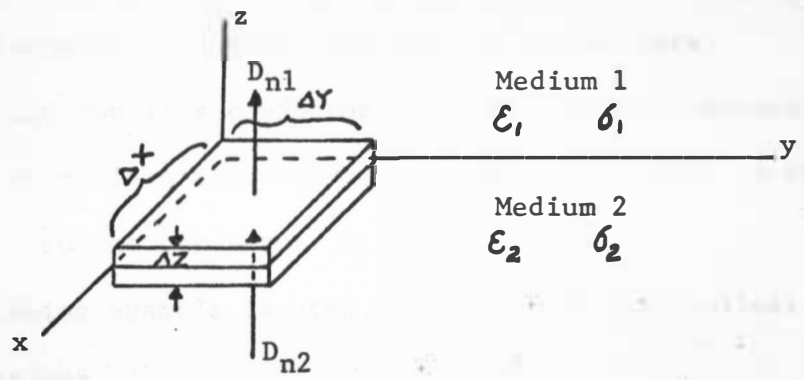

Fig. 6. The normal component of the flux density across a charge-free boundary.

Let the two dielectrics be perfect insulators, so σ_1 equals σ_2 which are both equal to zero. Assume the imaginary box is constructed as shown in Figure 6 with half of the box in each medium. Let D_{n1} and D_{n2} be the average flux densities normal to the box in the directions indicated in Figure 6. Gauss' law states that the surface integral of the normal component of the electric flux density D over any closed surface equals the charge enclosed;[11,12] therefore by letting ΔZ approach zero and applying Gauss' law to the top and bottom surfaces of the box then

the following relation is obtained.

$$D_{n1}\,\Delta X\,\Delta Y - D_{n2}\,\Delta X\,\Delta Y = \rho_s\,\Delta X\,\Delta Y$$

or

$$D_{n1} - D_{n2} = \rho_s \tag{18}$$

The average surface charge density on the boundary is ρ_s. This surface charge is not due to polarization. Equation (18) means that the normal component of the flux density changes at a charged boundary between two dielectrics by the amount of charge density on the surface of the boundary. Normally the charge density on the boundary between two dielectrics is zero. Then equation (18) reduces to

$$D_{n1} = D_{n2} \tag{19}$$

which means that the normal component of the flux density is continuous across the charge-free boundary between two dielectrics.

When medium two is a conductor, then the normal component of the flux density at a dielectric-conductor boundary is equal to the surface charge density on the conductor.[11,12,14]

The following example is used to illustrate the application of boundary relations.

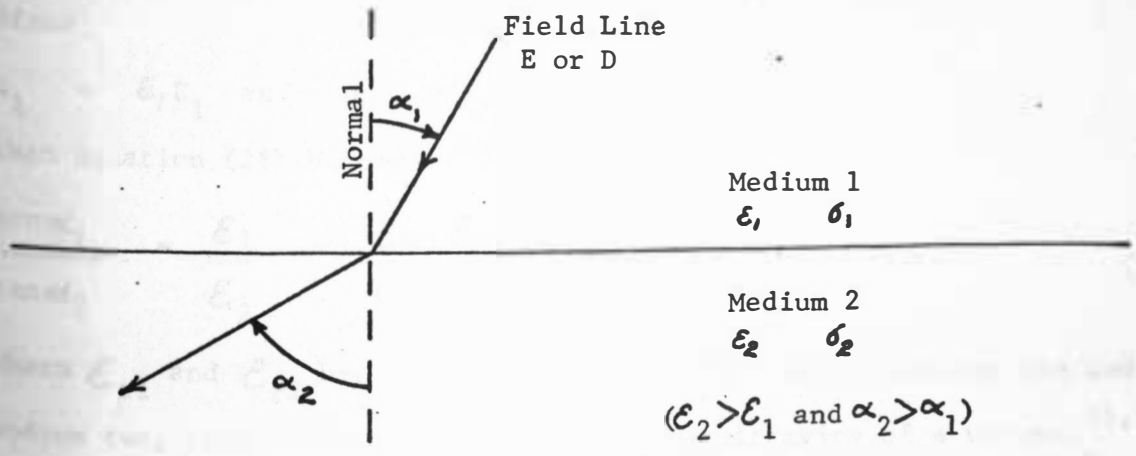

Fig. 7. Change in direction of field line across a boundary.

Let the boundary between two dielectric mediums be charge free and the permittivities be ε_1 and ε_2. The conductivities of the two mediums will be zero. Figure 7 illustrates the example. This example will be used to evaluate the relation between the angles shown in Figure 7.

From the boundary relations

$$D_{n1} = D_{n2} \tag{20}$$

$$E_{t1} = E_{t2} \tag{21}$$

therefore from Figure 7

$$D_{n1} = D_1 \cos \alpha_1 \tag{22}$$

$$D_{n2} = D_2 \cos \alpha_2 \tag{23}$$

and

$$E_{t1} = E_1 \sin \alpha_1 \tag{24}$$

$$E_{t2} = E_2 \sin \alpha_2 \tag{25}$$

Now dividing equation (20) by equation (21) and substituting equations (22), (23), (24), and (25) into the appropriate equations (20) and (21) the following relation is obtained.

$$\frac{D_1 \cos \alpha_1}{E_1 \sin \alpha_1} = \frac{D_2 \cos \alpha_2}{E_2 \sin \alpha_2} \tag{26}$$

Since

$$D_1 = \varepsilon_1 E_1 \quad \text{and} \quad D_2 = \varepsilon_2 E_2$$

then equation (26) becomes

$$\frac{\tan \alpha_1}{\tan \alpha_2} = \frac{\varepsilon_1}{\varepsilon_2} = \frac{\varepsilon_{r1} \varepsilon_o}{\varepsilon_{r2} \varepsilon_o} = \frac{\varepsilon_{r1}}{\varepsilon_{r2}} \tag{27}$$

where ε_{r1} and ε_{r2} are the relative permittivities of medium one and medium two, respectively, and ε_o is the permittivity of a vacuum.[11,12]

If medium two would have been a conductor, then $D_2 = E_2 = 0$

under static conditions. Then the boundary relations would have been

$$D_{n1} = \rho_s \quad \text{or} \quad E_{n1} = \frac{\rho_s}{\varepsilon_1} \tag{28}$$

$$E_{t1} = 0 \quad (\text{since } E_{t2} = 0) \tag{29}$$

With these relations

$$\alpha_1 = \tan^{-1} \frac{E_{t1}}{E_{n1}} = 0$$

This means that the electric field line at a dielectric conductor boundary is always perpendicular to the conductor surface.[11,12]

The boundary relations obtained for flux tubes in insulating media are analogous to the current tubes in conducting media. Also the conductivity of a conducting medium is analogous to the permittivity of an insulating media.[11,12,10] For the conducting media

$$J = \sigma E \text{ amp/meter}^2 \tag{30}$$

where σ is conductivity, E is the electric field intensity, and J is current density. Where for the insulating media

$$D = \varepsilon E \text{ coulombs/meter}^2 \tag{31}$$

where D is flux density, E is electric field intensity, and ε is permittivity. Therefore the same boundary relations found for a dielectric-dielectric medium can be used for the conductor to conductor medium and so forth by substituting J for D and σ for ε.[11,12]

TEST PROCEDURES AND EQUIPMENT

Gaseous Insulation Test Cells

1. General Description

The test cells used in the determination of the effect of the glass cylinder size on gaseous dielectric breakdown are shown in Figure 8. The two inch diameter test cell or the test cell on the right was constructed by M. J. Seavy and Sons. This cell was accepted as a tentative standard by the ASTM committee, Group 27[26] for the testing of gaseous insulation breakdown. The four inch diameter and six inch diameter test cells shown in Figure 8 were designed by Professor L. C. Whitman as suggested by the design of the Seavy test cell and the ASTM standards. These two cells were contructed by Wilbur V. Allen, a machinist in the Machine Shop at South Dakota State University.

2. Essential Features of the Test Cells

The cells consists of Corning Laboratory pyrex glass cylinders, with a dielectric constant of 5.1 at 1 megacycle[15] clamped by flanges to end plates which seal the cells and support the electrodes. The bottom electrode is grounded in each cell and is fixed to the bottom plate. The top electrode is held in place by the top plate and is adjustable by a suitable micrometer screw for setting the electrodes within a specified gap setting. The top and bottom plates have valved ports for evacuation and admission of the sample gas.

The electrode configurations used in the test cells were a 1" diameter brass sphere or alternately a 3/32" diameter tungsten rod with a sharp point to a 1-3/4" diameter brass grounded plane in each case. The

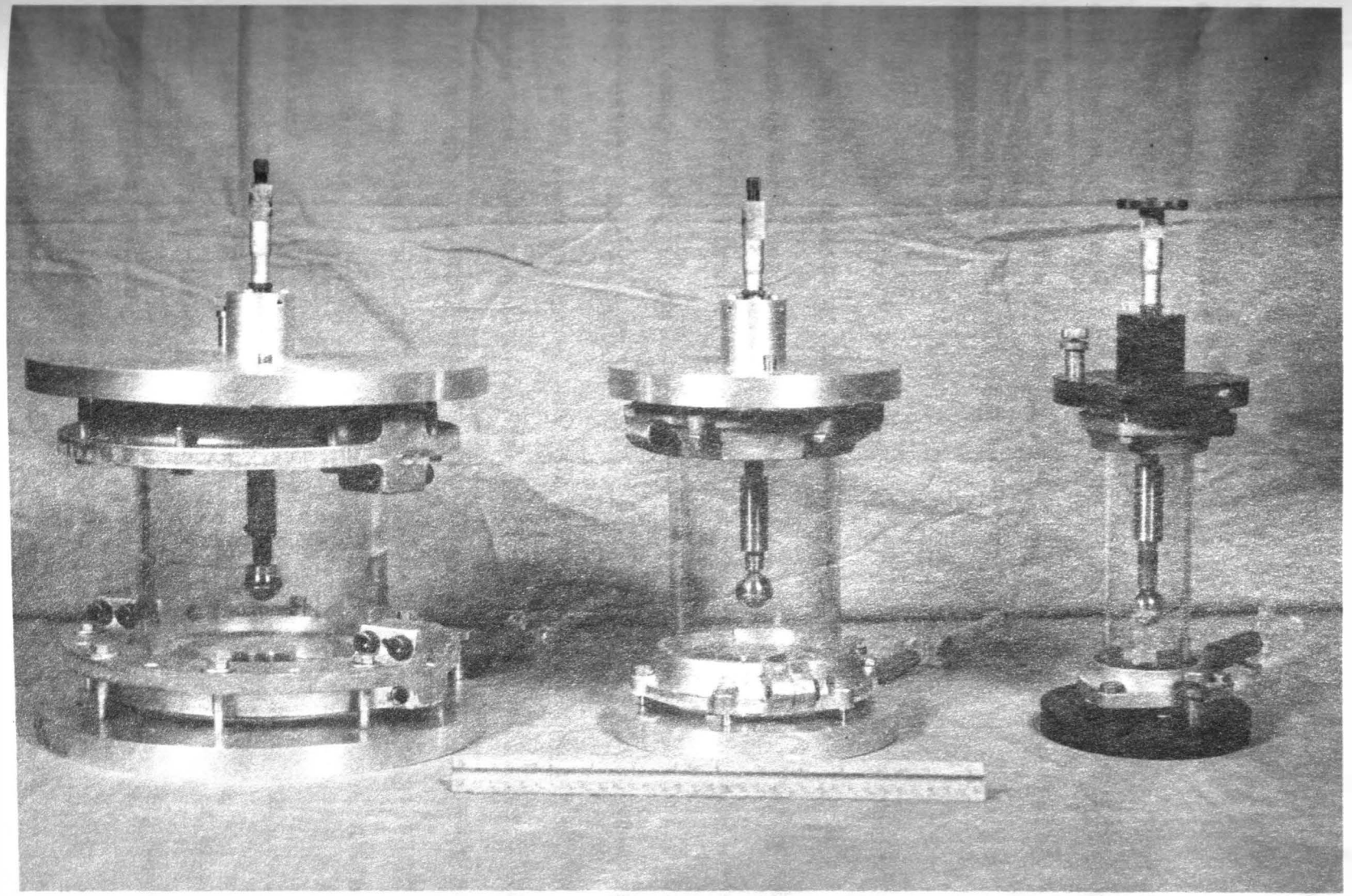

Fig. 8. The 6 inch diameter, 4 inch diameter and 2 inch diameter test cells from left to right.

composition of the brass used is unknown.

The name of each cell is specified by the inside diameter of the glass cylinder, such as the 2" diameter test cell has a 2" inside diameter glass cylinder.

The approximate internal volumes of each cell, not including the displacement of the electrodes, are 226.6 $in.^3$, 97.6 $in.^3$, and 20.8 $in.^3$ for the 6" dia., 4" dia., and 2" dia., test cells, respectively.

3. Operations

A. Method of Cleaning Test Cells

Before any test can be made with the test cells, the cells must be disassembled and thoroughly cleaned. The test cells are cleaned by first removing all detectable decomposition products and pits formed by the breakdown arc. This is done by sanding the electrodes with emery cloth (fineness 1 and 3/0) and then polishing them with a rouge wheel. The second step is to wash all the inside parts of the cells with laboratory glass cleaner and water. Then the parts are rinsed with distilled water and chemically pure acetone. The third step is to assemble the test cells and to evacuate them with a vacuum pump for at least 5-10 minutes. The vacuum pump is an oil seal type which would evacuate the cells to a pressure of approximately one millimeter of mercury.

B. Method of Filling Test Cells

The apparatus used in filling the test cells is shown in Figure 9. The cell and flasks F_1 and F_2 were evacuated with a vacuum pump. During evacuation stopcocks S_6 and S_5 were closed. Leveler tubes L_1 and L_2 contain silicone oil. These tubes are used to correct

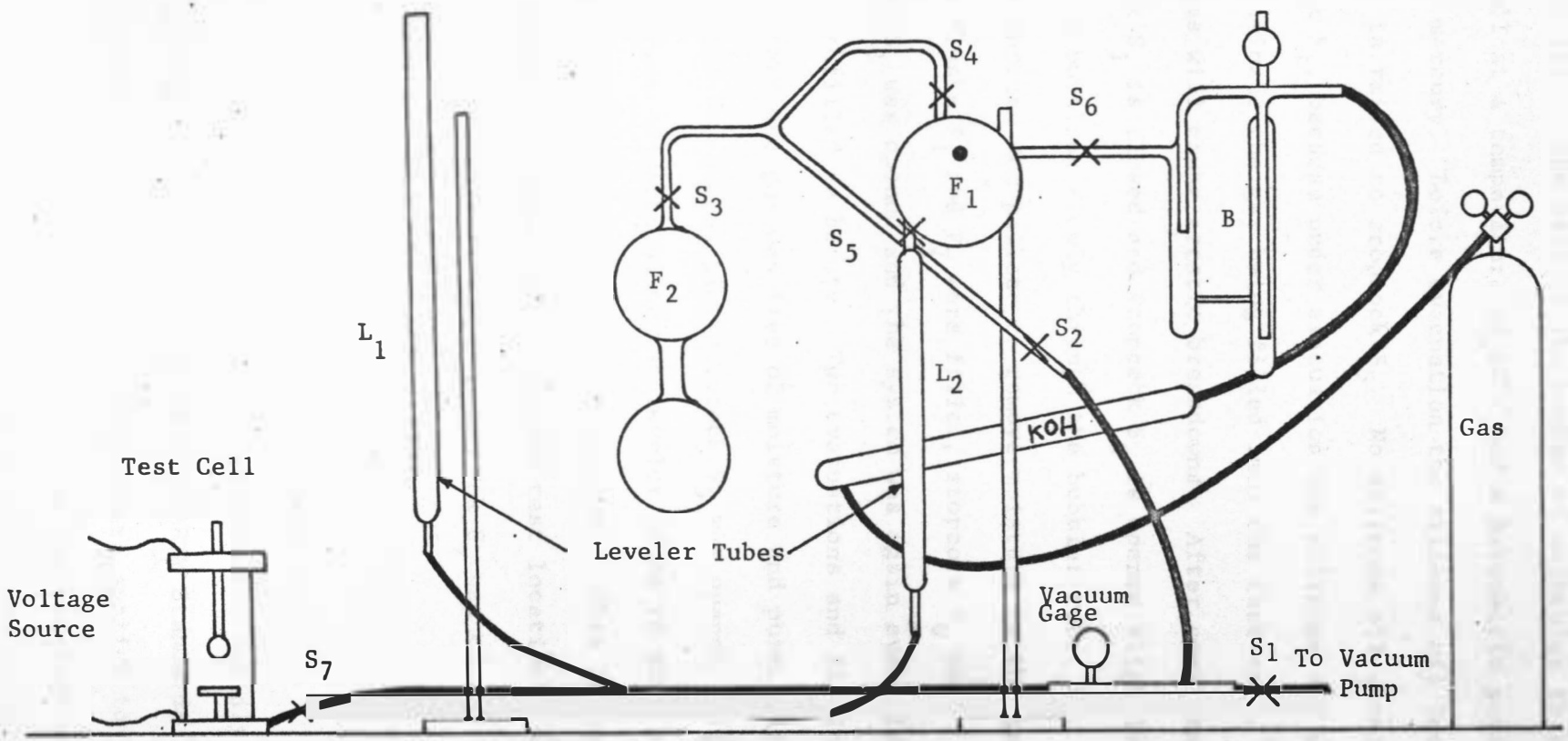

Fig. 9. Gas Filling Apparatus.

the number of molecules in the cell to the number of molecules there would be in the cell at a temperature of 80°F and a barometric pressure of 28.35 inches of mercury. Before evacuation the silicone oil level in leveler tube L_2 is raised to stopcock S_5. No silicone oil should be allowed in flask F_1, because under evacuation the silicone oil will evaporate and contaminate the gas being filled into the test cell. This oil vapor in the gas will cause erratic breakdowns. After complete evacuation stopcock S_1 is closed and stopcock S_6 is opened slightly until the gas starts bubbling slowly through the bubbler tube, B_1. The gas was passed through KOH pellets to remove moisture in the gas. After the cell and flasks F_1 and F_2 were filled, stopcock S_6 was closed and stopcock S_1 was opened and the system was again evacuated. Then the system was refilled as before. Two evacuations and fillings were used to insure that the gas was free of moisture and pure. After the cell was filled for the second time stopcock S_5 was opened and the pressure in the cell was adjusted using the leveler tubes to give a standard condition of 80°F and 28.35 inches of mercury. This temperature and pressure is the average condition at the test location. After relative gas density corrections were made, stopcock S_7 was closed and the test cell was ready for testing.

C. Voltage Application

1) Rapidly Applied 60 Cycle Voltage Test

All tests using the 60 cycle test set were rapidly applied 500 volts/sec. voltages in accordances with ASTM Standards D-149-64. Rapidly applied 500 volts/sec. voltages were applied to the 2" dia., 4" dia., and 6" dia. test cells for various gap settings rang-

ing from 100 mils to 1800 mils gap. Figure 10 shows the test set up for the 4" dia. test cell, but without the radium irradiation. At each gap setting 10 breakdown voltages with a rest of one minute between each breakdown were read and recorded. A correction of .4 KV was added to each of the 10 readings of each gap setting to correct for the lag (inertia) of the needle of the meter. The meter was a Westinghouse, rectifier type, AC voltmeter, which measured RMS voltages. Breakdown voltages were obtained in this manner for point to plane and 1" sphere to plane in nitrogen gas and air. When the above tests were made with nitrogen, the test cells were cleaned and refilled for every gap setting in order to keep the cell free from detectable decomposition products formed by the breakdown arc. The cells were filled with the gas filling apparatus. When the test cells were filled with air, a vacuum pump was used to circulate new air through the test cell for approximately one minute between each of the 10 breakdowns at each gap setting to eliminate decomposition products formed by the arc. The air was passed through KOH before entering the valve port at the top plate and evacuated out through the valve port at the bottom plate of the test cell by the vacuum pump. Open air was being circulated through the test cells; therefore, ambient temperatures and pressures must be recorded for each gap setting and the breakdown voltages for each gap setting must be corrected to standard breakdown conditions. Experimental correction factors were obtained for correcting the breakdown voltages and the methods used are shown in Appendix V and VI. Also during the above test with air, the cells were disassembled and cleaned for every other gap setting in order to keep the surface of the

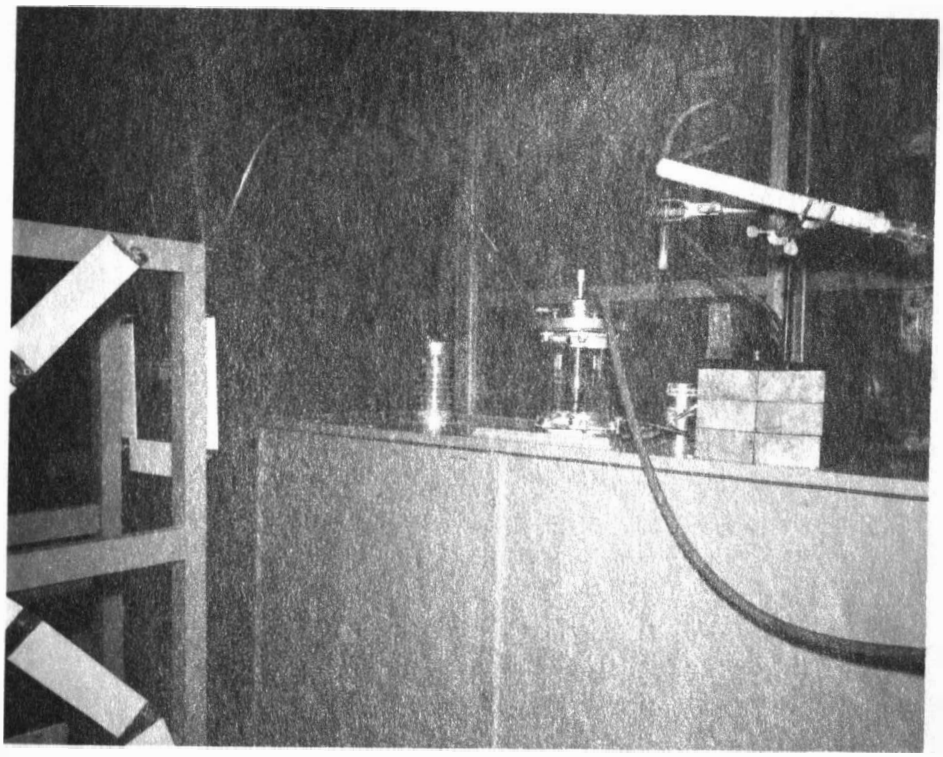

Fig. 10. Impulse test of air with 4 inch diameter test cell.

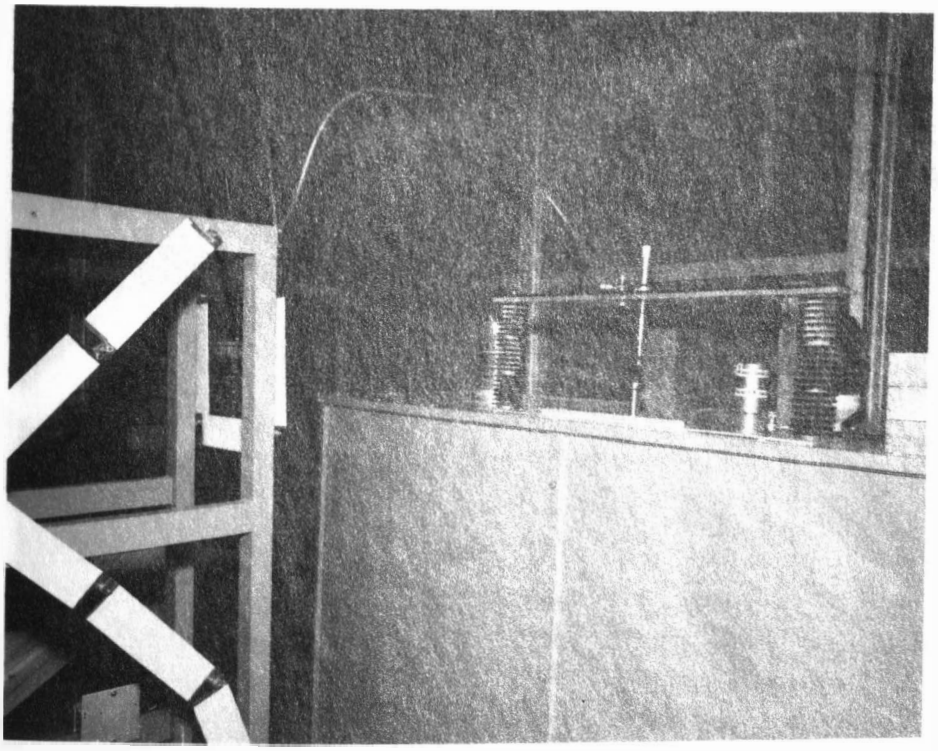

Fig. 11. Impulse test of air with open cell.

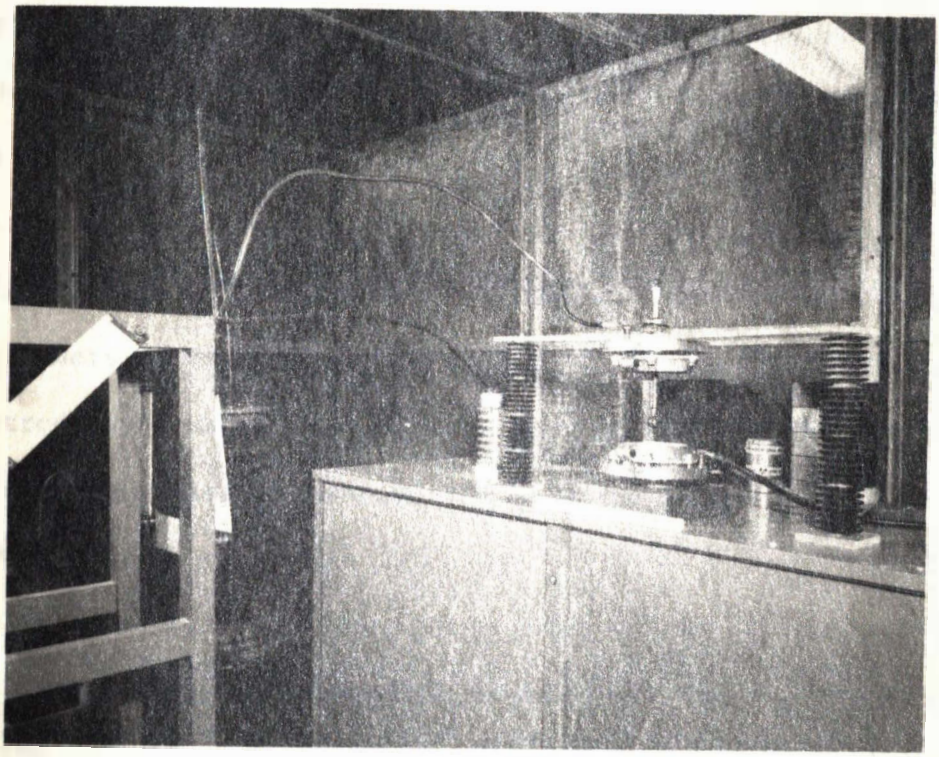

Fig. 12. Test apparatus used to determine the effect of the 4 inch diameter test cell clamps on the breakdown of air.

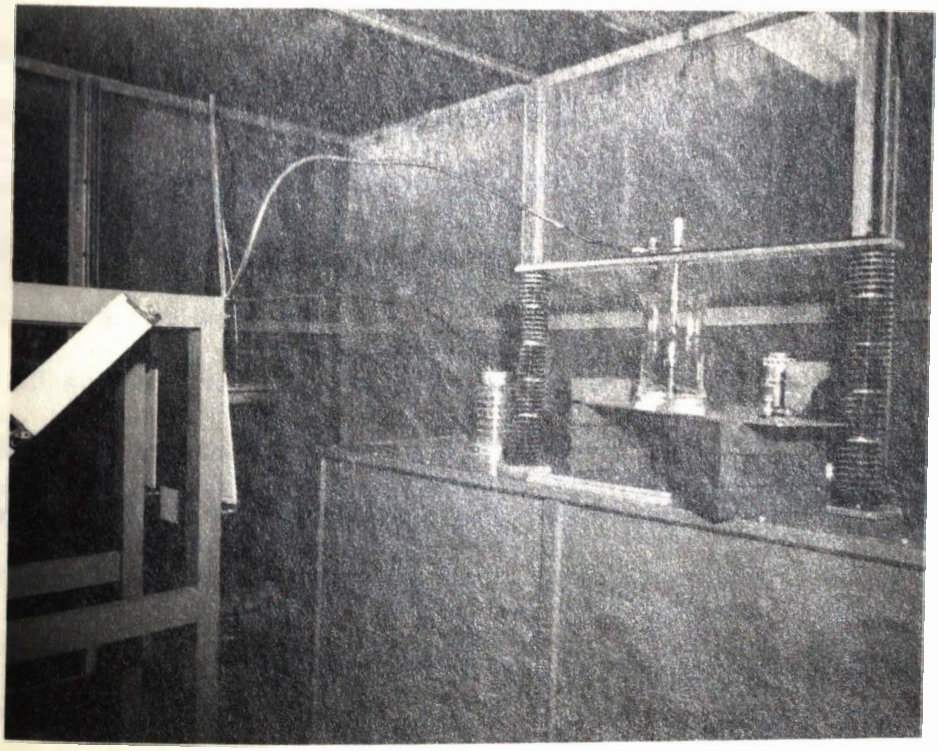

Fig. 13. Test apparatus used to determine the effect of the 4 inch diameter glass cylinder on the breakdown of air.

electrodes from contaminating films.

Rapidly applied, 500 volts/sec., 60 cycle voltages were applied to an open cell designed by the author as shown in Figure 11. Test data was recorded in the same manner as the above procedure for the 1" diameter sphere to plane and the point to plane electrodes in open air. Also data was recorded for the 2" dia., 4" dia., and 6" dia. glass cylinders centered about the open cell for open air and for the two electrode systems mentioned previously. Figure 13 shows the test set up for determining the effect of the 4" dia. glass cylinder on the breakdown of air in a uniform field, but without the radium irradiation. The open cell was also used to determine the effect of the clamps of each test cell on the breakdown of rapidly applied 60 cycle voltages in open air for the two electrode systems. The construction of the test apparatus for determining the effect of the clamps is shown in Figure 12, but without the radium irradiation. Data was recorded for these two electrode systems with the 2" dia., 4" dia., and 6" dia. clamps. In all the tests using the open cell an electric fan was used to remove the ionized air near the electrodes between each breakdown of the 10 breakdowns for each gap setting. The electric fan was turned off approximately 20 seconds before applying voltage. During any of the open cell tests, the ambient temperature, pressure, and humidity were recorded in order to correct the breakdown voltages to standard conditions. The method for correcting the breakdown voltages for various relative air densities to standard conditions is shown in Appendix V. Appendix VI shows that humidity has a negligible effect on breakdown of air for the two electrode systems.

2) Full Wave Impulse Voltage Test

Full wave (1½x40μsec.) positive and negative polarity impulse tests for air were made using the 1" sphere to plane and point to plane electrode systems. The 1½x40μsec. wave is obtained by a particular wave shaping circuit connected to the output of the impulse generator. The method used in obtaining this wave shaping circuit is shown in Appendix IV. The voltage at the output of the generator was indicated by the control panel meter and by a 507 Tektronix oscilloscope.

Full wave (1½x40μsec.) positive polarity impulses were applied to the 2" dia., 4" dia., and 6" dia. test cells for various gap settings ranging from 100 mils to 1800 mils gap. The test set up for the 4" dia. test cell is shown in Figure 10. At each gap setting an impulse voltage indicated by the panel meter setting was applied at a level that would cause 10% or less breakdowns out of 10 trials at the same panel meter setting. There was a 30 second interval between each trial. The panel meter setting was then raised one unit at a time with 10 trials at each panel meter setting until 90 to 100% of the 10 trials were breakdowns. After a two minute interval, this same 90 to 100% level was given 10 more trials at the same gap setting; then the panel meter setting was decreased by one unit and given 10 more trials. The panel meter setting was decreased until a 10% or less breakdown level was obtained. This same procedure was repeated for every gap setting for each test cell. Also a one minute interval was allowed between each voltage level, during this time the test cell was being circulated with air. This was done to eliminate any decomposition products due to arcing in the cell. The same vacuum pump that was used in the 60 cycle test was used to circulate the air through the cells. Also KOH was

used to eliminate moisture in the air entering the test cell. Also the electrode systems were cleaned for every other gap setting, in order to eliminate any erroneous breakdowns due to contaminating films forming on the electrodes and pits in the electrodes due to arcing. A sample of how the data was recorded for the above test is shown in Figure 14. The 50% breakdown level was used as the actual breakdown of air at each gap setting. The 50% breakdown voltages were obtained by plotting the percent breakdowns in each trial against the panel meter setting; the 50% panel meter setting was converted to voltage by the calibration curve in Appendix III. The 50% breakdown voltages for each gap setting were corrected from ambient to standard conditions. The determination of these correction factors are shown in Appendix V and VI.

The same test procedure as above was used to determine the 50% breakdown voltages for the open cell. The same electrode systems and polarity were used with the open cell. Test data for both electrode systems were obtained for the 2" dia., 4" dia., and 6" dia. glass cylinders centered about the open cell. Data was taken to determine if the clamps on each test cell had any effect on the breakdown strength of air for each electrode system using positive polarity. The apparatus used in making the previous tests is shown in Figure 13 with the 4" dia. glass cylinder.

Negative polarity impulse tests were made only on the open cell and with the 2" dia., 4" dia., and 6" dia. glass cylinders centered about the open cell with both electrode systems. The 50% breakdown voltages for negative polarity were obtained by the same procedure as for positive polarity, but data was taken for only a few gap settings ranging from 800 mils to 1400 mils gap. These breakdown

PANEL METER SETTING	TRIALS	OSCILLOSCOPE DEFLECTION (mm)
Cycle 1		(100% Atten.)
16.0	X O O O O O O O O O	43
17.0	O X X O O O O O X O	46
18.0	X O O X X X O X O X	48
19.0	X X X X X X X X X X	50
Cycle 2		(100% Atten.)
19.0	X X X X X X X X X X	50
18.0	X X X X X O X X X X	48
17.0	X O X X X X X O O X	46
16.0	O X X O X O O X O O	43
15.0	O O O O O O O O O O	40
	X = Breakdown O = No Breakdown	

Fig. 14. Method of Recording Data. 1½ x 40μ sec. Wave - Positive Polarity, 2" Dia. Test Cell, Dry Air, Point to Plane Electrode System, Gap Spacing - 1400 mils.

voltages obtained were also corrected from ambient to standard conditions. The correction factors were obtained by the same procedure as for positive polarity impulse voltages.

In all of the above open cell tests for positive and negative polarity a humidity correction factor was determined. The determination of this correction factor for each electrode system and polarity is shown in Appendix VI. The ambient temperature, barometric pressure, and relative humidity were recorded for every gap setting for all of the above tests.

In all of the above tests using the impulse generator, an irradiation source, consisting of a millicurie of radium placed in a lead container, was used to help prevent erratic breakdowns of the gas being used. This was suggested by the AIEE Standards #4, 1953, for measurement of breakdown voltages under 50 KV. This same radium source was used by Keith E. Crouch in his thesis titled, The Effect of Wave Shape on the Electrical Breakdown on Nitrogen Gas,[16] where more detailed information can be found on this particular radium source.

D. Voltage Sources

1) High Voltage 60 Cycle Test Set

The high voltage 60 cycle test set is a General Electric test set consisting of a control console panel and a high voltage testing transformer. This test set has a rated output of 0 to 75 KV. The control console panel has external terminals for connection of a high impedance voltmeter for accurate reading of the output voltage of the test transformer. The voltmeter used with this test set was a Westinghouse rectifier type AC voltmeter, which measured RMS voltages. The test set was designed to be corona free up to its top

rating.

2) Full Wave Impulse Voltage Test Set

The full wave impulse voltages were obtained from a Westinghouse, portable, impulse generator with a maximum rated output of 125 KV. The control cabinet contained a panel meter which was calibrated to indicate the output voltage of the generator for a particular wave shaping circuit. The generator used a Marx, parallel charge-series discharge of capacitors circuit. There were three capacitors, each having a 50 KV rating, in this unit. A circuit diagram of this generator is shown in Figure 15. Upon triggering, a mechanical arm shorted the first set of sphere gaps and caused the second and third set of sphere gaps to arc over and discharged the three capacitors in series across the output. Some of the voltage being discharged by the capacitors will be lost in the wave shaping circuit and across the air gaps between the internal spheres. A type 507 Tektronix oscilloscope was used with this test set as a reference indicator of the voltage output of the generator. The oscilloscope used a voltage divider in the wave shaping circuit to measure the output voltage. The connection of this oscilloscope as a voltage indicator is also shown in Figure 15. The oscilloscope was used to determine if the wave shaping circuit would give a $1\frac{1}{2} \times 40\ \mu$sec. wave. The calibration of the control panel meter and the oscilloscope is shown in the Appendix III.

Analog Field Plotting of Test Cells

1. General Description

The field plotting method of this thesis uses an anology method

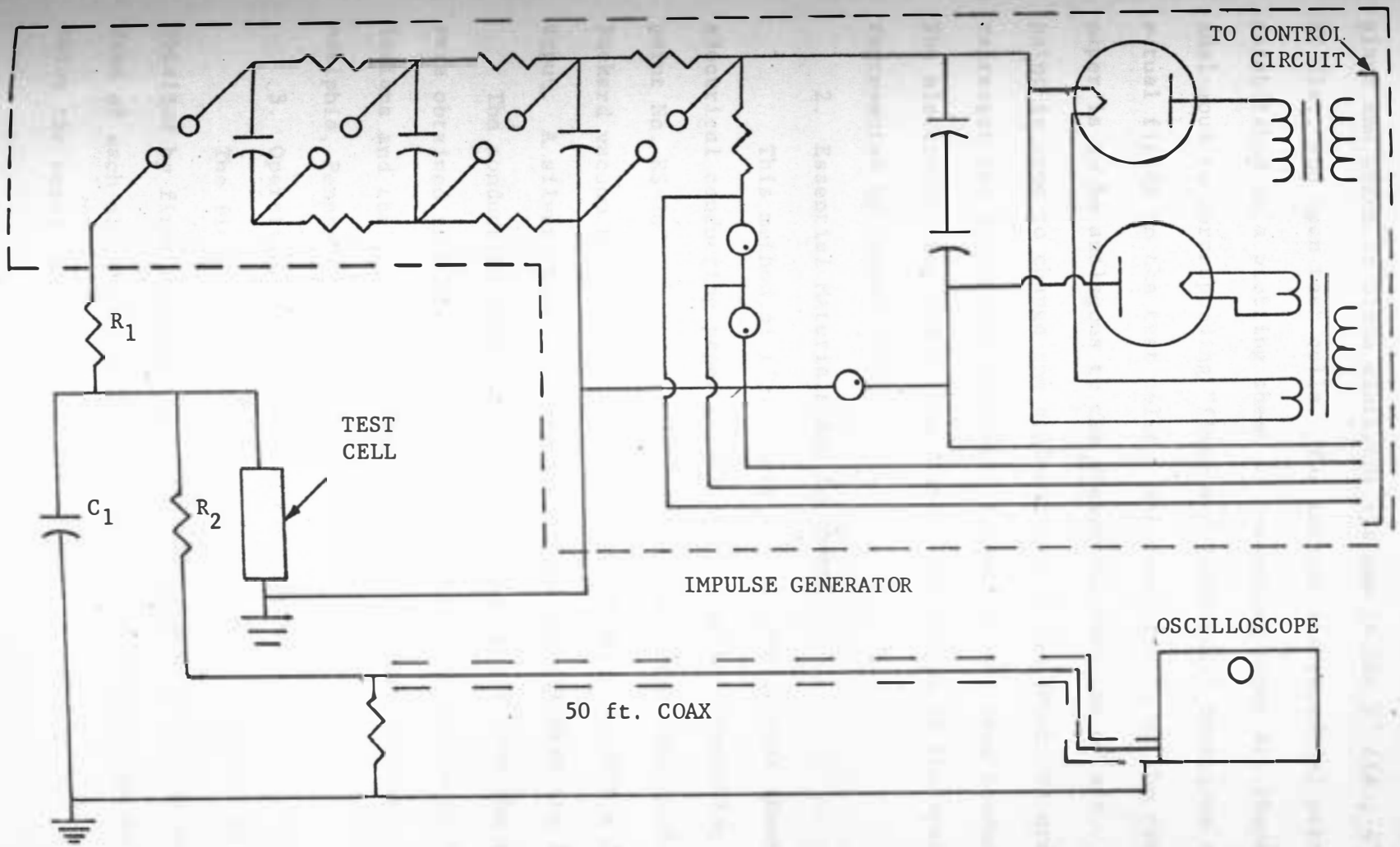

Fig. 15. Impulse Generator and Wave Shaping Circuit Diagram.[16]

to obtain the flux lines and equipotential lines of the 1" sphere to plane and point to plane electrode systems in the 2" dia., 4" dia., 6" dia., and open test cells. The current and potential patterns established on a plotting sheet of conducting paper are chosen to be analogous to corresponding "flux" and "potential" functions of the actual fields in the test cells. The conductivity of the conducting paper is to be analogous to the dielectric constant of air. Conducting paint is used to change the conductivity of the paper, in order to represent the dielectric constant of glass on the same conducting sheet. The electrodes, top and bottom plates, and clamps of the test cells are represented by copper foil.

2. Essential Materials and Equipment

This method of field plotting consists of thin sheets of electrical conducting paper (0.004 inches thick), conducting rubber paint No. RS-207A, 0.002 inches thick copper metal foil, a Hewlett Packard vacuum tube voltmeter and ammeter Model 410B with a 122 megaohm input. A silver, blue printing pencil was used to draw the field plots.

The conducting paper, conducting rubber paint, and the copper foil were obtained from the Westinghouse Electric Corporation at Muncie, Indiana and the Sunshine Scientific Instrument Corporation at Philadelphia, Pennsylvania.

3. Operations in Determining Field Plots

The field plots shown in the Figures of Appendix II were obtained by first drawing a schematic diagram of the cross-sectional area of each electrode configuration. Each configuration was drawn to twice the actual size in order to increase the accuracy of plotting.

The electrodes were attached to the conducting paper with conducting rubber paint. After sodering leads to the electrodes, a 20 volt DC supply was connected to the leads with the positive polarity terminal at the top electrode. The equipotential lines were then plotted with a Hewlett Packard vacuum tube voltmeter. The equipotential lines were plotted in 10 percent incremental voltage steps from 0 to 100 percent of the supplied voltage. The equipotential lines were obtained for all the test cells for both electrode systems and with and without the glass cylinders. The glass cylinder was represented on the conducting paper with the use of a certain mixture of conducting rubber paint and xylol. The mixture of the paint was such that the conductivity of the paper was five times greater when one coat of paint was applied. Since the dielectric constant of the glass was approximately five times greater than air, the conductivity of glass must be five times greater than air or the conducting paper.

The procedure for finding the flux lines for the cells with the glass is different than without the glass. The procedure for each will be discussed individually. To obtain the flux lines for the test cells without the glass, the copper foil electrodes were cut out and a new electrode system was attached to the paper. The conducting paper now had void areas where the original electrodes were positioned. A narrow slit was then cut between the point electrode or the 1" sphere electrode, depending on what configuration was being used, to the plane electrode. Then a narrow strip of copper foil was attached to each side of the narrow slit. These new electrodes were called current electrodes, because the equipotential lines plotted for these new electrodes

will be the current lines or flux lines of the original electrodes. In other words, the equipotential lines of one system are the current lines of the other system. This method of field plotting was suggested by reference 10. A large sheet of conducting paper must be used in order for the flux lines to come out perpendicular to the equipotential lines by this method. This method only applies to field plots in a single medium.

The flux lines for the test cells with the glass were drawn free hand, because of the failure of the above method to apply to a double medium. The flux lines were drawn by the method of curvilinear-squares. The following equation was used in determining the angle in which the flux lines would be refracted when crossing the boundary of two different mediums.

$$\frac{\text{Tan } \alpha_1}{\text{Tan } \alpha_2} = \frac{\varepsilon_1}{\varepsilon_2}$$

Explanation of this equation is given in the theory of this thesis.

RESULTS AND DISCUSSION

In order to determine the effect of different size glass cylinders on gaseous insulation breakdown, tests were run using the open cell with the 2" dia., 4" dia., and 6" dia. glass cylinders centered about the open cell. Test data was obtained for a 1" sphere to plane and a point to plane electrode systems with rapidly applied 60 cycle voltages (500 volts/sec.) and impulse voltages (positive and negative polarity). Test results are shown in the graphs of Figures 16, 17, 24, 25, and 31.

In Figure 16 the rapidly applied 60 cycle breakdown voltage decreases proportionally with a decrease in glass cylinder diameter and with an increase in gap spacing. At a gap spacing of 1800 mils the 2" dia., 4" dia., and 6" dia. glass cylinders centered about the open cell have a maximum deviation from the open cell breakdown voltages with no glass of -7.88%, -3.80%, and -1.52%, respectively. The values of maximum deviation for each gap spacing are shown in Table I. From Figure 16 it can be seen that the glass cylinder diameter does affect the breakdown voltage of a 1" sphere to plane electrode system under rapidly applied 60 cycle voltage. The effect of the glass cylinder only becomes significant for gap spacings above 1000 mils. For gap spacings below 1000 mils the maximum deviations for each size of glass cylinders are less than 5%. The effect of glass cylinder size on rapidly applied 60 cycle breakdown voltages can be explained by the field plots shown in Figures 32, 33, 34, 35, 36, 37, and 45. These Figures show how the flux lines are refracted due to the glass cylinder. The glass cylinders cause the flux lines to be refracted toward the electrodes, causing the

field to be more concentrated in the region of the electrodes. Since the wall of the 2" dia. glass cylinder is closer to the electrodes than the 4" dia., and 6" dia. glass cylinders, the concentration of the flux lines around the electrodes will be more noticeable than for the 4" dia. and 6" dia. glass cylinders. Also the 4" dia. glass cylinder will cause the flux lines to be more concentrated near the electrodes than the 6" dia. glass cylinder. The same concentration occurs for 6" dia. glass cylinder relative to the open cell with no glass cylinder. Since the 2" dia. glass cylinder centered about the open cell causes the field to be the most concentrated about the electrodes, the breakdown voltages should be the lowest. Therefore, the breakdown voltage should increase with the increase in glass cylinder diameter due to the decrease in the effect of the glass, which is verified by the experimental results shown in the graph of Figure 16.

The graph in Figure 17 shows how the rapidly applied 60 cycle breakdown voltage varies with different size glass cylinders centered about the open cell for a point to plane electrode system. It can be seen by observing Figure 17 that no definite effect of glass cylinder size can be distinguished from the curves. Table II shows that the maximum deviation at some of the lower gap spacings are just as high as for some of the higher gap spacings. The author believes that the maximum deviation should have increased gradually with an increase in gap spacing. It is well known that a point to plane electrode system causes very erratic results. This is one of the reasons why the AIEE Standard 4, A.S.A., c68.1, (1953) does not approve of this type of electrode arrangement for voltage measurements in dielectric tests.

These erratic results, which may not be noticeable by the investigator, are due to the fact that after successive trials the breakdown voltage will vary as the point becomes less sharp and due to the fact that corona discharges occur around sharp points.[17,18] These may be some of the reasons why no definite effect of glass cylinder size on rapidly applied 60 cycle breakdown voltage could be observed in the graph of Figure 17. However, the curves in Figure 17 do show that the 2" dia. and 4" dia. glass cylinders affect the rapidly applied 60 cycle breakdown voltage much more then the 6" dia. glass cylinder at the higher gap spacings. One of the reasons for this lower breakdown voltage at high gap spacings can be explained by observing the field plots shown in Figures 38, 39, 40, 41, 42, 43, and 44. The field plots show that the glass cylinders cause the flux lines to be refracted toward the electrodes, the same as the field plots for the 1" sphere to plane, causing the field to be more concentrated around the electrodes; therefore, causing the breakdown voltage to be lower. This may be the reason why the breakdown voltages are lower for the open cell with the 2" dia. and 4" dia. glass cylinders. No definite answer can be given by the author for the reason why the breakdown voltages were different and why the trend of the curves are like they are in the graph of Figure 17.

In order to determine the effect of the glass cylinder on rapidly applied 60 cycle breakdown voltage within the test cell, the effect of the clamps should be considered. Figure 18 shows how the breakdown voltage varies with different size and configuration of clamps for each test cell for a 1" sphere to plane electrodes. From Figure 18 and Table III it can be seen that the clamps have no significant effect

on breakdown voltage relative to the breakdown voltages obtained for the open cell. The maximum deviation from the reference curve (open cell) is 3.39% at 1200 mils gap for all three test cells without the glass cylinders. The maximum deviation from the mean breakdown voltage is 2.61% at 1200 mils gap shown in Table III.

Figure 19 shows how the rapidly applied 60 cycle voltage varies with different size and configuration of clamps for each test cell with a point to plane electrode system. Table IV shows that the clamps affect the breakdown voltage most significantly between the gap spacings of 400 mils and 1400 mils. From Table IV it can be seen that the breakdown voltages of the 6" dia. test cell without the glass cylinder closely approximates the breakdown voltages obtained with the open cell. The 2" dia. test cell and the 4" dia. test cell without the glass seem to have some effect on the breakdown voltage. However, it must be considered that a point to plane electrode system was being used, so erratic results must be considered. The author believes that the effects of the clamps should not have been significant, since they were not significant for the 1" sphere to plane electrodes. No definite conclusion can be obtained from the results suggesting that the clamps did have a significant effect. Further research must be done in order to reduce erratic results obtained with a point to plane electrode system before definite conclusions can be obtained.

In Figures 32, 34, 35, 38, 40, and 42 show how the field is distributed in the test cells without the glass cylinder for the 1" sphere to plane and point to plane electrodes. When comparing these field plots to Figures 44 and 45, it can be seen that the clamps do

change the pattern of the field. But from the experimental results obtained the effect of the clamps on the rapidly applied 60 cycle breakdown voltages for the 1" sphere to plane indicate no significant effect. For the point to plane electrodes the effect of the clamps is unpredictable, experimentally, even though the field plots indicate some effect.

Figure 20 shows a comparison of the rapidly applied 60 cycle breakdown voltages at various gap spacings for the 2" dia., 4" dia., and 6" dia. test cells with a 1" sphere to plane electrode system when changing the air in the cells for every breakdown. The test results for Figure 21 were obtained by the same procedure as those in Figure 20 except the air in the test cells was not changed during the test. In Figure 21 the curves are broken between the 800 mils and the 1000 mils gap spacing, because the test cells were disassembled and cleaned after obtaining the average breakdown voltages for gap spacings between 0 and 800 mils. These two Figures give a comparison of how the breakdown voltage varies in the test cells when the gas or air in the cells is changed or not changed after each breakdown. When comparing the curves in Figures 20 and 21, it can be seen that the breakdown voltages obtained in the 2" dia. test cell changes for the upper gap spacings depending on if the air in the cell is changed or not changed after every breakdown. The rapidly applied 60 cycle breakdown voltage at 1800 mils gap spacing when not changing the air in the 2" dia. test cell is 2.3 KV higher than the breakdown voltage obtained when changing the air in the cell after every breakdown. The rapidly applied 60 cycle breakdown voltages obtained for each gap spacing for the 4" dia. and

6" dia. test cells when changing the air in the cells or not changing the air in the cells is approximately the same. One of the reasons for the breakdown voltage to increase when not changing the air in the 2" dia. test cell may be due to a contaminating film, which may have caused the work function of the electrodes to increase; therefore, suppressing the admission of elecions during the pre-spark period. These electrons from the electrodes help in avalanching a breakdown. This contaminating film may have formed due to ozone in the cell, which is formed by previous breakdowns. Ozone formed by corona or during breakdown may deteriorate the surface of the electrodes.[17] Contaminating films on the electrodes were most noticeable in the 2" dia. test cell, which may be due to the smaller volume of gas contained by this cell compared to the other cells. The 2" dia. test cell has an internal gas volume of 20.8 $in.^3$ where the internal gas volume of the 6" dia. and 4" dia. test cells is 226.6 $in.^3$ and 97.6 $in.^3$, respectively.

In order to determine if ozone was the major cause of the contaminating films on the electrodes, the author decided to run tests on pure nitrogen gas in the test cells for the 1" sphere to plane electrodes, since pure nitrogen contains no oxygen. Figure 22 shows the results of these tests for gap spacings between 1000 mils and 1800 mils. Again very noticeable contaminating films were formed on the electrodes of the 2" dia. test cell. From Figure 22 it can be seen that the general trend of the curves is the same as those curves in Figure 21. Therefore, the author believes that nitrogen gas is the cause of the contaminating films rather than ozone gas in the cells. Since the effect of the contaminating films was reduced when changing

the air in the cells after each breakdown, as can be seen from Figure 20, the author decided to purge the enclosed test cells in all of the following tests with new air in order to obtain accurate results. Now observing Figure 20 again the general trend of the curves is similar to the curves obtained in Figure 16. Therefore, the major differences in the curves in Figure 20 seems to be due to the effect of the different size glass cylinders. The breakdown voltages for each gap spacing for each test cell is slightly higher in Figure 20 than the breakdown voltages for each gap spacing in Figure 16. This is due to the fact that the breakdown voltages obtained in Figure 16 are for open air which contains some moisture content where the breakdown voltages obtained in Figure 20 are for dry air. Dry air will have a higher breakdown voltage per gap spacing than moist air.

Figure 23 shows a comparison of test results obtained for the 2" dia., 4" dia., and 6" dia. test cells with a point to plane electrode system in dry air. Each data point is an average of 10 breakdowns in which the air was changed in the cells for each breakdown. From this Figure 23 it can be seen that the rapidly applied 60 cycle breakdown voltage does change with different size test cells. The rapidly applied 60 cycle breakdown voltage increases almost linearly with an increase in gap spacing for the 2" dia. test cell where the rapidly applied 60 cycle breakdown voltage varies parabolically with gap spacing for the 6" dia. and 4" dia. test cells. The only reason the author can suggest for the difference in the curves is that each test cell contains a different volume of gas. The author believes that the difference could not be due to the effect of the glass cylinders.

If the glass cylinders were affecting the breakdown of the gas, the 2" dia. glass cylinder would have the lowest breakdown voltage for each gap spacing. The author suggests that further research is required, in order to obtain a definite answer for the differences in the curves.

Figure 24 gives a comparison of the 50% impulse breakdown voltages per gap spacing obtained for the open cell and for the 2" dia., 4" dia., and 6" dia. glass cylinders centered about the open cell with a 1" sphere to plane electrode and for positive polarity. The results in Figure 24 were obtained in order to determine the effect of the different size glass cylinders upon impulse voltage breakdown. When observing Table V it can be seen that the percent deviations from the reference curve, which is the open cell, are all within experimental accuracy for impulse voltage tests, except for the breakdown voltages for the 1400, 1600, and 1800 mils gap spacing for the 6" dia. glass cylinder. Even though the test run with the 6" dia. glass cylinder had the highest percent deviation from the reference curve, the author believes that the deviation is not large enough to suggest that the difference is due to the effect of the glass cylinder. Also if the glass cylinders were causing the differences in the curves, the 2" dia. glass should have the greatest effect. The author believes that all of the percent deviations shown in Table V are within experimental accuracy of the equipment being used. When observing Figure 24 and Figure 16, the effect of the different size glass cylinders can be seen to have a smaller effect on impulse breakdown voltages for air then for rapidly applied 60 cycle voltages.

Figure 25 gives a comparison of the impulse breakdown voltages

obtained for a point to plane electrode system in the open cell and for different size glass cylinders centered about the open cell. Table VI gives the percent deviation from the reference curve (open cell) for the breakdown voltages obtained for the point to plane electrodes within different size glass cylinders. When observing Figure 25 and Table VI, it can be seen that there is no significant effect of the different size glass cylinders. Therefore, the author believes that the effect of the glass cylinders can be neglected.

One of the reasons for the insignificant effect of the glass cylinders on impulse voltage breakdowns is that the impulse wave has a smaller power capacity then 60 cycle voltages; therefore, the field of the impulse wave will be less effective at the walls of the glass cylinder. Also the impulse voltages being applied are of much shorter time duration than the rapidly applied 60 cycle voltages.

Figure 26 and Table VII show a comparison of the 50% impulse breakdown voltages (positive polarity) obtained for the 1" sphere to plane without the glass cylinders for open air. From Table VII it can be seen that the percent deviation of the breakdown voltages obtained for the test cells without the glass cylinders are all less then 5.0% from the breakdown voltages obtained with the open cell test. Therefore, the effect of the clamps on the breakdown voltage of open air with the 1" sphere to plane electrodes is insignificant. The effect of the clamps on impulse breakdown voltage of open air with the point to plane electrodes was also found to be insignificant by observation of Figure 27 and Table VIII.

Figures 28 and 29 show a comparison of the breakdown voltages

obtained for dry air within the enclosed test cells for the 1" sphere to plane and the point to plane electrode systems, respectively. In Figure 28 the positive polarity impulse breakdown voltages for the upper gap spacings could not be obtained for dry air within the 2" dia. and 4" dia. test cells with the impulse generator used in these tests. A 50% breakdown voltage could not be obtained for gap spacing above 1000 mils in the 2" dia. test cell and for gap spacing above 1200 mils in the 4" dia. test cell. The same test was repeated again at a later date on the 2" dia. and 4" dia. test cells, but the same effect was observed at the upper gap spacings. This effect seems to be more noticeable in the 2" dia. test cell than in the 4" dia. test cell, because the highest gap spacing at which a 50% breakdown voltage could be obtained in the 4" dia. test cell was 1200 mils where in the 2" dia. test cell the highest gap spacing was 1000 mils. As can be seen in Figure 28, the breakdown voltages could be obtained for all gap spacing in the 6" dia. test cell with a 1" sphere to plane electrodes. However, the 50% breakdown voltages for the 6" dia. test cell can be seen to increase quite rapidly with the increase in gap spacings above 1400 mils. This seems to be the trend of all the curves in Figure 28. The author believes that this rapid increase in the 50% breakdown voltages at the upper gap spacings is dependent on the volume of gas contained by each test cell. Since the highest 50% breakdown voltage that could be obtained with the 2" dia. test cell (gas volume-20.8 $in.^3$), the 4" dia. test cell (gas volume- 97.6 $in.^3$), and the 6" dia. test cell (gas volume- 226.6 $in.^3$) was at the gap spacings of 1000 mils, 1200 mils, and 1800 mils, the volume of gas in the cells seems to be

the influencing factor. The author suggest this explanation, since the air in the test cells was changed after every 3 impulses applied to the cells; therefore, contamination in the cells is limited, which could cause the breakdown voltages to increase.

Figure 29 shows the results obtained when positive polarity impulse voltages were applied to the test cells with point to plane electrodes in dry air. From Table X it can be seen that the highest maximum deviation from the mean breakdown voltage is 1.91% at the 1800 mils gap spacing. Since this maximum deviation is very low and within experimental accuracy, all of the test cells can be considered to give the same results when being used to obtain the positive polarity impulse breakdown voltages of dry air with a point to plane electrode system.

Some tests were also run on a point to plane and a 1" sphere to plane electrodes in the open cell and with different size glass cylinders centered about the open cell for open air under negative polarity impulse voltages. The tests were run for gap spacing between 800 mils and 1400 mils. As can be seen from Figure 30 and Table XI, the glass cylinder size on the breakdown of air with the point to plane electrode system has an insignificant effect. But from Figure 31 and Table XII the breakdown of open air with the 1" sphere to plane electrodes is only affected by the 2" dia. glass cylinder. The breakdown voltages obtained for the 4" dia. and 6" dia. glass cylinders centered about the open cell have a percent deviation from the reference curve (open cell) of less than 2.0% at all gap spacings. Therefore, the trend seems to be that the smaller the glass cylinder the greater the effect on

breakdown. This effect causes the breakdown voltage to increase at each gap spacing according to Figure 31. Therefore, the results obtained from the field plots shown in Figures 32, 33, 34, 35, 36, 37, and 45 do not correspond. The field plots indicate that the field around the electrodes increases as the diameter of the glass cylinder decreases, which in turn would cause the breakdown voltage to decrease. Therefore, it would seem that the reason for the higher breakdown voltages at each gap spacing for the 1" sphere to plane electrodes surrounded by the 2" dia. glass cylinder could not be due to the glass cylinder. The author believes that more investigation is needed with negative polarity impulse voltages, in order to determine the real cause of the increase in breakdown voltage when the 2" dia. glass cylinder is used.

The field plots in Figures 46 and 47 were obtained by the same procedure as was done in obtaining the field plots in all the previous Figures, except that the negative terminal of the DC supply was attached to the top electrode. These field plots of Figures 46 and 47 were drawn in order to determine if the field around the electrodes changes depending upon what polarity is applied to the top electrode. If one compares Figures 46 and 47 to the corresponding Figures 41 and 35 with positive polarity at the top electrode, it can be seen that the field around the electrodes is essentially the same. Therefore, the different size glass cylinders will affect the negative polarity and positive polarity breakdowns in the same manner.

The maximum gap spacing at which all three test cells give the same experimental results for a 1" sphere to plane electrode system

under rapidly applied 60 cycle voltages is 1400 mils. At this gap spacing the maximum deviation from the mean breakdown voltage is 4.8% at 1400 mils gap spacing. The results in Figure 23 show that there is no gap spacing in which all three test cells with a point to plane electrode system under rapidly applied 60 cycle voltages would give essentially the same results. Since the 6" dia. glass cylinder seems to have the least effect on breakdown of open air as can be seen by Figure 16, it would seem that the 6" dia. test cell would be the most appropriate in determining the dielectric strength of insulating gases with a point to plane electrode system.

When testing the dielectric strength of dry air under positive polarity impulse voltages and with a 1" sphere to plane, all of the test cells can be considered to give good experimental results up to a gap spacing of 1000 mils. All of the gap spacings from 1000 mils and below have breakdown voltages within 5.0% of the maximum deviation from the mean breakdown voltages as shown in Table IX. Figure 29 and Table X show that all of the test cells give essentially the same breakdown voltages at all gap spacing from 0 to 1800 mils when using a point to plane electrode system under positive polarity impulse voltages.

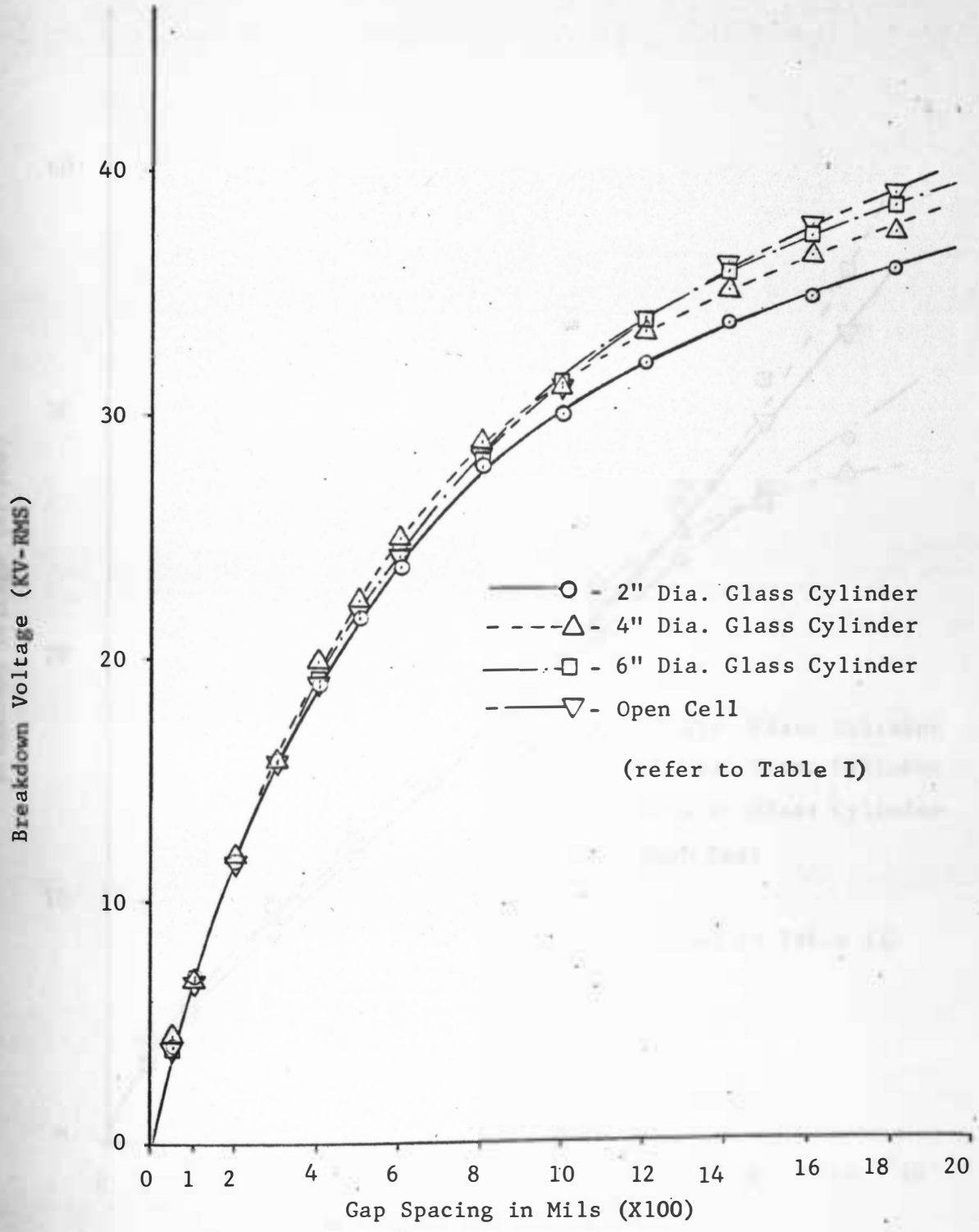

Fig. 16. Rapidly Applied 60 Cycle Breakdown Voltage (500 volts/sec) in KV vs. Gap Spacing in Mils for Open Air with a 1" Sphere to Plane Electrode System. Standard Conditions: 28.35 in. of Hg. and 80°F.

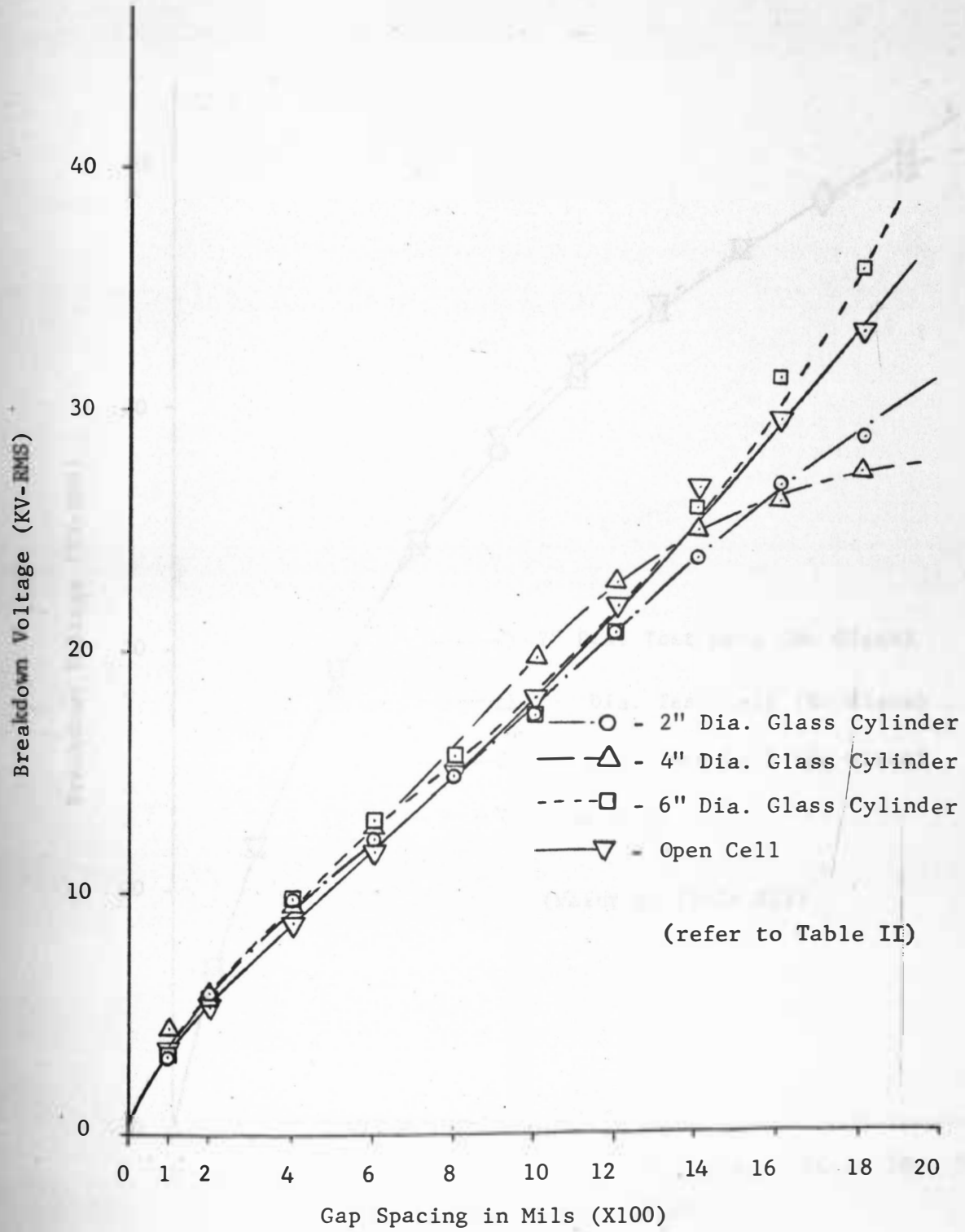

Fig. 17. Rapidly Applied 60 Cycle Breakdown Voltage (500 volts/sec) in KV vs. Gap Spacing in Mils for Open Air with a Point to Plane Electrode System. Standard Conditions: 28.35 in. of Hg. and 80°F.

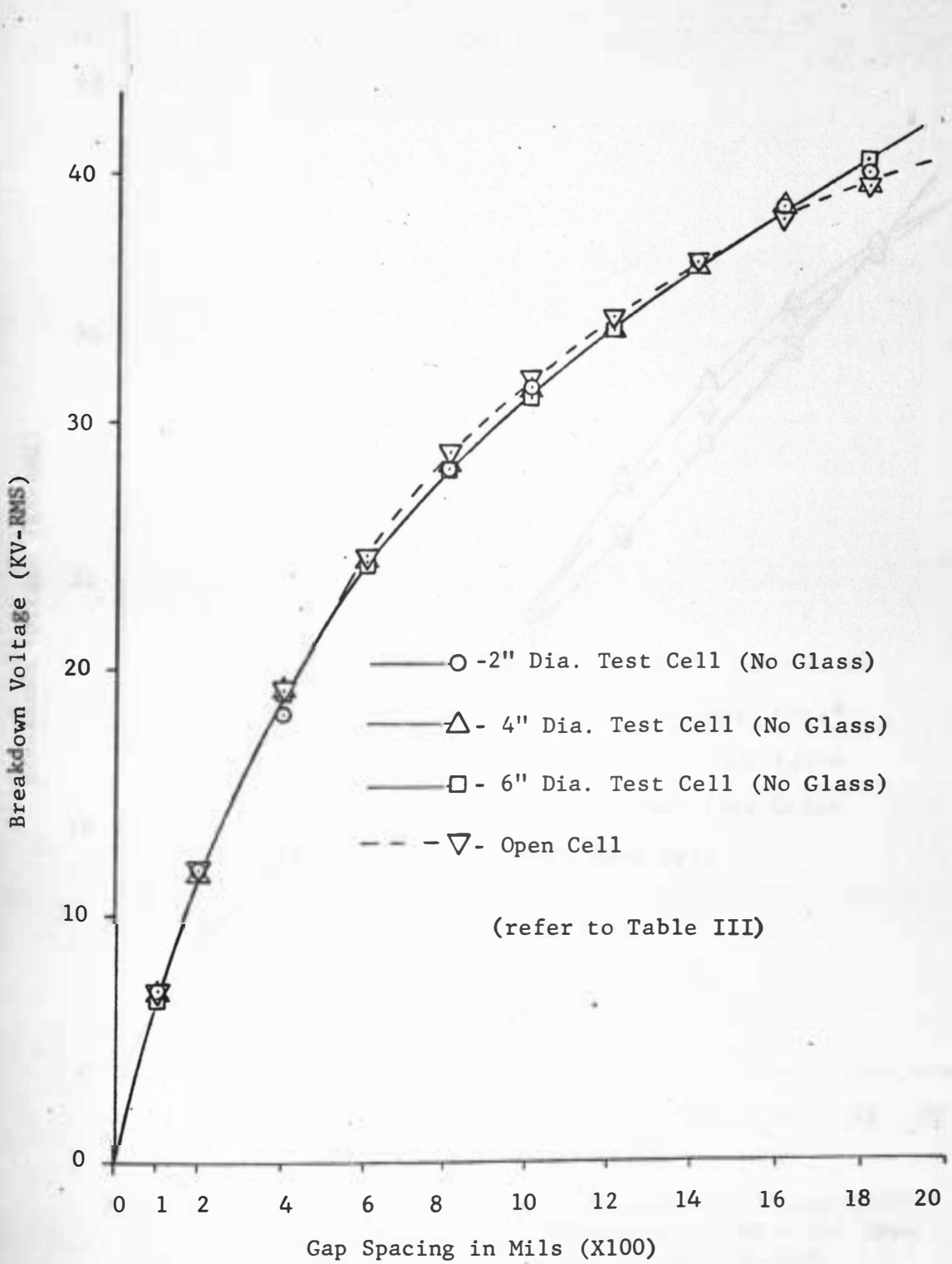

Fig. 18. Rapidly Applied 60 Cycle Breakdown Voltage (500 volts/sec) in KV vs. Gap Spacing in Mils for Open Air With a 1" Sphere to Plane Electrode System. Standard Conditions: 28.35 in. of Hg. and 80^{o}F.

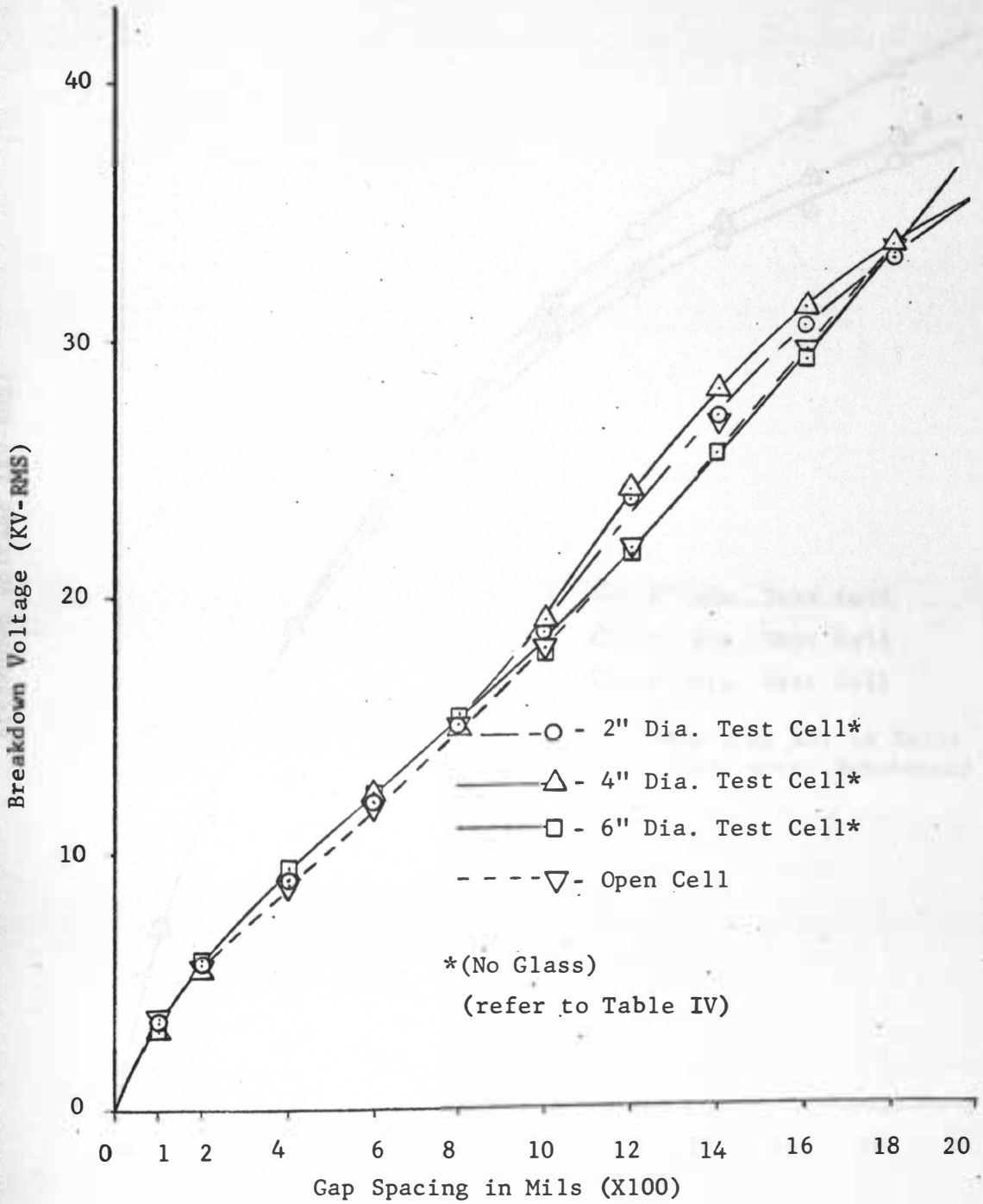

Fig. 19. Rapidly Applied 60 Cycle Breakdown Voltages (500 volts/sec) in KV vs. Gap Spacing in Mils for Open Air With a Point to Plane Electrode System. Standard Conditions: 28.35 in. of Hg. and 80°F.

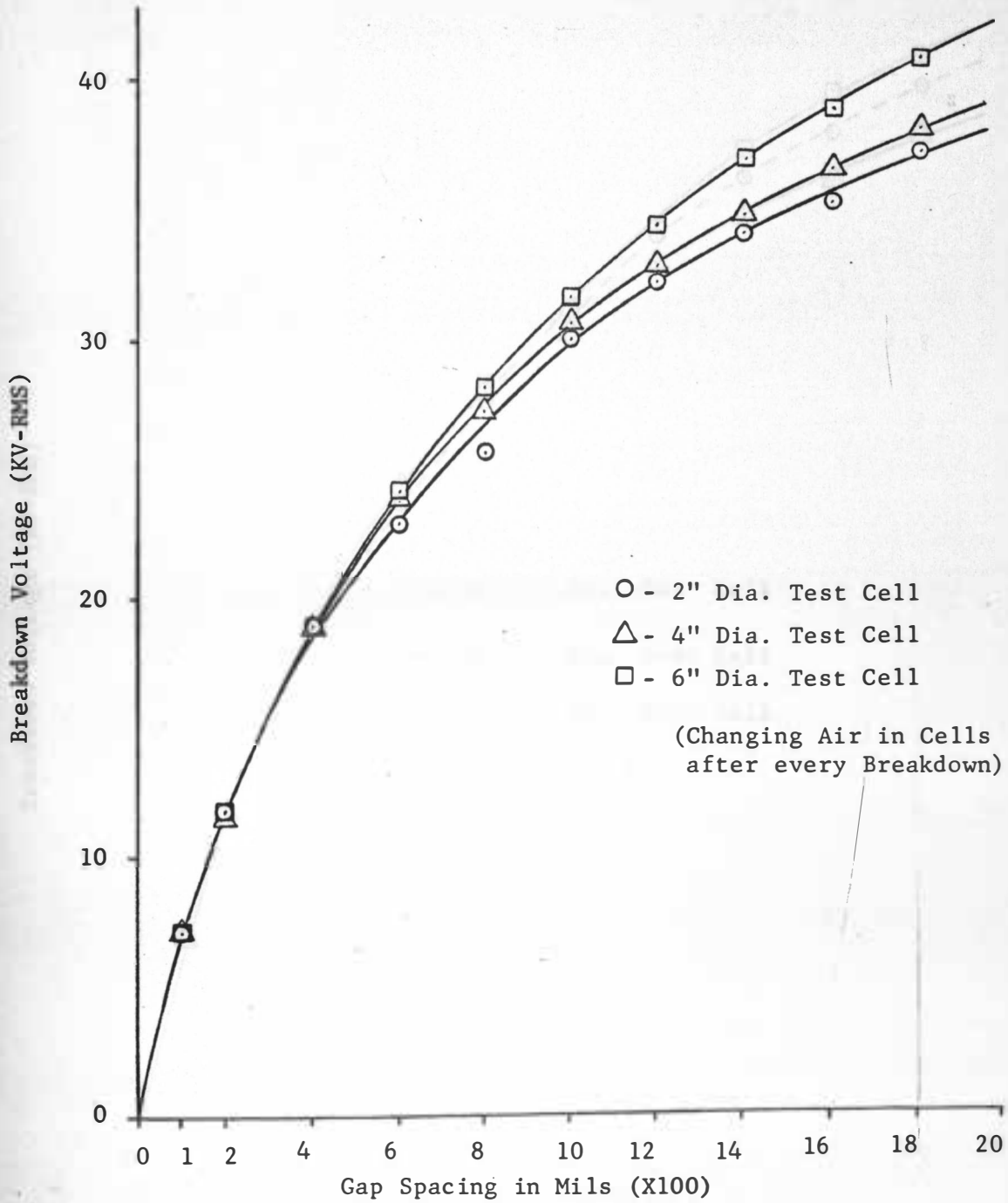

Fig. 20. Rapidly Applied 60 Cycle Breakdown Voltages (500 volts/sec) in KV vs. Gap Spacing in Mils for Dry Air with a 1" Sphere to Plane Electrode System. Standard Conditions: 28.35 in. of Hg. and 80°F.

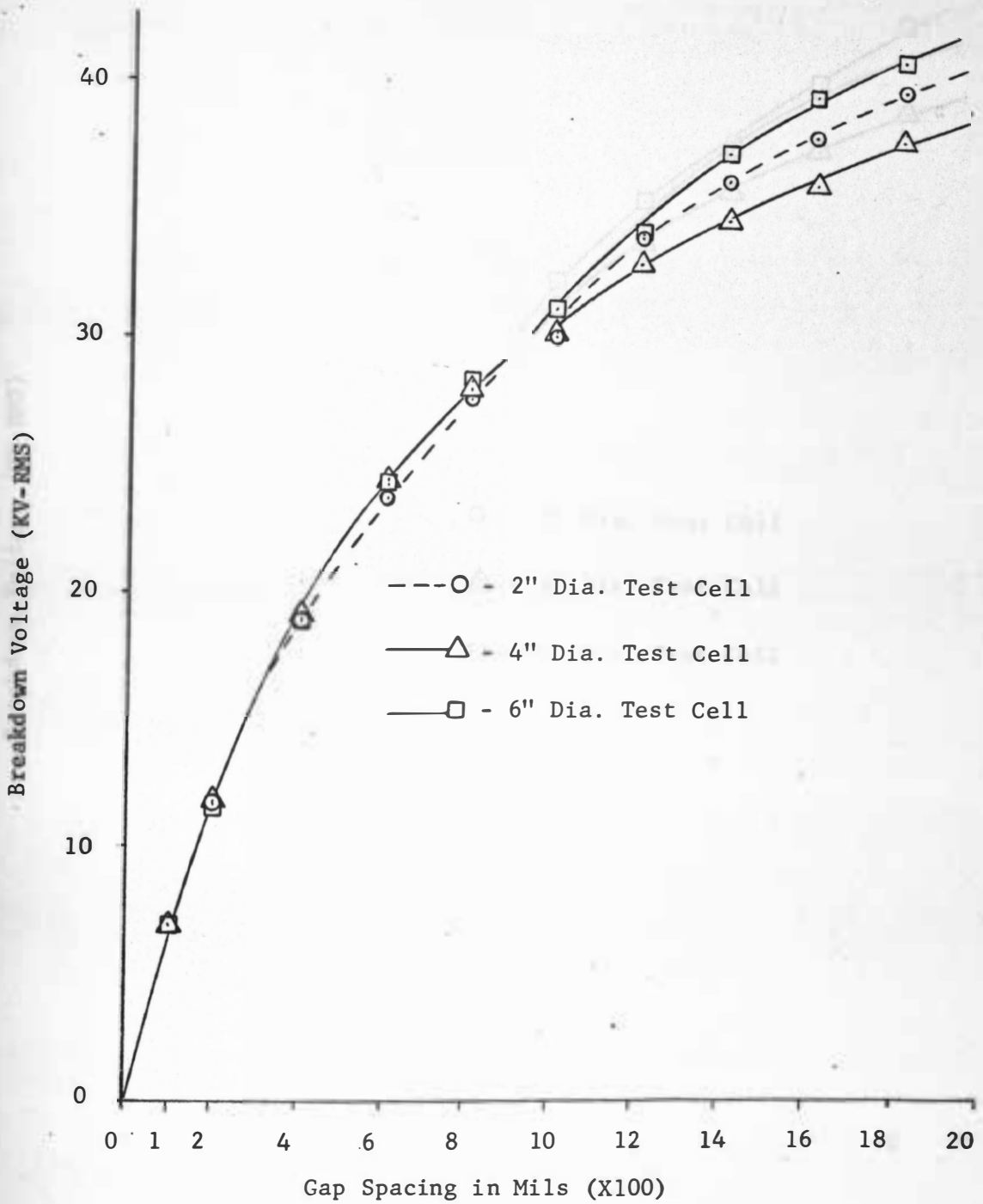

Fig. 21. Rapidly Applied 60 Cycle Breakdown Voltages (500 volts/sec) in KV vs. Gap Spacing in Mils for Dry Air With a 1" Sphere to Plane Electrode System. (No Change of Air in Cells During Tests). Standard Conditions: 28.35 in. of Hg. and 80°F.

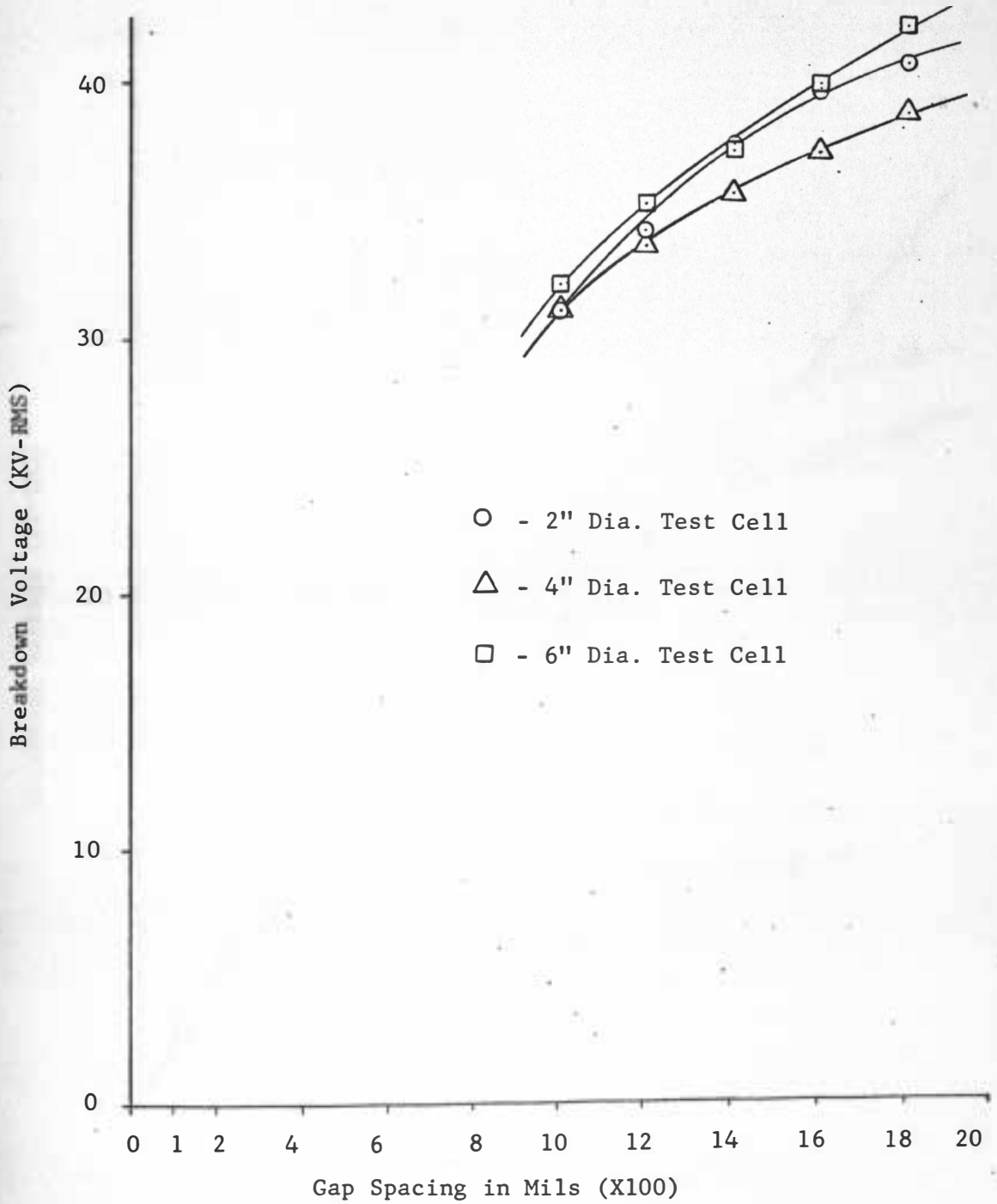

Fig. 22. Rapidly Applied 60 Cycle Breakdown Voltage (500 volts/sec) in KV vs. Gap Spacing in Mils for Dry N_2. With a 1" Sphere to Plane Electrode System. (No Change of Gas In Cells During Test). Standard Conditions: 28.35 in. of Hg. and 80°F.

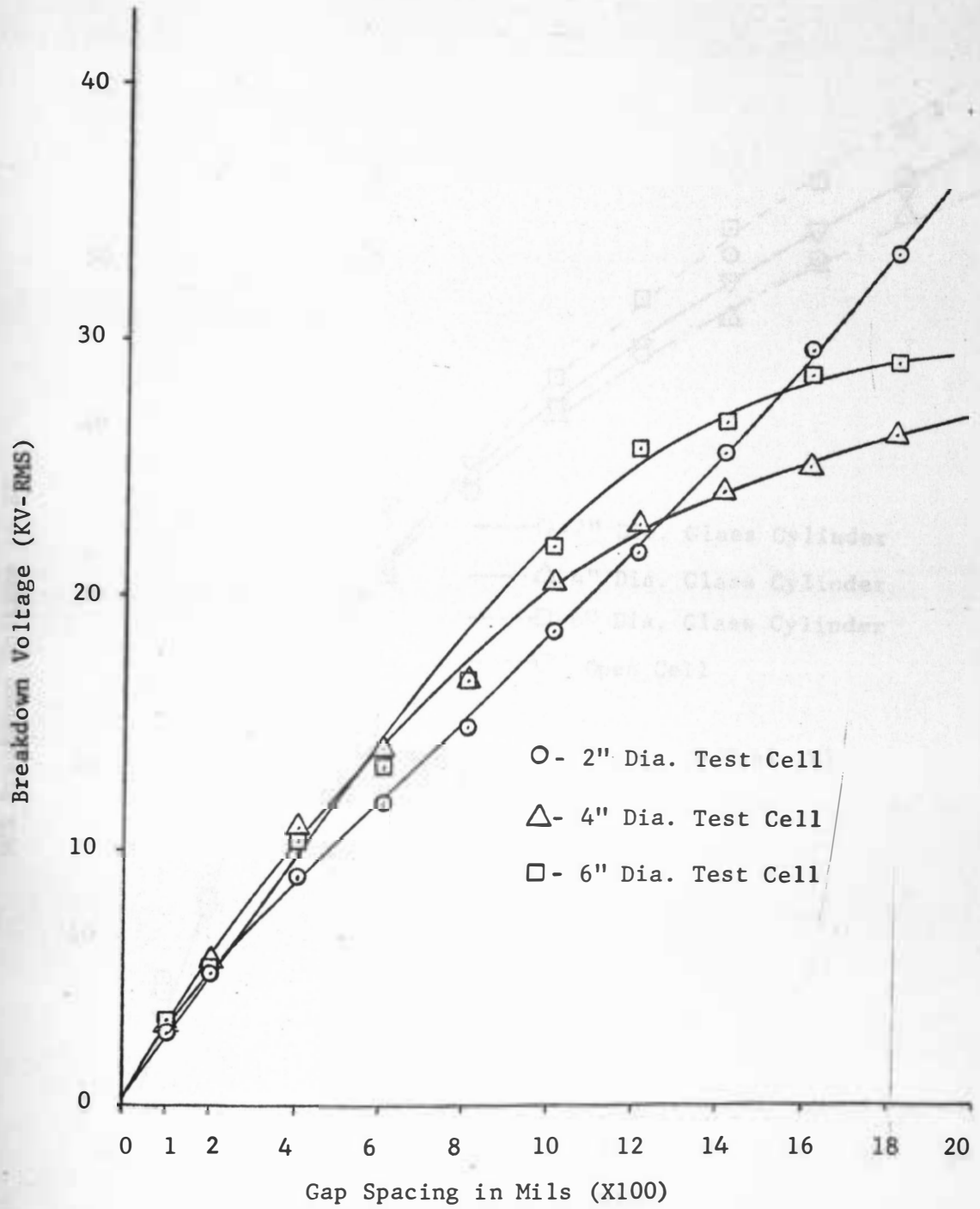

Fig. 23. Rapidly Applied 60 Cycle Breakdown Voltage (500 Volt/sec) in KV vs. Gap Spacing in Mils for Dry Air With a Point to Plane Electrode System (Changing Air in Cell After Every Breakdown). Standard Conditions: 28.35 in. of Hg. and 80°F.

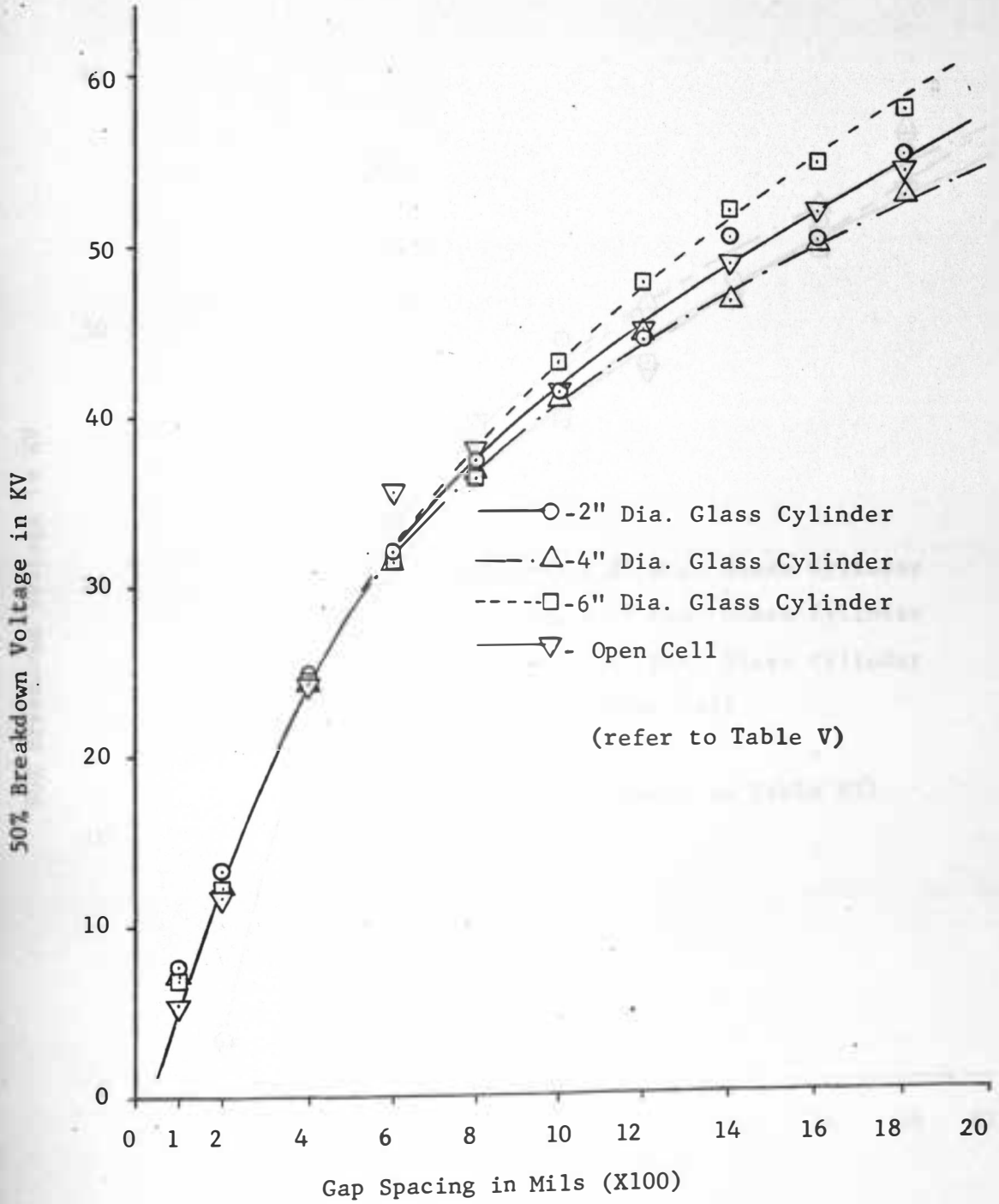

Fig. 24. 50% Breakdown Voltage in KV vs. Gap Spacing in Mils for Open Air With a 1½-40 μsec. Impulse Wave, Positive Polarity for a 1" Sphere to Plane Electrode System.
Standard Conditions: 28.35 in. of Hg. and 80°F.

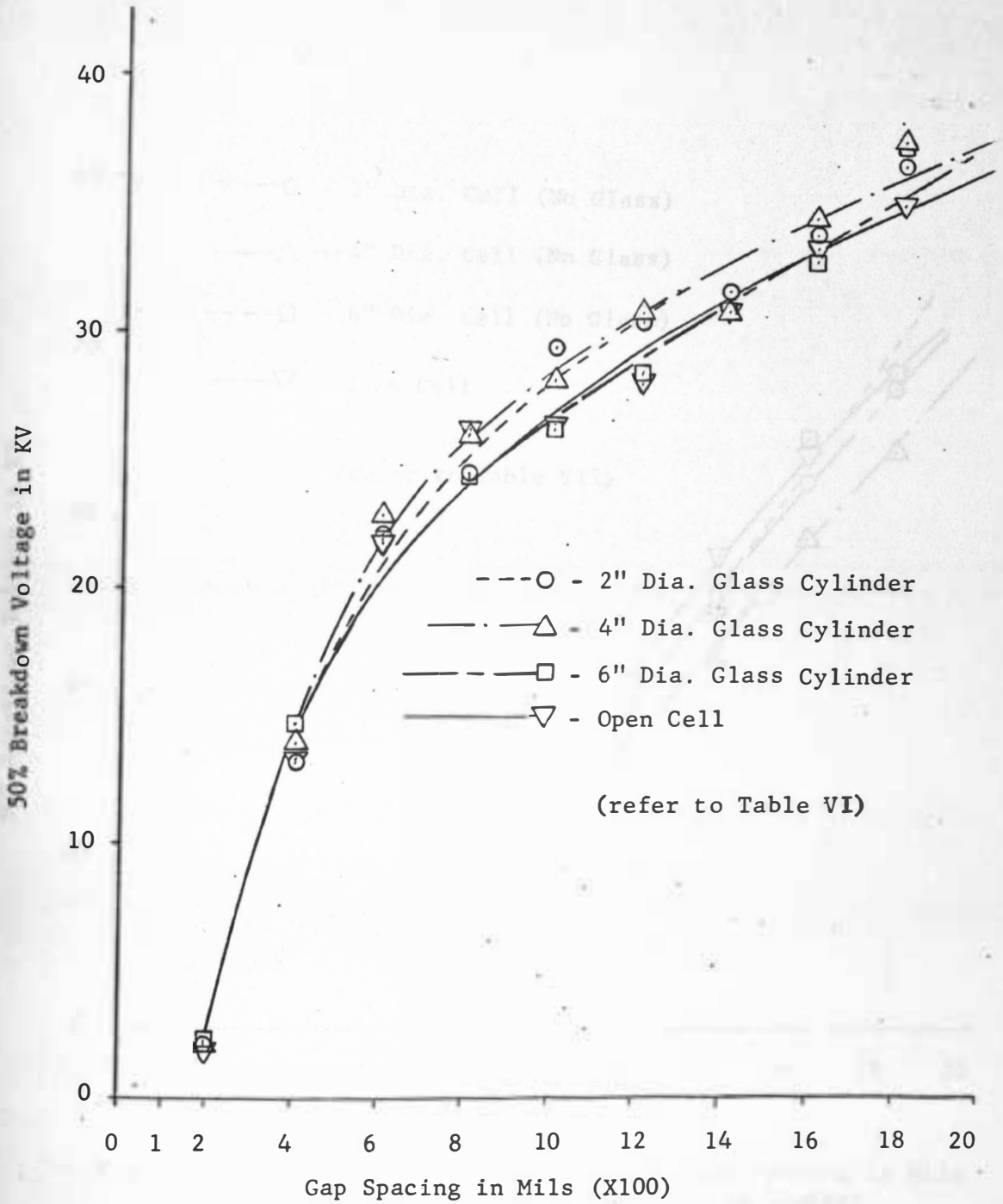

Fig. 25. 50% Breakdown Voltage in KV vs. Gap Spacing in Mils for Open Air With a 1½-40μsec. Impulse Wave, Positive Polarity for a Point to Plane Electrode System.
Standard Conditions: 28.35 in. of Hg. and 80°F.

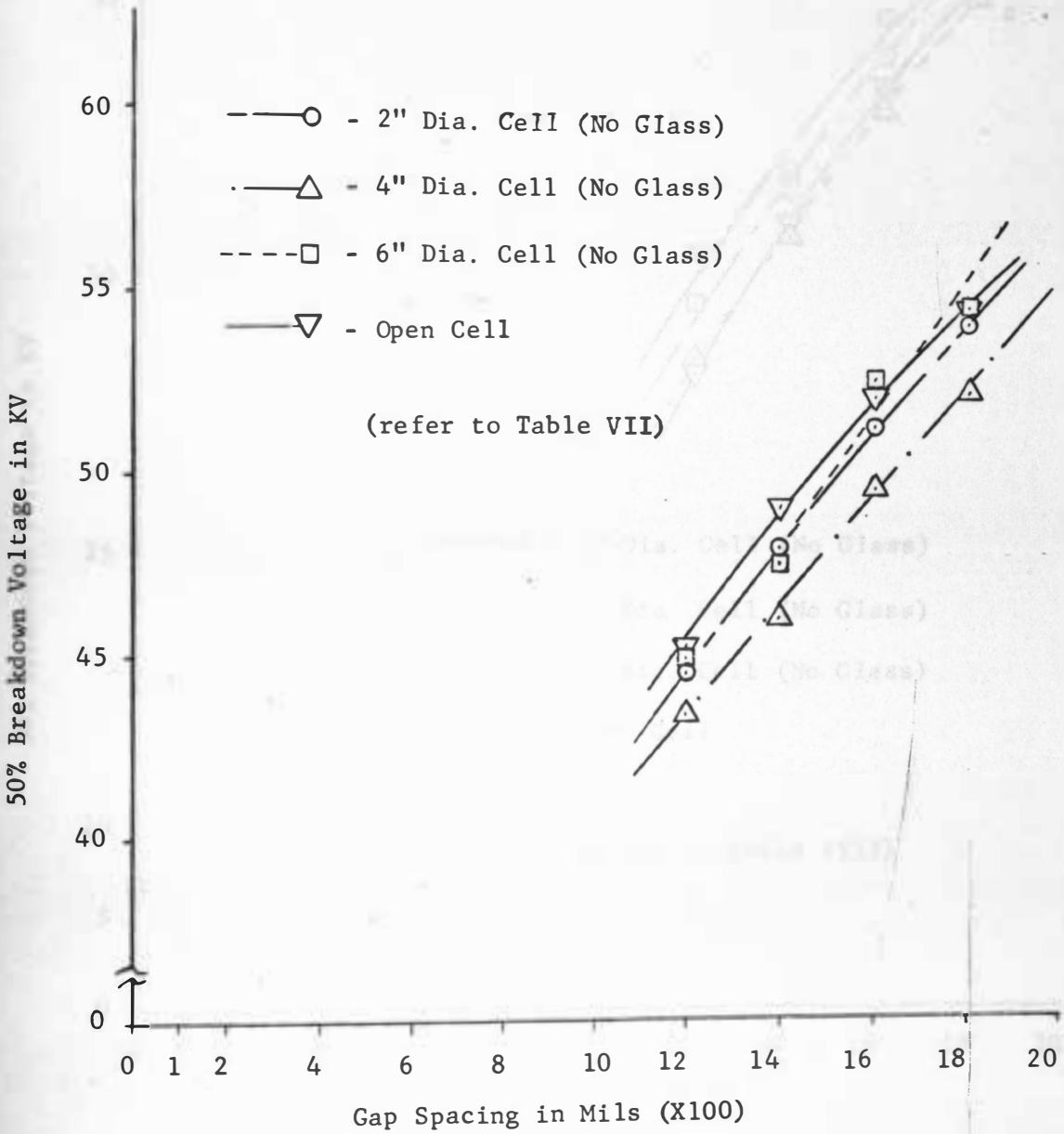

Fig. 26. 50% Breakdown Voltage in KV vs. Gap Spacing in Mils for Open Air. Positive Polarity, 1½-40 μsec. Impulse Wave for a 1" Sphere to Plane Electrode System.
Standard Conditions: 28.35 in. of Hg. and 80°F.

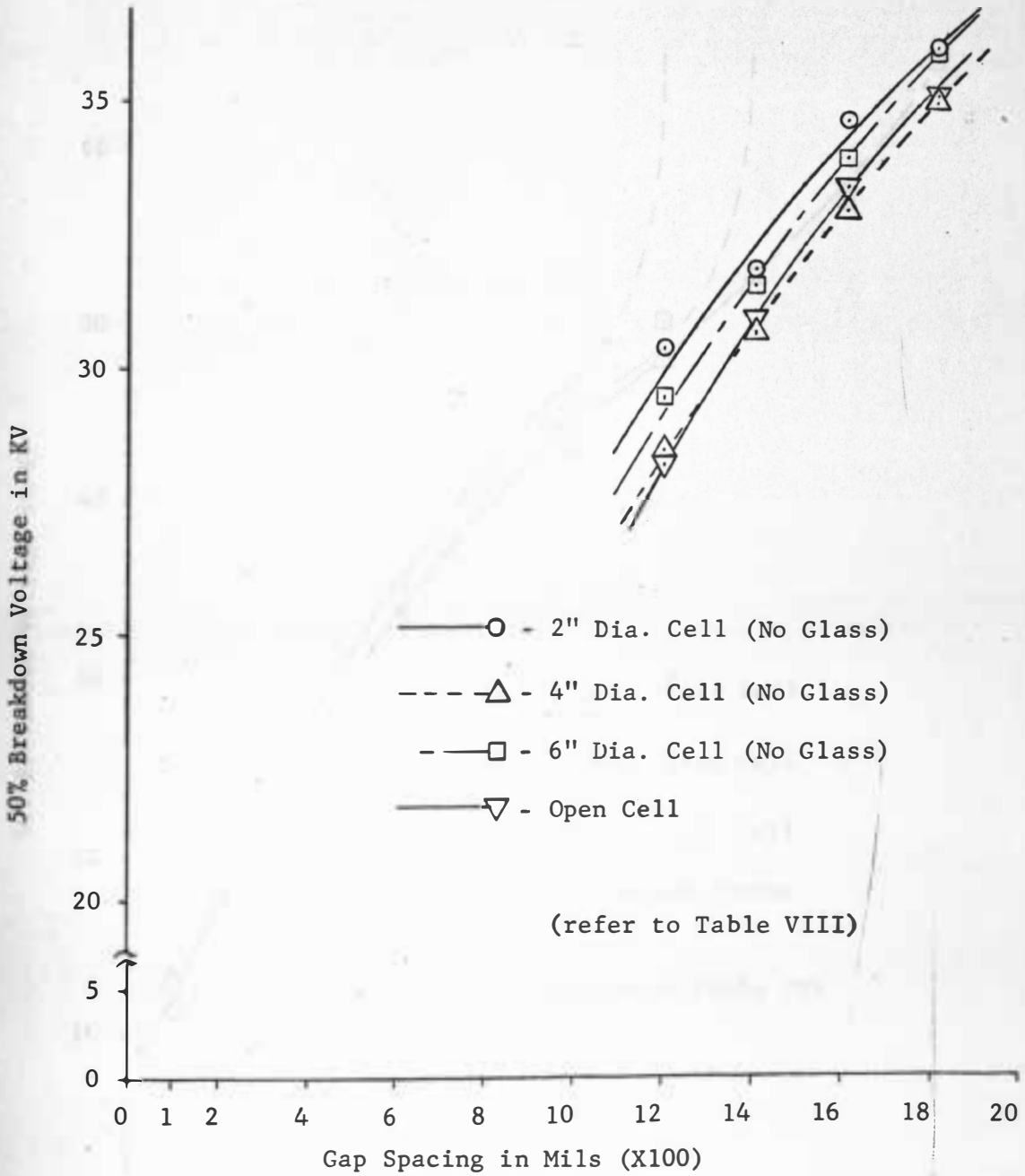

Fig. 27. 50% Breakdown Voltage in KV vs. Gap Spacing in Mils for Open Air. Positive Polarity, 1½ x 40 μ sec. Impulse Wave for a Point to Plane Electrode System. Standard Conditions: 28.35 in. of Hg. and 80°F.

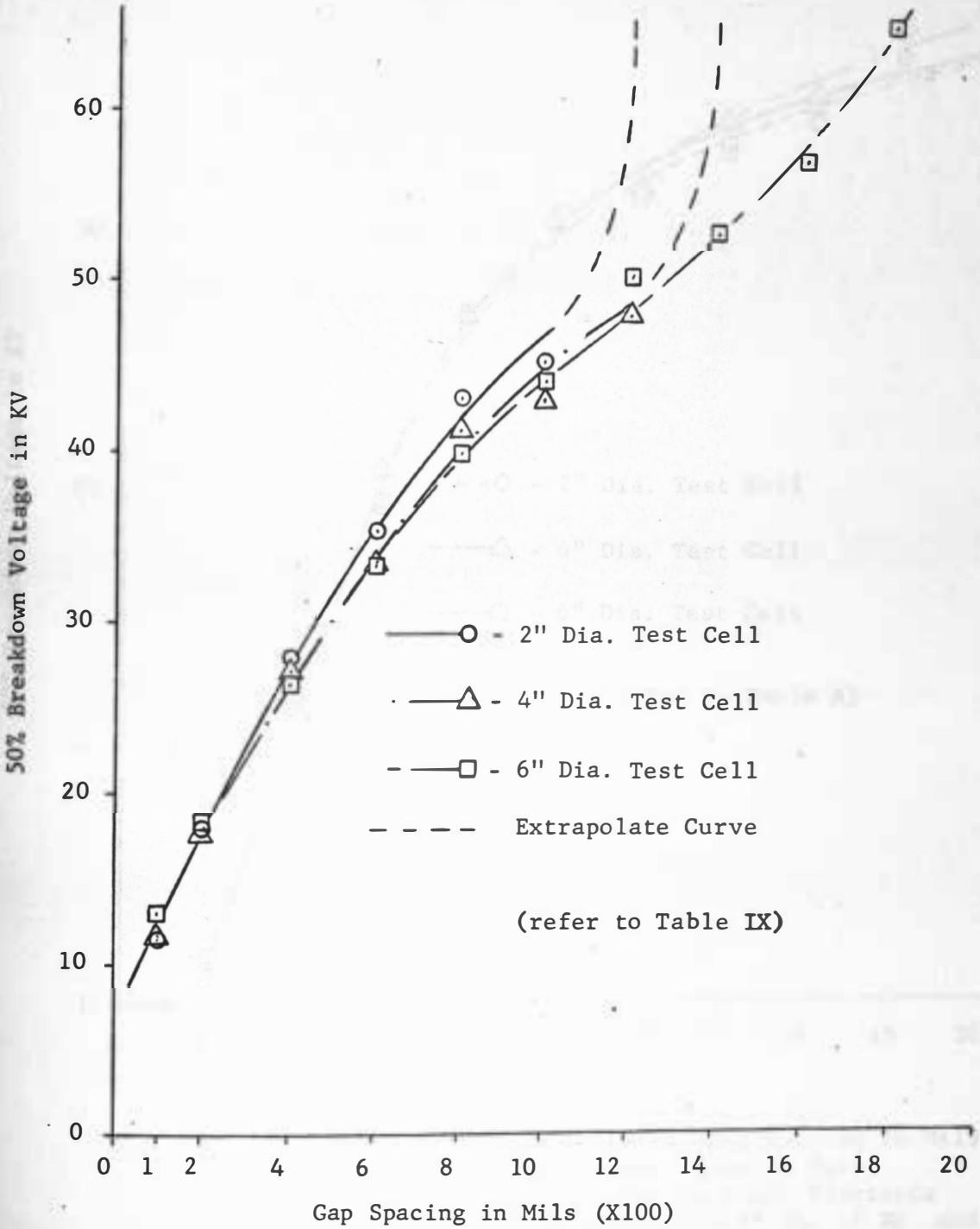

Fig. 28. 50% Breakdown Voltage in KV vs. Gap Spacing in Mils for Dry Air With a 1½-40μsec. Impulse Wave, Positive Polarity for a 1" Sphere to Plane Electrode System. Standard Conditions: 28.35 in of Hg. and 80°F. (Changing Air in Cells After every Panel Meter Setting).

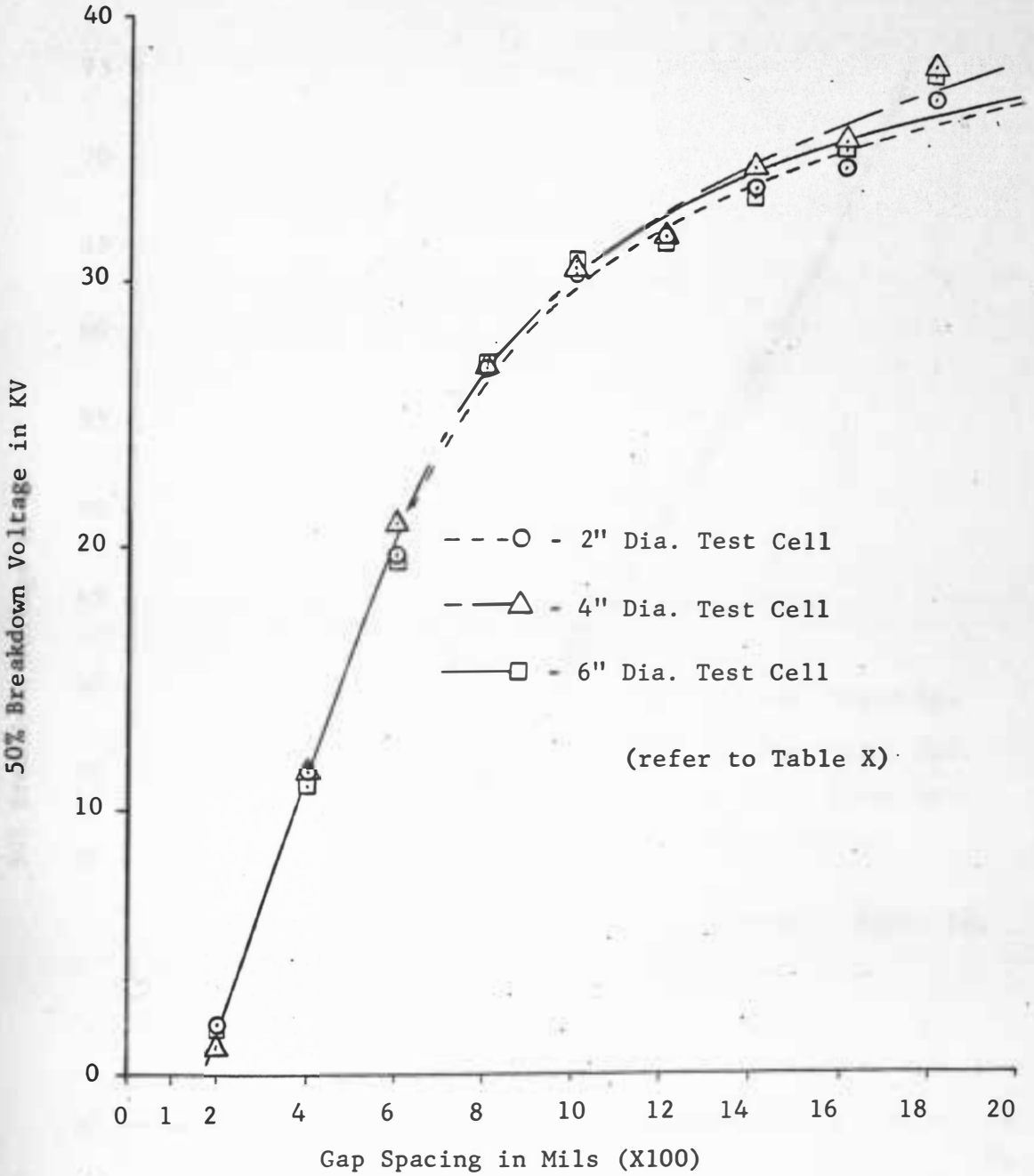

Fig. 29. 50% Breakdown Voltage in KV vs. Gap Spacing in Mils for Dry Air With a 1½-40 μsec. Impulse Wave, Positive Polarity for a Point to Plane Electrode System. Standard Conditions: 28.35 in. of Hg. and 80°F. (Changing Air in Cells After Every Panel Meter Setting).

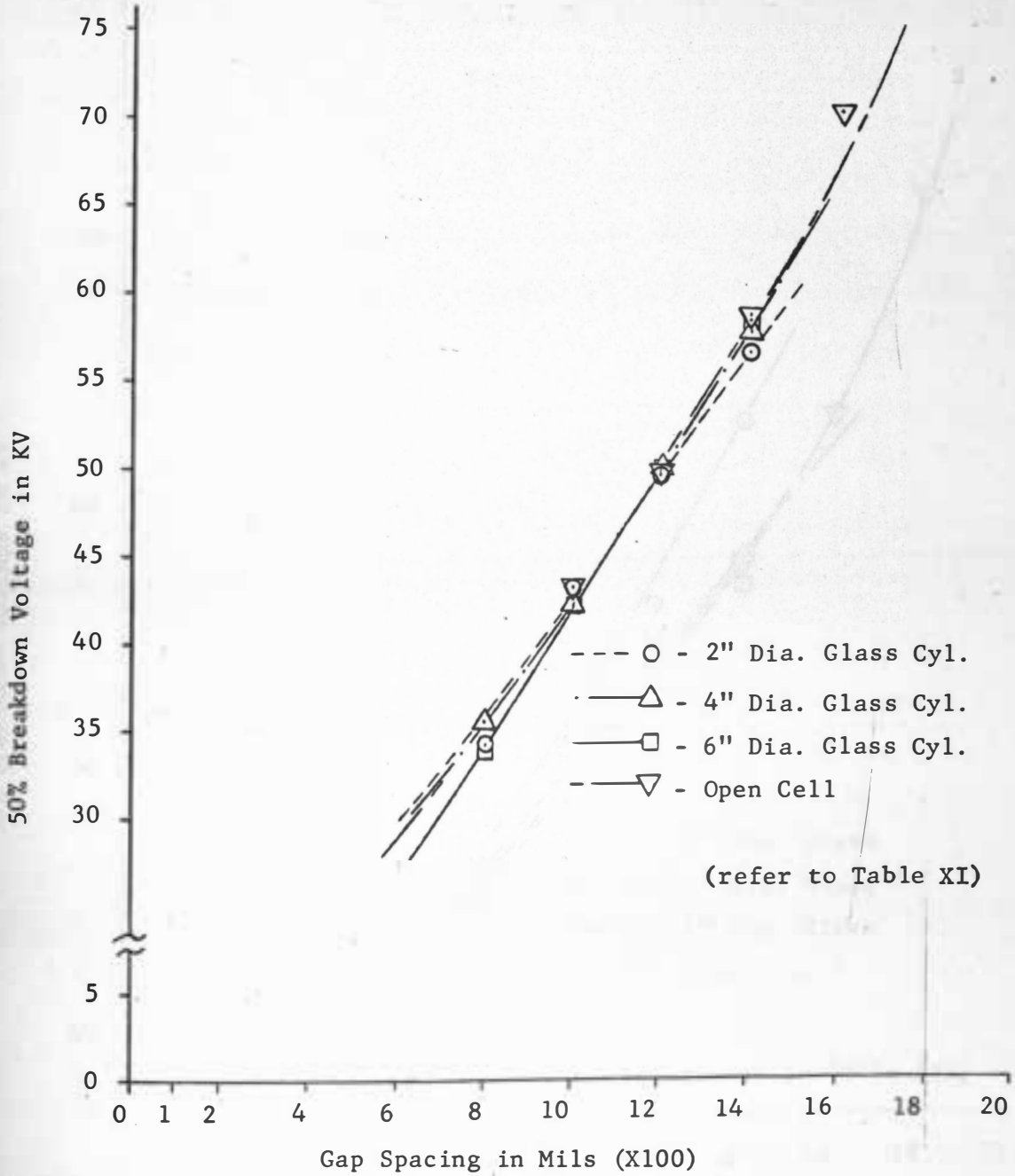

Fig. 30. 50% Breakdown Voltage in KV vs. Gap Spacing in Mils for Open Air With a 1½ x 40 μsec. Impulse Wave, Negative Polarity for a Point to Plane Electrode System.
Standard Conditions: 28.35 in Hg. and 80°F.

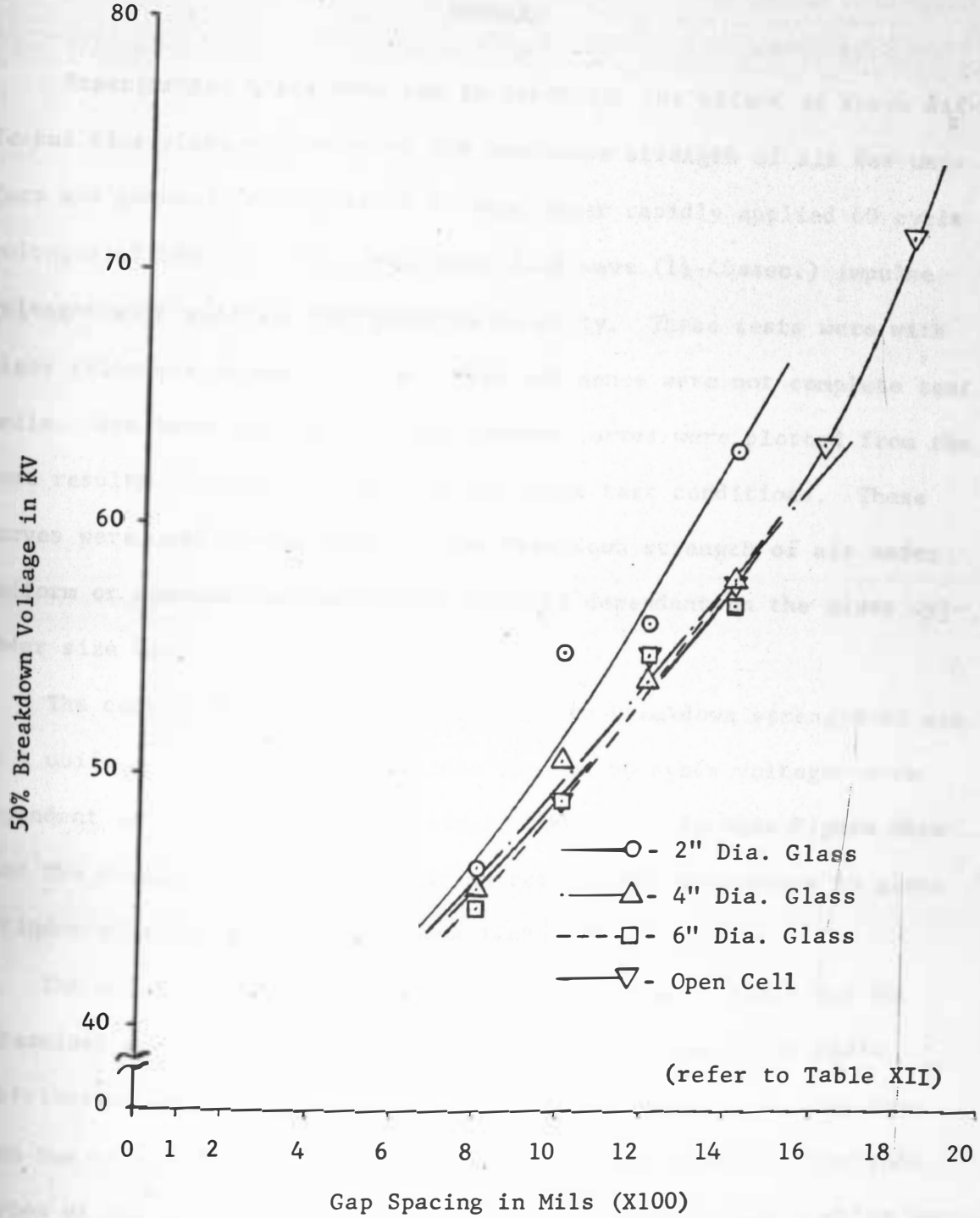

Fig. 31. 50% Breakdown Voltage in KV vs. Gap Spacing in Mils for Open Air With a 1½-40μsec. Impulse Wave, Negative Polarity for 1" Sphere to Plane Electrode System.
Standard Conditions: 28.35 in. Hg. and 80°F.

SUMMARY

Experimental tests were run to determine the effect of three different size glass cylinders on the breakdown strength of air for uniform and non-uniform electrode systems under rapidly applied 60 cycle voltages of 500 volts/sec. and under full wave (1½-40μsec.) impulse voltages with positive and negative polarity. These tests were with glass cylinders around the electrodes and hence were not complete test cells. Breakdown voltage vs. gap spacing curves were plotted from the test results obtained for each of the above test conditions. These curves were used to determine if the breakdown strength of air under uniform or non-uniform conditions would be dependent on the glass cylinder size used in test cells.

The curves in Figure 16 showed that the breakdown strength of air in a uniform field and under rapidly applied 60 cycle voltages were dependent on the glass cylinder size. The curves in this Figure show that the breakdown strength of air decreased with a decrease in glass cylinder size for gap spacing above 1000 mils.

The effect of the different size glass cylinders could not be determined from the test results obtained for a non-uniform field distribution under rapidly applied 60 cycle voltages, which may have been due to the erratic characteristic of a point to plane electrode system or due to some unknown, uncontrolled, outside effects which overwhelmed the effect of the glass cylinders. The only parameters that were considered and corrected for in these tests were the ambient temperature, pressure, and humidity.

For impulse tests with uniform and non-uniform field conditions, the effect of the different size glass cylinders on the breakdown of air were not as noticeable as compared to rapidly applied 60 cycle tests. The breakdown curves obtained under impulse tests were found not to have the same general trend as the breakdown curves obtained for the rapidly applied 60 cycle test under the same test conditions. This can be seen when the breakdown voltages of air for various gap spacings ranging from 100 to 1800 mils were compared with the results obtained from tests run with the different size glass cylinders centered about the open cell and from tests run with only the open cell for both uniform and non-uniform field conditions under impulse voltages and rapidly applied 60 cycle voltages.

The second series of tests that were run were the impulse test and rapidly applied 60 cycle test on the completely enclosed test cells with uniform and non-uniform electrode systems. All of the test cells had definitely different breakdown voltage curves for both tests with exception of the positive polarity impulse test with the point to plane electrode system. The author's intention of these experimental tests was to try to see if the variation in the breakdown curves were due to the effect of the glass cylinders. In order to reduce the number of breakdown influencing variables, the test cells were purged with dry air, since contamination was found to cause the breakdown voltages of air to change after a series of breakdowns. Dry air was used to eliminate any effect that may be due to the variation of vapor pressure throughout the tests. After considering all variable parameters, including ambient temperature and pressure, the results obtained for each test cell were compared and analyzed.

After comparing the results, it was found that the breakdown voltage curves obtained for the enclosed test cells, under the rapidly applied 60 cycle voltages and for the 1" sphere to plane electrodes, had the same general trend as the breakdown voltage curves obtained for just the glass cylinders centered about the open cell with the same test conditions. This was found not to be true for the same tests only with the point to plane electrode system. The author believed that there were some other outside effects causing the trouble, such as the clamps used with each test cell.

In order to eliminate any doubt that the clamps were causing some effect on the breakdown strength of air, an apparatus was designed by the author to hold the top plate and clamp of each test cell above the bottom plate and clamp; therefore, the glass cylinder could be removed. Tests were then run for both voltage sources and the results obtained show that the clamps used with each test cell do not have a significant effect to be even considered upon the breakdown of air for both uniform and non-uniform fields. For positive polarity impulse tests the breakdown voltage curves obtained for the enclosed test cells with the point to plane electrodes were approximately the same, but with the 1" sphere to plane electrodes the curves varied a great deal at the upper gap spacings. In fact the breakdown voltage increases so rapidly at the upper gap spacings in the 2" dia. and 4" dia. test cells that no data points could be obtained above 1000 and 1200 mils, respectively. The author believed that this rapid increase in breakdown voltage may have been due to the difference in gas volume contained by each cell, but further investigation would be required to prove this explanation.

In order to determine what sort of effect the different size glass cylinders could be expected with experimental results for the enclosed test cells, two dimensional field plots were drawn for each test cell and for the open cell with uniform and non-uniform electrode systems. These field plots, shown in Appendix II, show that the glass cylinders cause the flux lines to be refracted in toward the electrodes; therefore, increasing the field concentration around the electrodes. The amount of increase in field concentration around the electrodes is dependent upon the size of the glass cylinders. The smaller the glass cylinder diameter becomes the greater the increase in the field distribution about the electrodes and the lower the breakdown strength of the gas. This was experimentally verified only by the rapidly applied 60 cycle test for the uniform field or the 1" sphere to plane electrodes at the gap spacings above 1000 mils.

Since the experimental results and the field plots obtained in this thesis did not correspond under all test conditions, it would be ridiculous for one to select one test cell over another and to specify the range of gap spacing that should be used depending on the size of the cell without further investigation. The author would like to suggest from experience with these test cells that in general the 6" dia. test cell would be the most appropriate for obtaining the breakdown strength of various gases above a one inch gap spacing, since this test cell seems to be the least affected by its surrounding. But for gap spacings below one inch, the standard Seavy test cell (2" dia. cell) will in general give good results and would be more economical. The major factor in determining what size test cell and gap spacings should

be used is dependent upon the purpose of its application and to what accuracy the results are desired.

In general, the experimental tests made in this thesis were few in number. Therefore, the data is not sufficient for determining the magnitude of significance of various effects, but is nevertheless an important guide and gives some insight into what can be expected when testing the breakdown strength of gases.

LITERATURE CITED

1. M. L. Manning, "Gaseous Insulation: Its Importance and Need for Test Methods," ASTM Special Technical Publication No. 346, Alpha, N. J., (1963) pp. 3-20.

2. "Symposium On Electrical Insulating Gases," ASTM Special Technical Publication No. 346, Alpha, N. J., (December, 1963) pp. 67-85.

3. M. L. Manning, "Experience with the AIEE Subcommittee Test Cell for Gaseous Insulation," Paper 59-114, presented at AIEE Winter General Meeting, (February, 1959).

4. R. L. Ramey, Physical Electronics, Belmont, California: Wadsworth Publishing Company, (1962) pp. 193-243.

5. J. C. Devins and A. H. Sharbaugh, "The Fundamental Nature of Electrical Breakdown," Electro-Technology, (February, 1961) pp. 104-122.

6. L. B. Loeb, Fundamental Processes of Electrical Discharge of Gases, New York: John Wiley and Sons, Inc., (1939) pp. 408-432.

7. F. M. Penning, Electrical Discharges In Gases, New York: Macmillan Company, (1957) pp. 26-40.

8. H. Raether, Electron Avalanches and Breakdown in Gases, Washington: Butterworths, (1964) pp. 90-148.

9. J. R. Faillace and L. Robins, "The Rigorous Solution of a Field Problem by Means of the Card Programmed Calculator," Conference Paper No. 55-805, read at the AIEE Fall General Meeting, Chicago, Illinois, (1955).

10. Sunshine Scientific Instrument, Instructions Analog Field Plotter, Engineering Department, Instruction Manual 1M24-1.

11. J. D. Kraus, Electromagnetics, New York: McGraw-Hill Book Company, Inc., (1953) pp. 29-30, 52-56, 80-88, 128-138.

12. E. Weber, Electromagnetic Fields, New York: John Wiley and Sons, Inc., (1950).

13. J. P. Neal, Introduction To Electrical Engineering Theory, McGraw-Hill Book Company, Inc., (1960) pp. 154-166, 192-206.

14. C. A. Holt, Introduction to Electromagnetic Fields and Waves, New York: John Wiley and Sons, Inc., (1963).

15. Pyrex Brand Laboratory Glassware, Corning Glass Works, Corning, New York, (1963) LG-3 Catalog, p. 206.

16. K. E. Crouch, "The Effect of Wave Shape on the Electrical Breakdown of Nitrogen Gas," South Dakota State University, Brookings, South Dakota, Thesis, (June, 1966).

17. F. H. Kreuger, Discharge Detection in High Voltage Equipment, New York: American Elsevier Publishing Company, Inc., (1965) pp. 1-46.

18. American Standard for Measurement of Voltage in Dielectric Tests, AIEE Standard 4, A.S.A., c68.1, (1953).

19. J. L. Threlkeld, Thermal Environmental Engineering, Englewood Cliffs, New Jersey: Prentice-Hall, Inc., (1962) pp. 163-168, 464-471.

20. M. Mason and W. Weaver, The Electromagnetic Field, New York: Dover Publications, Inc., (1929) pp. 116-121.

21. W. H. Hayt, Jr., Engineering Electromagnetics, New York: McGraw-Hill Book Company, Inc., (1958) pp. 49-53, 110-112, 123-126, 142-154, 133-138.

22. L. V. Bewley, Two Dimensional Fields in Electrical Engineering, New York: Dover Publications, Inc., (1963) pp. 167-172, 196-200.

23. L. B. Loeb and J. M. Meek, The Mechanism of the Electric Spark, Stanford: University Press, (1941) pp. 34-107.

24. J. M. Meek and J. D. Craggs, Electrical Breakdown of Gases, London: Oxford University Press, (1953) pp. 282-288.

25. F. Liewellyn-Jones, Ionization and Breakdown in Gases, New York: John Wiley and Sons, (1957) pp. 80-82.

26. Tentative Method of Test for Dielectric Breakdown Voltage and Dielectric Strength of Insulating Gases at Commercial Power Frequencies, ASTM Standard Group Method D-27.

27. A. Pedersen, Janos Lebeda, and Svend Vibholm, "Analysis of Spark Breakdown Characteristics for Sphere Gaps," IEEE Transactions on Power Apparatus and Systems, Vol., PAS-86, No. 8 (August, 1967) pp. 975-978.

28. T. A. Phillips, L. M. Robertson, A. F. Rohlfs, and R. L. Thompson, "Influence of Air Density on Electrical Strength of Transmission Line Insulation," IEEE Transactions on Power Apparatus and Systems, Vol., PAS-86, No. 8, (August, 1967) pp. 948-961.

29. C. M. Foust, H. P. Kuehni, and N. Rohats, "Impulse Testing Technique," General Electric Review, Vol. 35, No. 7, (July, 1932)

30. Proposed Guide for Transformer Impulse Test, AIEE Standard 93, (December, 1962).

31. L. C. Whitman, "Impulse Voltage Tests on Air and C_3F_8," IEEE Transactions on Electrical Insulation, Vol. EI-1, No. 2, (November, 1965).

32. C. N. Works and D. Berg, "Portable 125 KV Impulse Generator," Insulation, Vol. 8, No. 12, (November, 1962) pp. 41-45.

33. Yarlagadda Radha Drishna Rao, "Some Electrical Characteristics of C_3F_8 and Air with Various Electrode Systems," South Dakota State University, Brookings, South Dakota, Thesis, (December, 1961).

34. C. M. Foust and P. H. McAuley, "Recommendations for High Voltage Testing," Paper No. 40-38, presented at AIEE Winter Convention, (January, 1940).

35. Report of Committee D-27 on Electrical Insulating Liquids and Gases presented at Annual Meeting of AMTM, (June-July, 1966).

36. H. K. Farr and W. A. Keen, Jr., "Improving Field Analogues Through Conformal Mapping," Transactions Paper, Paper No. 55-105, presented at the AIEE Winter General Meeting, (February, 1955).

APPENDIX ONE

TABLE I

Comparison of Rapidly Applied 60 Cycle Breakdown Strength of Open Air at Various Gap Spacings With a 1" Sphere to Plane Electrode System in the Open Cell and With Different Size Glass Cylinders Centered About the Open Cell. (refer to Fig. 16)
Standard Conditions: 28.35 in. of Hg. and 80°F.

Gap Spacing (mils)	Rapidly Applied 60 Cycle Breakdown Voltages				Percent Deviation From Reference Curve (Open Cell)			Maximum Deviation from the Mean.
	Open Cell (KV)	6" Dia. Glass (KV)	4" Dia. Glass (KV)	2" Dia. Glass (KV)	6" Dia. Glass (%)	4" Dia. Glass (%)	2" Dia. Glass (%)	(%)
100	6.8	6.8	6.8	6.8	0.00	0.00	0.00	0.00
200	11.7	11.7	11.7	11.7	0.00	0.00	0.00	0.00
400	18.8	19.2	19.5	18.8	+2.12	+3.72	0.00	2.09
600	24.1	24.4	24.9	23.7	+1.24	+3.32	-1.65	2.46
800	28.3	28.3	28.6	27.6	0.00	+1.06	-2.47	2.13
1000	31.6	31.4	31.3	30.2	-0.63	-0.95	-4.43	2.89
1200	34.1	34.1	33.5	32.2	0.00	-1.75	-5.57	3.88
1400	36.2	35.8	35.2	33.8	-1.10	-2.76	-6.63	3.97
1600	37.8	37.5	36.6	35.1	-0.79	-3.17	-7.14	4.35
1800	39.3	38.7	37.8	36.2	-1.52	-3.81	-7.88	4.73

TABLE II

Comparison of Rapidly Applied 60 Cycle Breakdown Strength of Open Air at Various Gap Spacings With a Point to Plane Electrode System in the Open Cell and With Different Size Glass Cylinders Centered About the Open Cell. (refer to Fig. 17)
Standard Conditions: 28.35 in. of Hg. and 80°F.

Gap Spacing (mils)	Rapidly Applied 60 Cycle Breakdown Voltages				Percent Deviation From Reference Curve (Open Cell)			Maximum Deviation from the Mean.
	Open Cell (KV)	6" Dia. Cell (KV)	4" Dia. Cell (KV)	2" Dia. Cell (KV)	6" Dia. Cell (%)	4" Dia. Cell (%)	2" Dia. Cell (%)	(%)
100	3.5	3.7	3.7	3.6	+5.7	+5.7	+2.86	2.77
200	5.5	6/0	6.0	5.9	+9.09	+9.09	+7.27	5.17
400	8.7	9.5	9.5	9.3	+9.19	+9.19	+6.89	5.43
600	11.7	12.6	12.6	12.2	+7.69	+7.69	+4.27	4.88
800	14.9	15.3	16.1	14.7	+2.68	+8.05	-1.34	5.92
1000	18.2	18.0	19.7	17.7	-1.09	+8.24	-2.74	7.06
1200	21.7	21.4	22.7	20.8	-1.38	+4.60	-4.15	5.09
1400	25.4	25.4	24.4	23.8	0.00	-3.93	-6.30	3.64
1600	29.4	30.2	26.5	26.7	+2.72	-9.86	-9.18	7.09
1800	33.6	35.9	27.5	29.3	+6.84	-18.15	-12.80	13.61

TABLE III

Comparison of Rapidly Applied 60 Cycle Breakdown Strength of Air at Various Gap Spacings With a 1" Sphere to Plane Electrode System in the Open Cell and The Test Cells Without the Glass Cylinders. (refer to Fig. 18)
Standard Conditions: 28.35 in. of Hg. and 80°F.

Gap Spacing (mils)	Rapidly Applied 60 Cycle Breakdown Voltages				Percent Deviation From Reference Curve (Open Cell)			Maximum Deviation from the Mean.
	Open Cell (KV)	6" Dia. Cell (KV)	4" Dia. Cell (KV)	2" Dia. Cell (KV)	6" Dia. Cell (%)	4" Dia. Cell (%)	2" Dia. Cell (%)	(%)
100	6.7	6.7	6.7	6.7	0.00	0.00	0.00	0.00
200	11.5	11.5	11.5	11.5	0.00	0.00	0.00	0.00
400	19.1	19.1	19.1	19.1	0.00	0.00	0.00	0.00
600	24.6	24.2	24.2	24.2	-1.62	-1.62	-1.62	1.23
800	28.8	28.1	28.1	28.1	-2.43	-2.43	-2.43	1.76
1000	31.8	31.2	31.2	31.2	-1.88	-1.88	-1.88	1.59
1200	35.3	34.1	34.1	34.1	-3.39	-3.39	-3.39	2.61
1400	36.6	36.4	36.4	36.4	-0.54	-0.54	-0.54	0.54
1600	39.5	39.7	39.7	39.7	+0.50	+0.50	+0.50	0.25
1800	39.9	40.8	40.8	40.8	+2.25	+2.25	+2.25	1.72

TABLE IV

Comparison of Rapidly Applied 60 Cycle Breakdown Strength of Open Air at Various Gap Spacings With a Point to Plane Electrode System in the Open Cell and the Test Cells Without the Glass Cylinders. (refer to Fig. 19)
Standard Conditions: 28.35 in. of Hg. and 80°F.

Gap Spacing (mils)	Rapidly Applied 60 Cycle Breakdown Voltages				Percent Deviation From Reference Curve (Open Cell)			Maximum Deviation from the Mean.
	Open Cell (KV)	6" Dia. Cell (KV)	4" Dia. Cell (KV)	2" Dia. Cell (KV)	6" Dia. Cell (%)	4" Dia. Cell (%)	2" Dia. Cell (%)	(%)
100	3.5	3.5	3.5	3.5	0.00	0.00	0.00	0.00
200	5.6	5.8	5.8	5.8	+3.57	+3.57	+3.57	2.61
400	8.6	9.3	9.3	9.3	+8.14	+8.14	+8.14	5.81
600	11.6	12.3	12.3	12.3	+6.03	+6.03	+6.03	4.29
800	14.7	15.3	15.3	15.3	+4.08	+4.08	+4.08	2.97
1000	18.0	18.3	19.3	19.2	+1.66	+7.22	+6.66	3.74
1200	21.7	21.7	24.1	23.3	0.00	+11.05	+7.37	6.16
1400	25.6	25.5	28.2	27.2	-0.39	+10.15	+6.25	6.02
1600	29.7	29.5	31.5	30.7	-0.67	+6.06	+3.36	3.96
1800	33.8	33.8	34.1	33.5	0.00	+0.88	-0.88	0.88

TABLE V

Comparison of the 50% Impulse Breakdown Voltages for Open Air For Various Gap Spacings With a 1" Sphere to Plane Electrode System in the Open Cell and With Different Size Glass Cylinders Centered about the Open Cell. Positive Polarity, 1½-40μsec. Wave. Standard Conditions: 28.35 in. of Hg. and 80°F. (refer to Fig. 24)

Gap Spacings	50% Impulse Breakdown Voltages				Percent Deviation From Reference Curve (Open Cell)			Maximum Deviation from the Mean.
	Open Cell	6" Dia. Glass	4" Dia. Glass	2" Dia. Glass	6" Dia. Glass	4" Dia. Glass	2" Dia. Glass	
(mils)	(KV)	(KV)	(KV)	(KV)	(%)	(%)	(%)	(%)
100	5.5	5.5	5.5	5.5	0.00	0.00	0.00	0.00
200	12.5	12.5	12.5	12.5	0.00	0.00	0.00	0.00
400	24.2	24.2	24.2	24.2	0.00	0.00	0.00	0.00
600	32.5	32.1	31.8	32.5	-1.23	-2.15	0.00	1.24
800	38.0	38.1	36.8	38.0	+0.26	-3.16	0.00	2.39
1000	41.8	43.2	40.8	41.8	+3.35	-2.39	0.00	3.10
1200	45.5	47.7	44.3	45.5	+4.83	-2.64	0.00	4.38
1400	49.0	51.8	47.4	49.0	+5.71	-3.26	0.00	5.07
1600	52.2	55.5	50.2	52.2	+6.32	-3.83	0.00	5.71
1800	55.2	59.0	52.7	55.2	+6.88	-4.53	0.00	6.31

TABLE VI

Comparison of 50% Impulse Breakdown Voltages for Open Air for Various Gap Spacings With a Point to Plane Electrode System in the Open Cell and With Different Size Glass Cylinders Centered About the Open Cell. Positive Polarity, 1½-40 μ sec. Wave. Standard Conditions: 28.35 in. of Hg. and 80°F. (refer to Fig. 25)

Gap Spacings (mils)	50% Impulse Breakdown Voltages				Percent Deviation From Reference Curve (Open Cell)			Maximum Deviation from the Mean.
	Open Cell (KV)	6" Dia. Glass (KV)	4" Dia. Glass (KV)	2" Dia. Glass (KV)	6" Dia. Glass (%)	4" Dia. Glass (%)	2" Dia. Glass (%)	(%)
200	2.1	2.1	2.1	2.1	0.00	0.00	0.00	0.00
400	14.4	14.4	14.4	14.4	0.00	0.00	0.00	0.00
600	20.4	20.4	21.8	21.0	0.00	+6.86	+2.94	3.83
800	24.2	24.2	26.1	25.2	0.00	+6.85	+4.13	4.82
1000	27.0	26.7	28.6	28.3	-1.11	+5.92	+4.81	3.62
1200	29.4	29.2	30.9	30.7	-0.68	+5.10	+5.00	3.00
1400	31.5	31.3	32.8	32.8	-0.63	+4.13	+4.13	2.49
1600	33.4	33.5	34.6	34.6	+0.29	+3.59	+3.59	1.76
1800	35.1	35.5	36.2	36.3	+1.14	+3.13	+3.42	1.99

TABLE VII

Comparison of 50% Impulse Breakdown Voltage in KV for Open Air at Various Gap Spacings for a 1" Sphere to Plane Electrode System in the Test Cells Without the Glass Cylinders. Positive Polarity, 1½ x 40 μsec. Wave. (refer to Fig. 26)
Standard Conditions: 28.35 in. of Hg. and 80°F.

Gap Spacings mils)	50% Impulse Breakdown Voltages				Percent Deviation From Reference Curve (Open Cell)			Maximum Deviation from the Mean.
	Open Cell (KV)	6" Dia. Cell* (KV)	4" Dia. Cell* (KV)	2" Dia. Cell* (KV)	6" Dia. Cell* (%)	4" Dia. Cell* (%)	2" Dia. Cell* (%)	(%)
1200	45.4	44.5	43.4	44.5	-1.98	-4.40	-1.98	2.25
1400	48.8	48.0	46.5	48.0	-1.64	-4.71	-1.98	2.71
1600	51.8	51.7	49.4	51.1	-0.19	-4.63	-1.35	1.57
1800	54.6	55.3	52.4	54.0	+1.28	-4.03	-1.10	3.14

*(No Glass)

TABLE VIII

Comparison of 50% Impulse Breakdown Voltage of Open Air For Various Gap Spacings With a Point to Plane Electrode System in the Open Cell and in Different Size Test Cells Without the Glass Cylinders. Positive Polarity, 1½-40 μsec. Wave. Standard Conditions: 28.35 in. of Hg. and 80°F. (refer to Fig. 27)

Gap Spacings (mils)	Impulse Breakdown Voltages				Percent Deviation From Reference Curve (Open Cell)			Maximum Deviation from the Mean.
	Open Cell (KV)	6" Dia. Cell* (KV)	4" Dia. Cell* (KV)	2" Dia. Cell* (KV)	6" Dia. Cell* (%)	4" Dia. Cell* (%)	2" Dia. Cell* (%)	(%)
1200	28.2	29.3	28.5	30.0	+3.90	+1.06	+5.00	3.45
1400	31.0	31.7	31.0	32.3	+2.26	0.00	+4.19	2.53
1600	33.5	34.1	32.3	34.4	+1.79	-3.58	+2.68	3.87
1800	35.4	36.0	35.2	36.2	+1.69	-0.56	+2.26	1.40

*(No Glass)

TABLE IX

Comparison of 50% Breakdown Voltage (Impulse, Positive Polarity 1½-40 μsec. Wave) for Dry Air at Various Gap Spacings With a 1" Sphere to Plane Electrode System in Different Test Cells. Standard Conditions: 28.35 in. of Hg. and 80°F. Changing Air in Cells for Every Breakdown. (refer to Fig. 28)

Gap Spacings (mils)	50% Impulse Breakdown Voltages			Mean Value (KV)	Maximum Deviation from the Mean. (%)
	6" Dia. Cell (KV)	4" Dia. Cell (KV)	2" Dia. Cell (KV)		
100	12.2	12.2	12.2	12.2	0.00
200	17.8	17.4	17.8	17.6	1.13
400	26.5	26.5	27.4	26.8	2.24
600	33.7	34.0	35.6	34.4	3.49
800	39.7	40.1	42.1	40.6	3.69
1000	44.2	45.1	47.1	45.5	3.52
1200	48.1	48.7	unattainable	unattain-able	----
1400	52.9	unattain-able	unattain-able	----	----
1600	58.0	unattain-able	unattain-able	----	----
1800	64.8	unattain-able	unattain-able	----	----

TABLE X

Comparison of 50% Breakdown Voltage (Impulse, Positive Polarity 1½-40μsec. Wave) for Dry Air at Various Gap Spacings With a Point to Plane Electrode System in Different Test Cells. Standard Conditions: 28.35 in. of Hg. and 80°F. Changing Air in Cells After Every Breakdown. (refer to Fig. 29)

Gap Spacings (mils)	50% Impulse Breakdown Voltages			Mean Value (KV)	Maximum Deviation from the Mean. (%)
	6" Dia. Cell (KV)	4" Dia. Cell (KV)	2" Dia. Cell (KV)		
200	1.5	1.5	1.5	1.5	0.00
400	11.2	11.2	11.2	11.2	0.00
600	20.3	20.3	20.3	20.3	0.00
800	26.7	26.7	26.3	26.5	0.75
1000	30.3	30.3	29.9	30.1	0.66
1200	32.6	32.7	32.2	32.5	0.92
1400	34.2	34.6	33.8	34.2	1.17
1600	35.5	36.1	35.1	35.5	1.69
1800	36.5	37.4	36.1	36.7	1.91

TABLE XI

Comparison of 50% Impulse Breakdown Voltage of Open Air for Various Gap Spacings With a Point to Plane Electrode System in the Open Cell and With Different Size Glass Cylinders Centered About the Open Cell. Negative Polarity, 1½-40 μsec. Wave. (refer to Fig. 30) Standard Conditions: 28.35 in. of Hg. and 80°F.

Gap Spacings	Impulse Breakdown Voltages				Percent Deviation From Reference Curve (Open Cell)			Maximum Deviation From The Mean.
	Open Cell	6" Dia. Glass	4" Dia. Glass	2" Dia. Glass	6" Dia. Glass	4" Dia. Glass	2" Dia. Glass	
(mils)	(KV)	(KV)	(KV)	(KV)	(%)	(%)	(%)	(%)
800	36.1	33.9	35.5	35.5	-5.01	-1.66	-1.66	3.69
1000	42.5	42.1	42.3	42.3	-0.94	-0.47	-0.47	0.47
1200	50.0	50.2	50.0	49.9	+0.40	0.00	-0.20	0.40
1400	58.1	58.7	58.0	56.7	+1.03	-0.17	-2.40	2.07

TABLE XII

Comparison of 50% Impulse Breakdown Voltage of Open Air For Various Gap Spacings With a 1" Sphere to Plane Electrode System in the Open Cell and With Different Size Glass Cylinders centered about the Open Cell. Negative Polarity, 1½-40 μsec. Wave. Standard Conditions: 28.35 in. of Hg. and 80°F. (refer to Fig. 31)

Gap Spacings (mils)	Impulse Breakdown Voltages				Percent Deviation From Reference Curve (Open Cell)			Maximum Deviation from the Mean.
	Open Cell (KV)	6" Dia. Glass (KV)	4" Dia. Glass (KV)	2" Dia. Glass (KV)	6" Dia. Glass (%)	4" Dia. Glass (%)	2" Dia. Glass (%)	(%)
800	45.5	44.9	45.8	46.7	-1.31	+0.66	+2.63	2.19
1000	49.2	49.0	49.7	51.6	-0.41	+1.02	+4.88	3.41
1200	53.2	53.3	53.8	57.2	+0.19	+1.13	+7.52	5.15
1400	57.8	58.1	57.9	63.2	+0.52	+0.17	+9.34	6.75

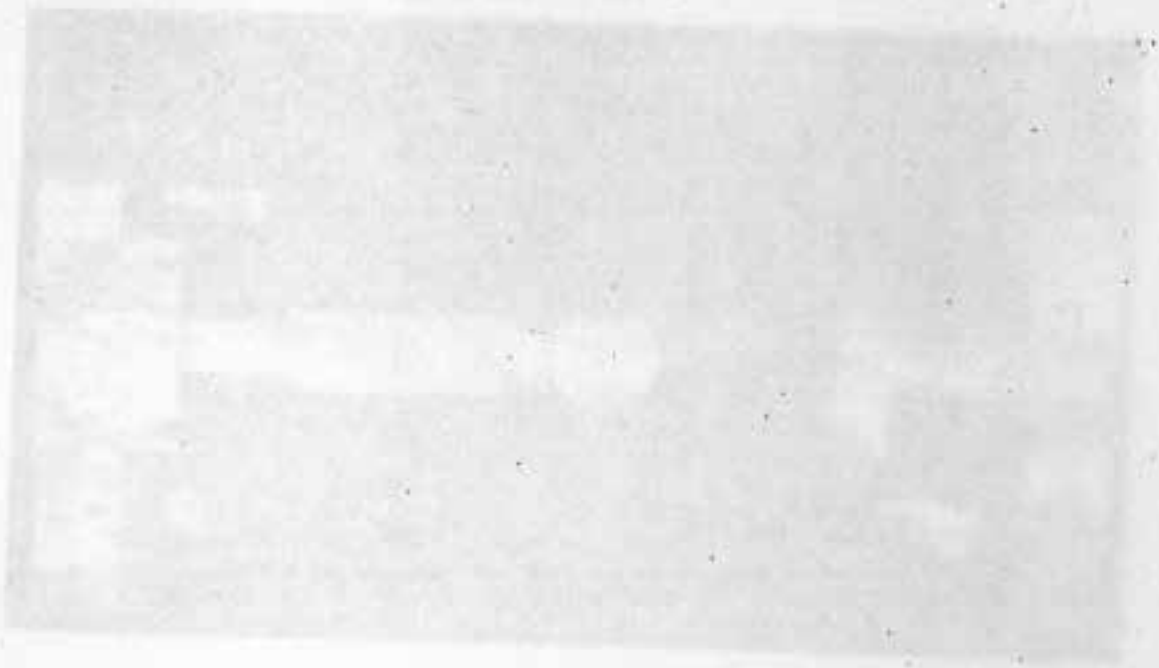

APPENDIX TWO

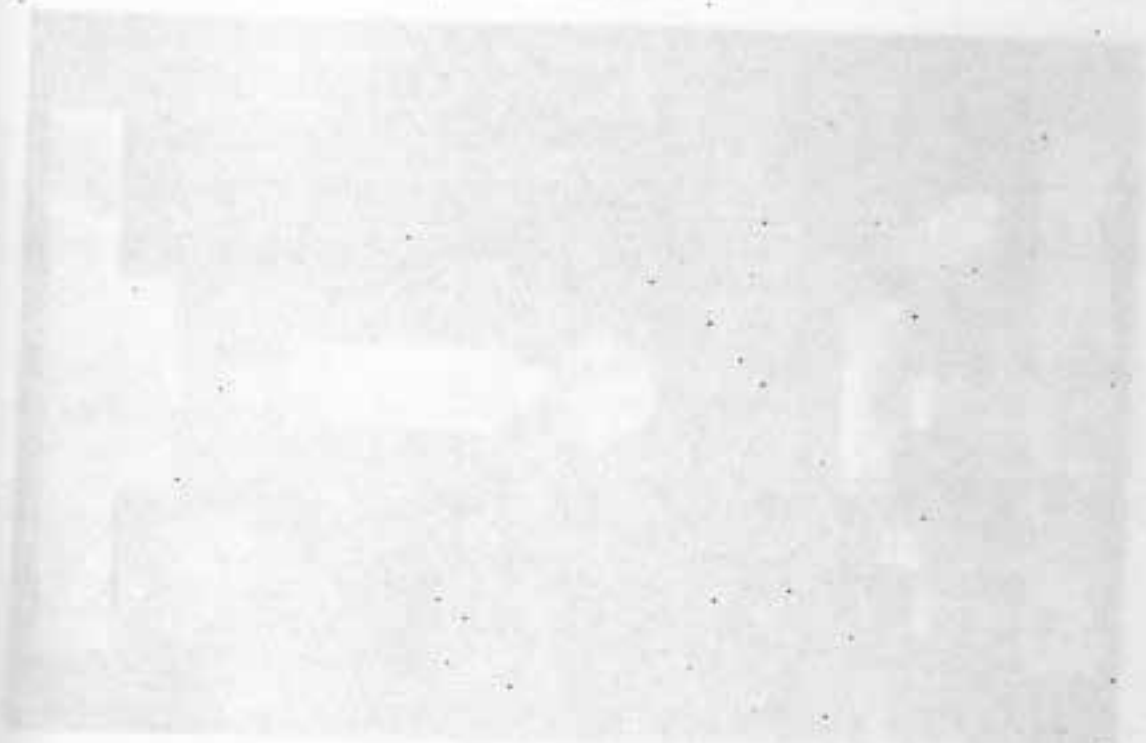

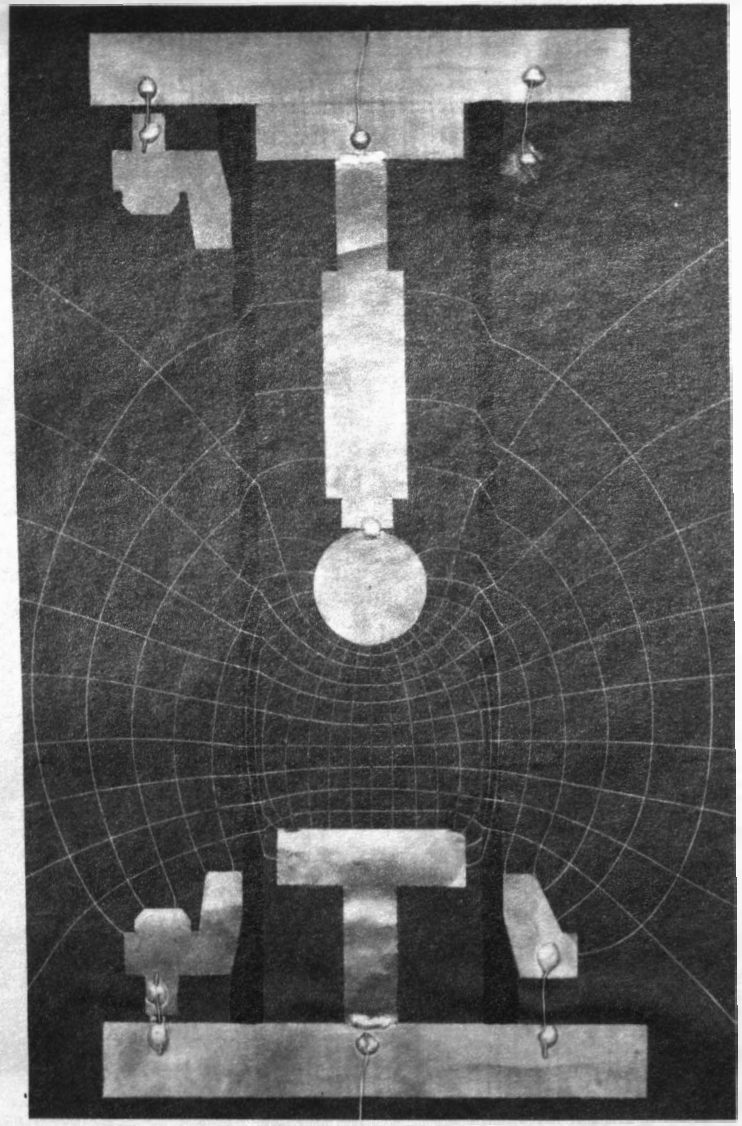

Fig. 33. Two inch diameter test cell with the glass cylinder.

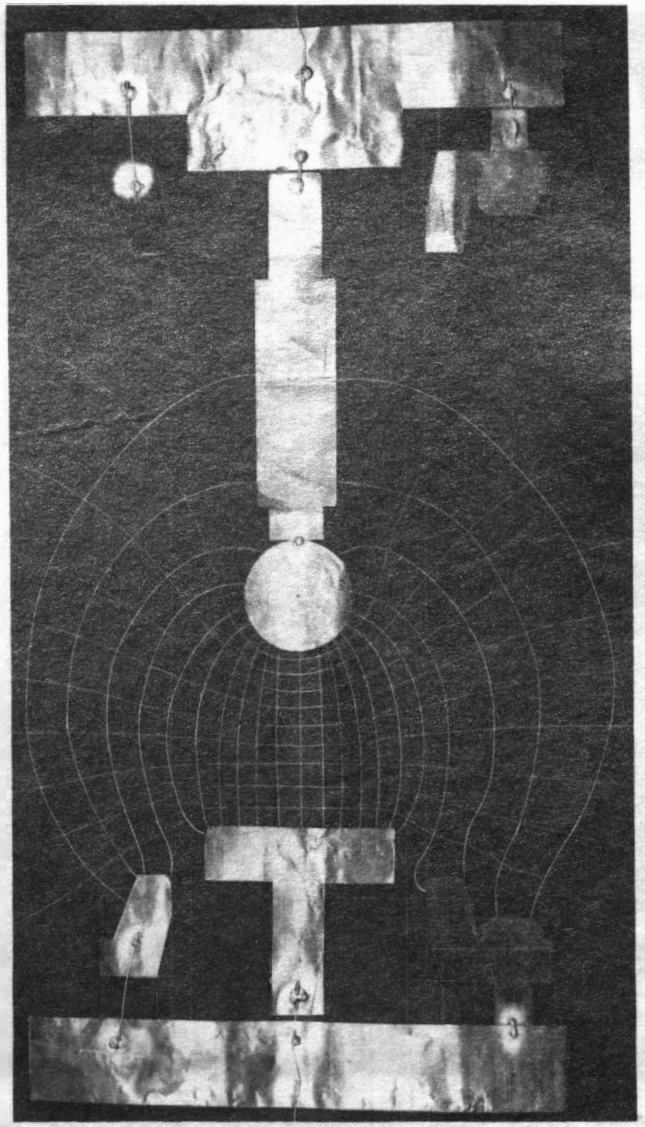

Fig. 32. Two inch diameter test cell without the glass cylinder.

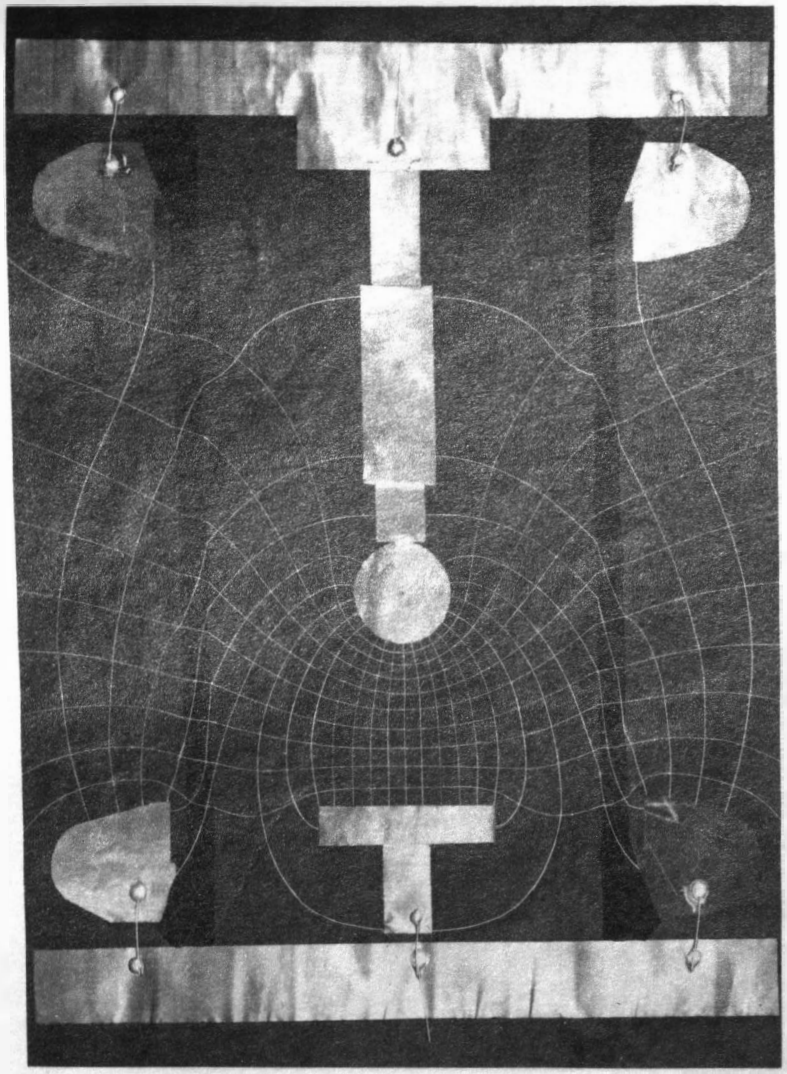

Fig. 35. Four inch diameter test cell with the glass cylinder.

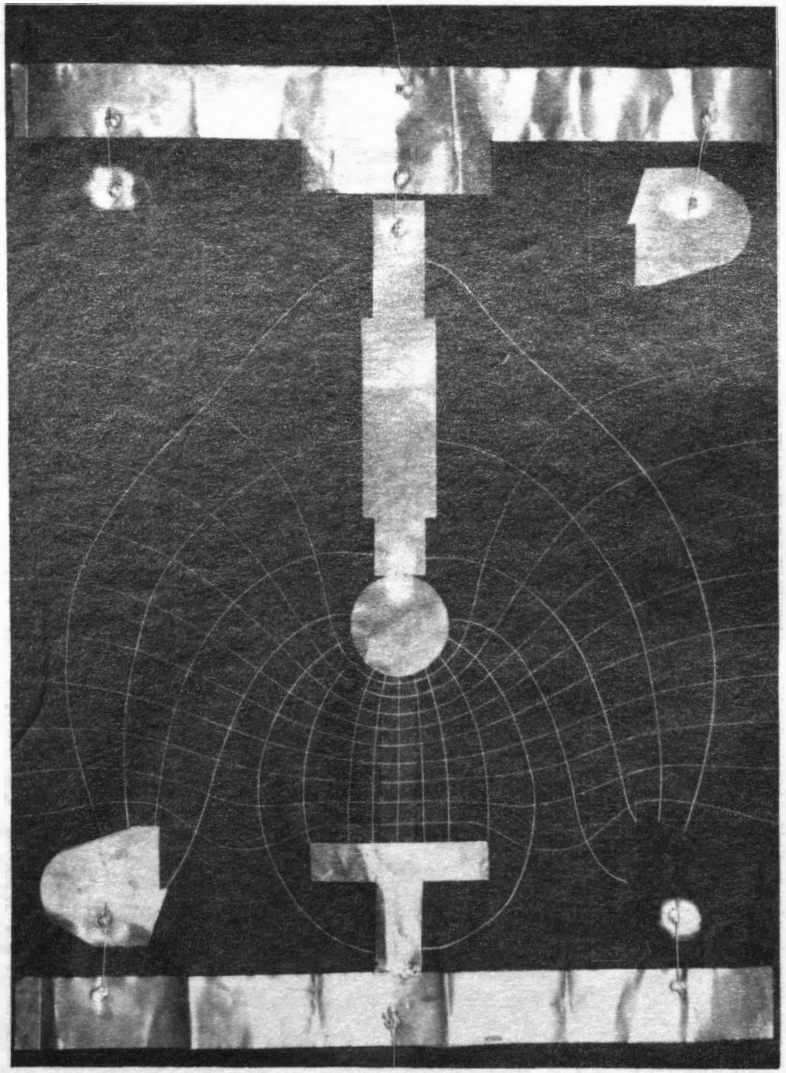

Fig. 34. Four inch diameter test cell without the glass cylinder.

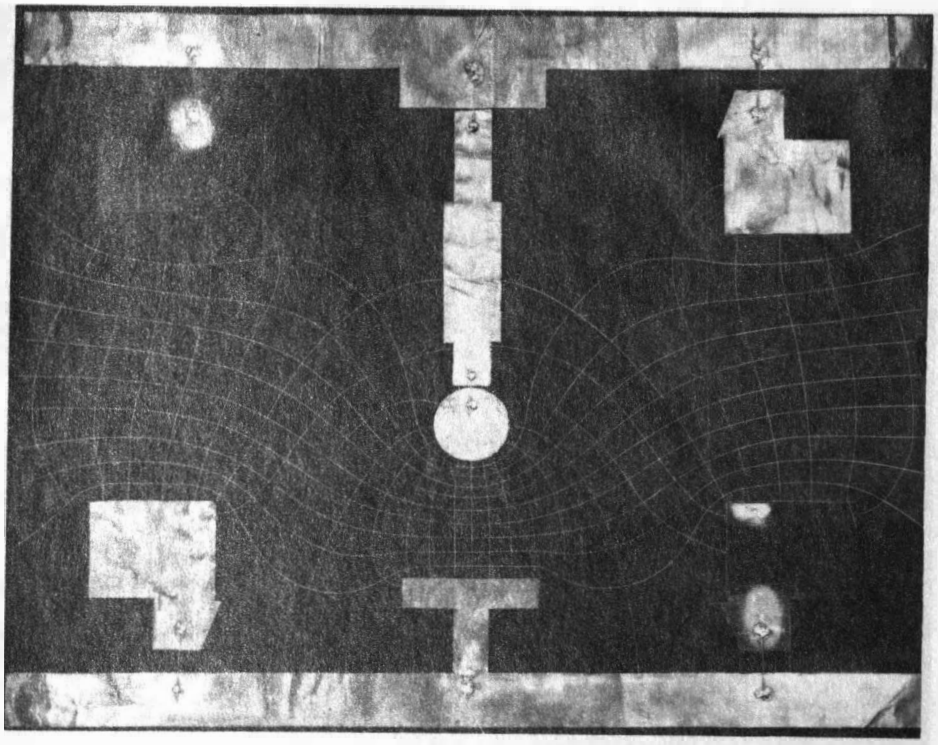

Fig. 36. Six inch diameter test cell without the glass cylinder.

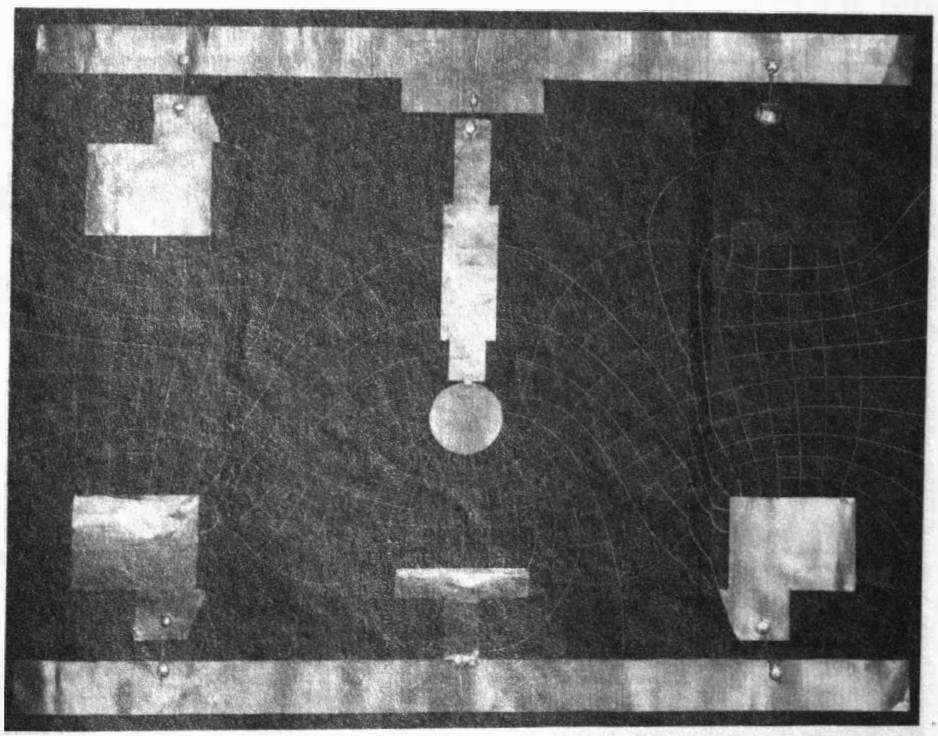

Fig. 37. Six inch diameter test cell with the glass cylinder.

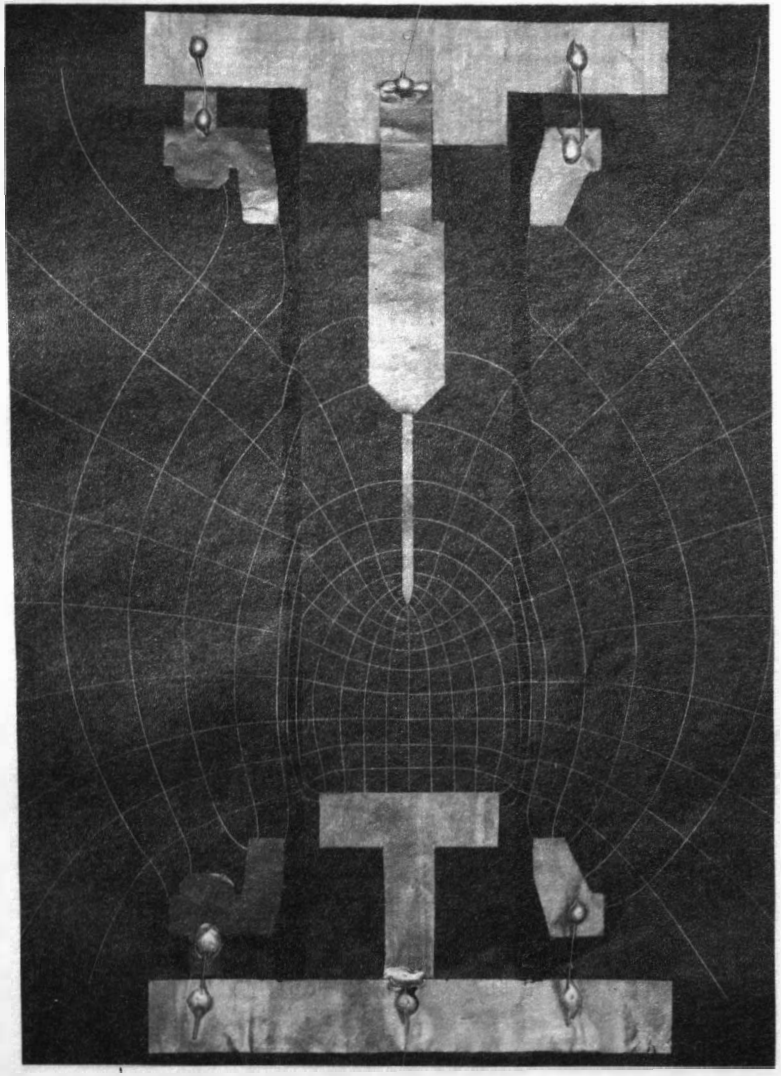

Fig. 39. Two inch diameter test cell with the glass cylinder.

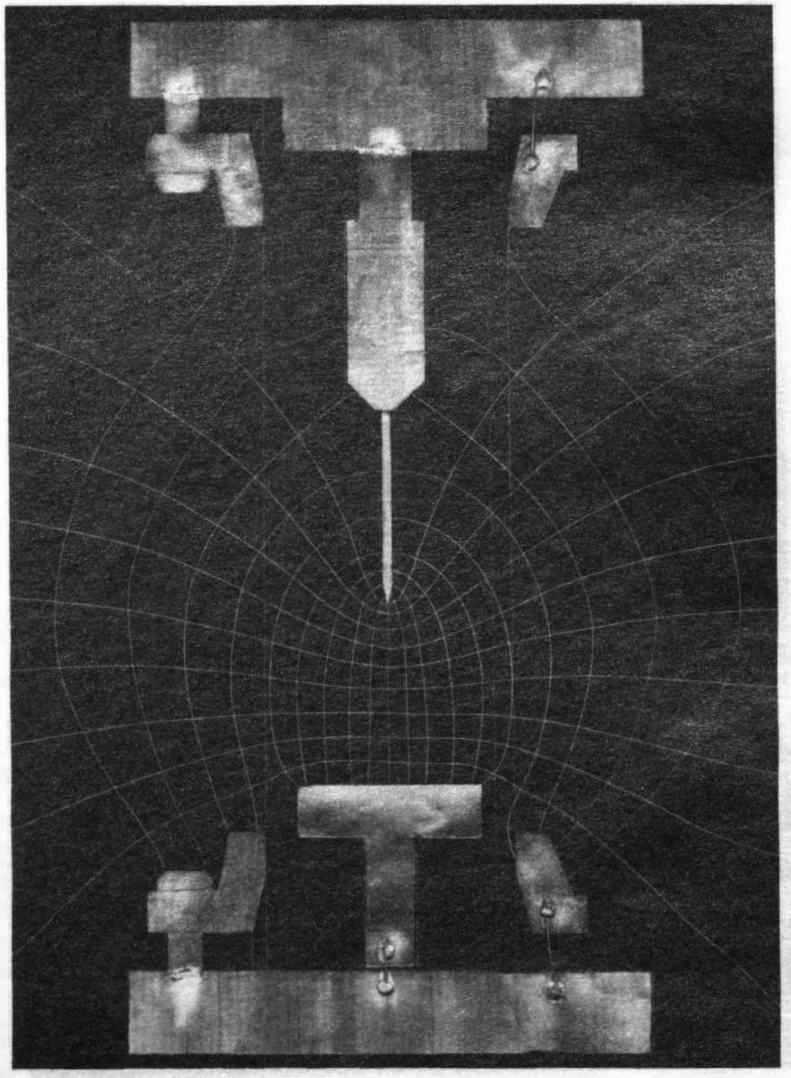

Fig. 38. Two inch diameter test cell without the glass cylinder.

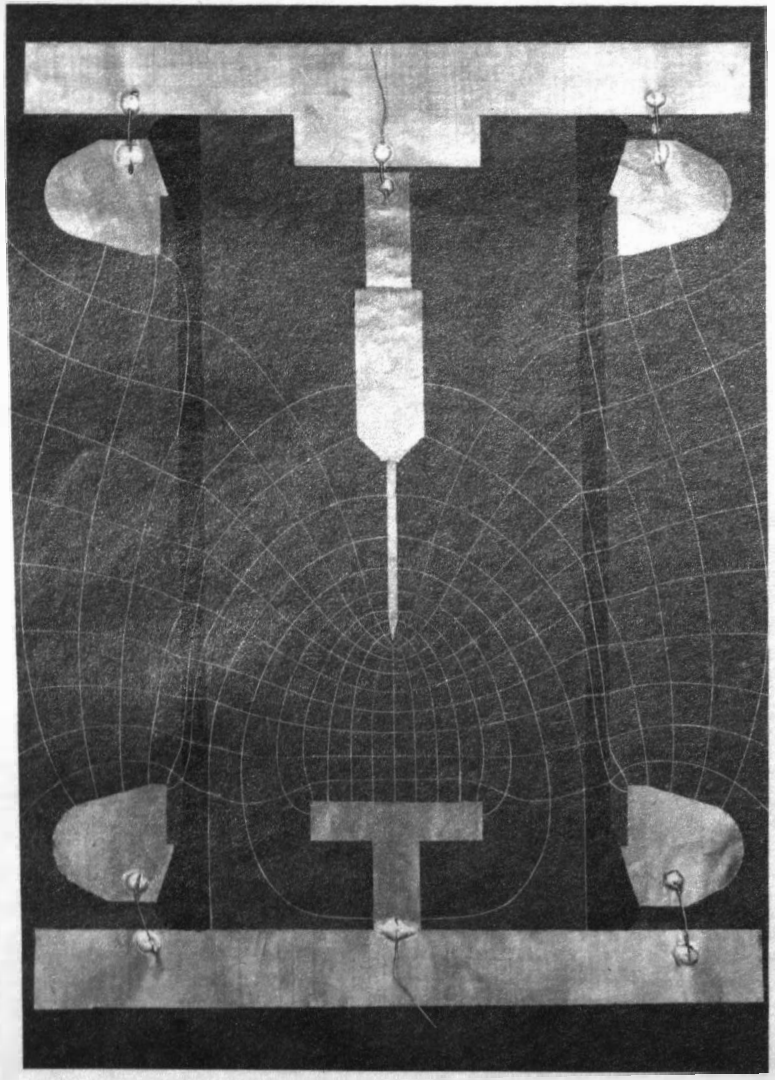

Fig. 41. Four inch diameter test cell with the glass cylinder.

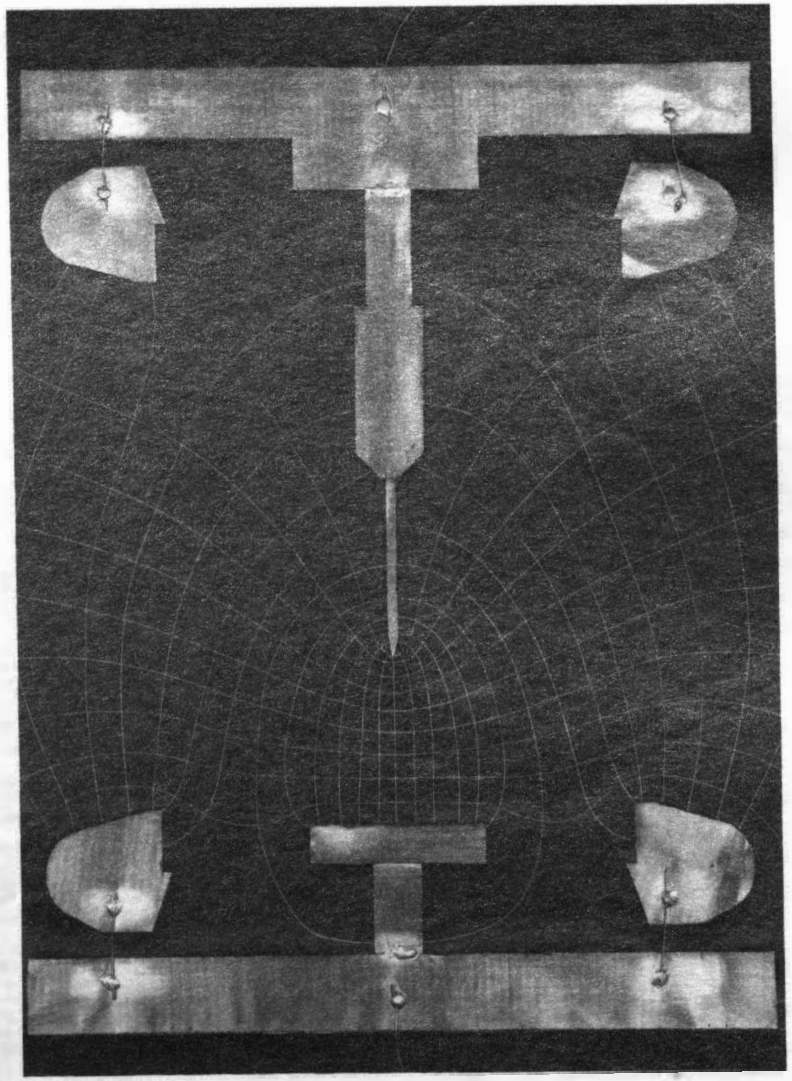

Fig. 40. Four inch diameter test cell without the glass cylinder.

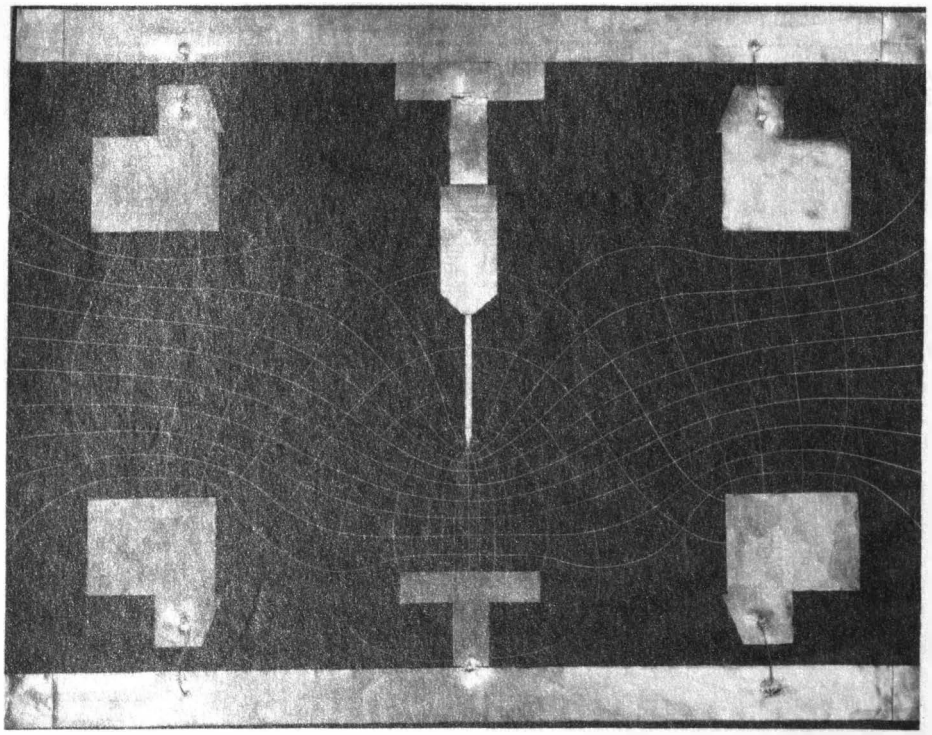

Fig. 42. Six inch diameter test cell without the glass cylinder.

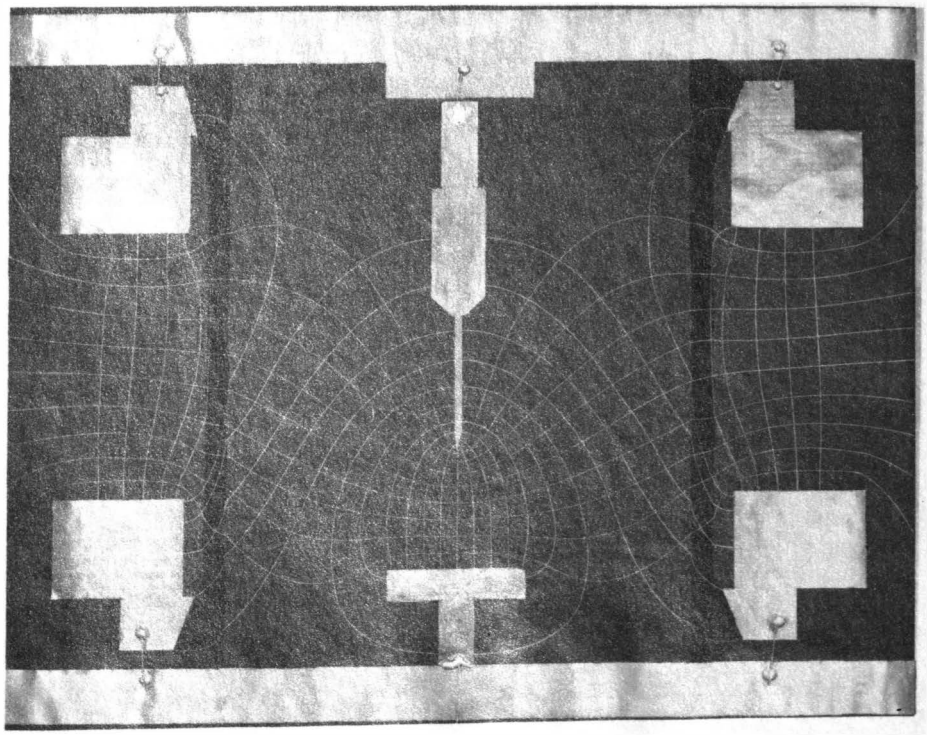

Fig. 43. Six inch diameter test cell with the glass cylinder.

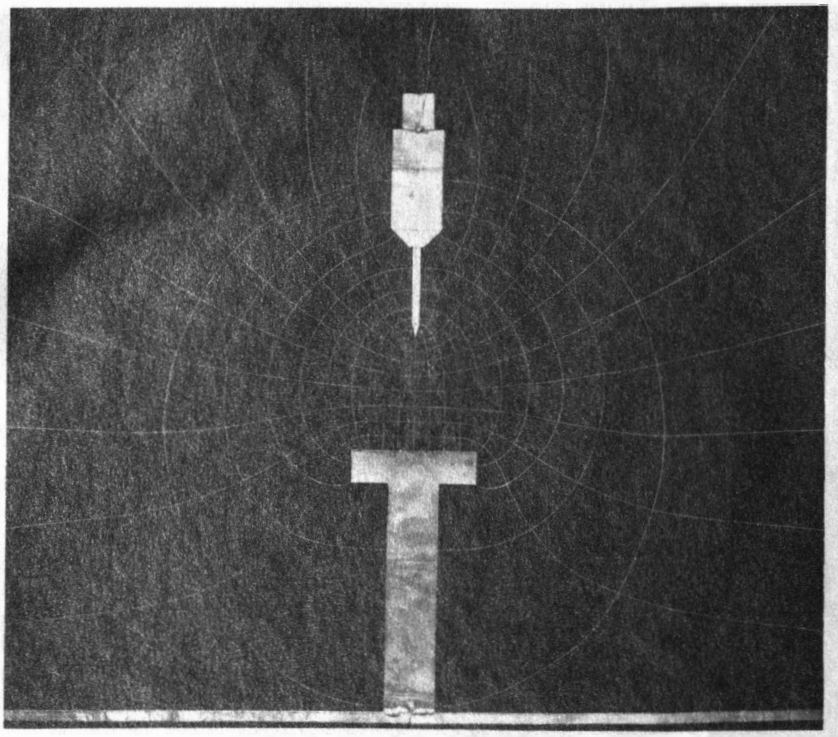

Fig. 44. Field plot of open cell with point to plane electrodes.

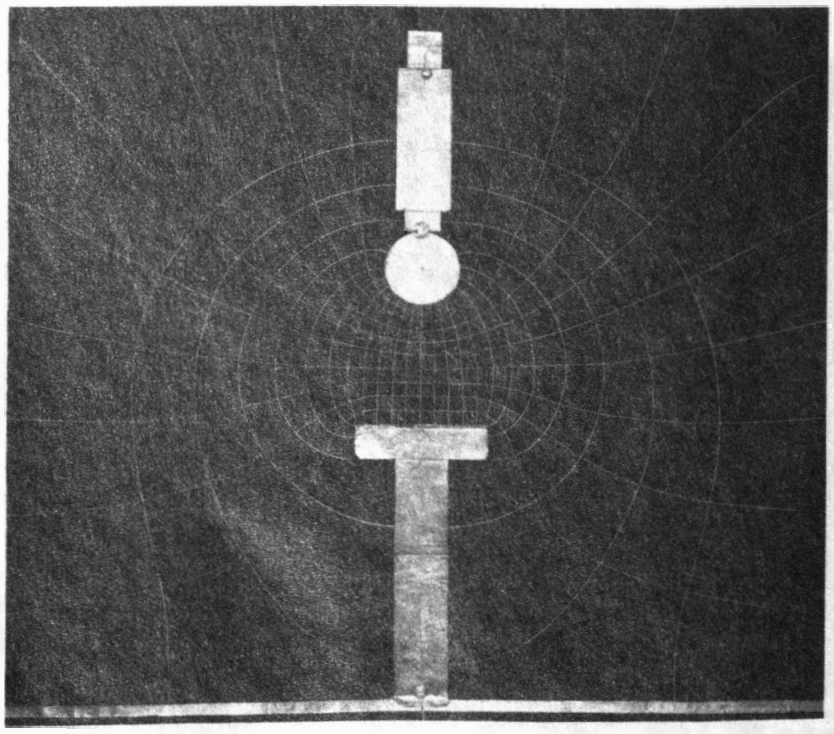

Fig. 45. Field plot of open cell with 1 inch diameter sphere to plane electrodes.

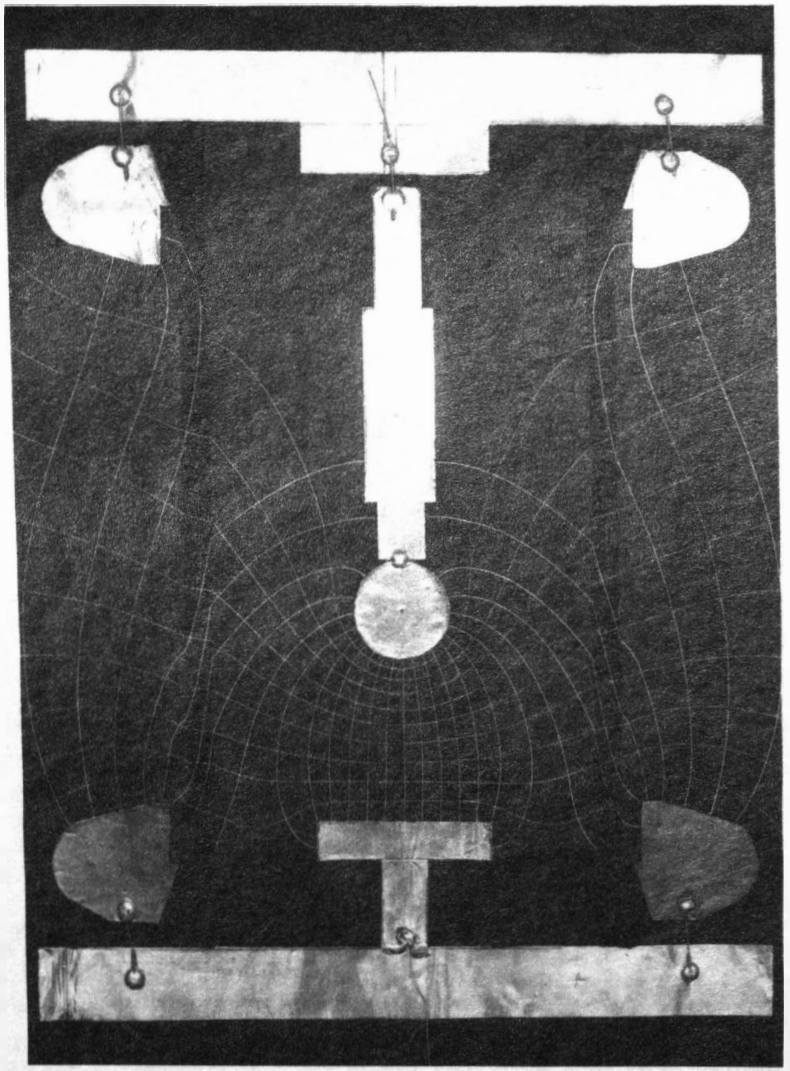

Fig. 47. Four inch diameter test cell with 1 inch diameter sphere to plane electrodes and with glass cylinder. (Top electrode negative polarity).

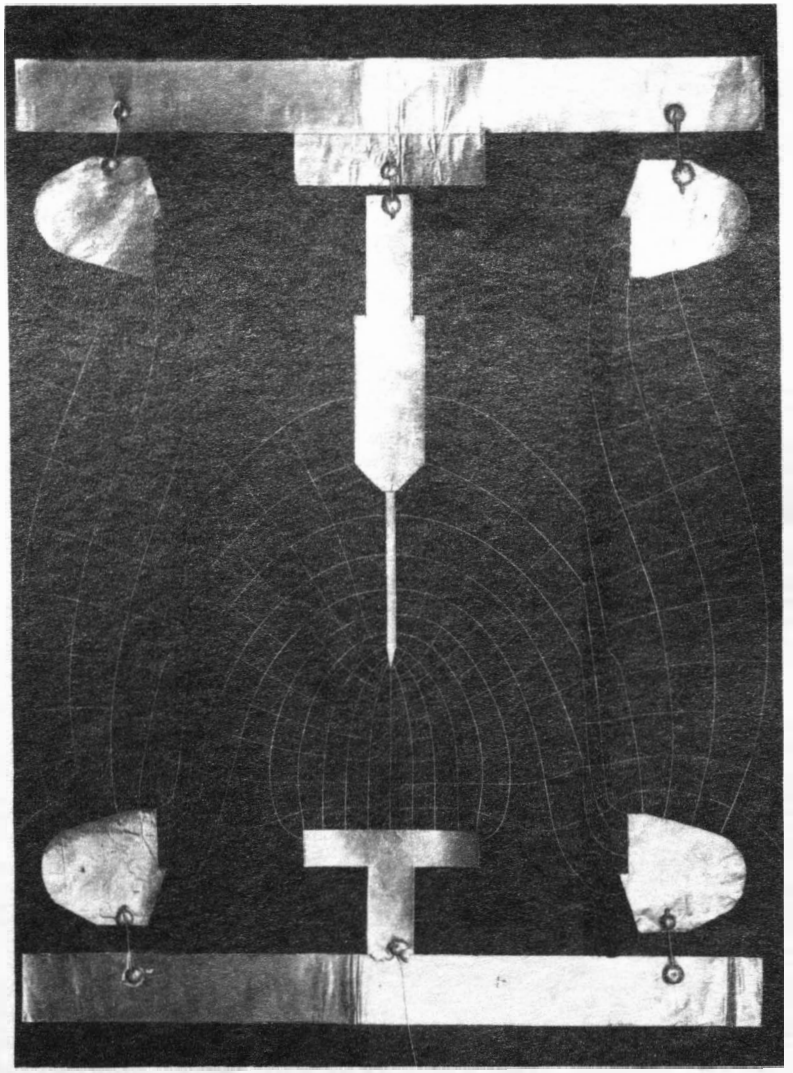

Fig. 46. Four inch diameter test cell with point to plane electrodes and with glass cylinder (Top electrode negative polarity).

APPENDIX THREE

CALIBRATION OF IMPULSE GENERATOR

The panel meter on the control cabinet of the impulse generator does not give a direct reading of the output voltage; therefore, the meter and the 507 oscilloscope must be calibrated to the output voltage of the generator. The procedure used in calibrating the generator was prescribed by AIEE Standard #4, 1953, using the 6.25 cm sphere gaps and the standard wave, 1½-40μsec. The relative humidity correction factors were also given in the AIEE Standard #4, 1953.[18] By this prescribed method the 50% breakdown voltages were found in terms of the control panel meter setting and the oscilloscope deflections. The calibration curve of breakdown voltages (KV) versus panel meter setting for positive and negative polarity is shown in Figure 49.

Figure 48 shows a comparison of the output voltage calibration of the generator by means of the 6.25 cm sphere gaps to the voltage divider readings on the type 507 oscilloscope. Only a few gap settings for positive polarity are compared for an example. The AIEE Standard #4, 1953, require that these two methods of reading the output voltages must be within five percent of the lower value.[18]

The equation derived for converting oscilloscope deflection to breakdown voltage is the following:

$$E = \frac{(\text{Scope deflec. in cm.})_X}{(\text{attenuation})} \frac{(50\ v)}{(\text{cm})} X \left\{ \frac{R_3 R_4}{R_3+R_4} \right\} X \left(R_2 + \frac{R_3 R_4}{R_3+R_4}\right) X (10^{-3}) \qquad (1)$$

where E is the peak voltage across the test speciment measured by the oscilloscope, R_1, R_2, and R_3 are resistors in the wave shaping circuit for a 1½ x 40μsec. wave, and R_4 is the input resistance of the oscilloscope.

Figure 50 of Appendix IV shows the position of the resistors in the wave shaping circuit. Substituting into equation (1) the values of the resistors, the equation becomes

$$E = \frac{\text{(Scope deflec. in cm.)}}{\text{(attenuation)}} \times (3.95 \text{ KV/cm.}) \qquad (2)$$

This equation was used to determine the peak voltages measured by the oscilloscope in the following Figure.

Gap	Attenuation on Scope	Scope Deflection	Output Voltage on Scope	Output Voltage from Spheres	Error
(mils)		(cm)	(KV)	(KV)	(%)
400	0.6	4.70	31.0	30.4	1.97
800	0.3	4.32	56.8	55.9	1.61
1000	0.2	3.47	68.4	66.3	3.17
1300	0.2	4.18	82.6	81.1	1.85

Fig. 48. Comparison of the output voltage calibration of the generator by means of the 6.25 cm. sphere gaps to the voltage divider readings on the Type 507 oscilloscope with positive polarity for a 1½x40 μsec. wave. The output voltages are 50% breakdown voltages of air.

Note: The oscilloscope was only used as a check on the output voltage obtained with the spheres. The breakdown voltages obtained in all tests were taken from the panel meter settings and not from the oscilloscope readings.

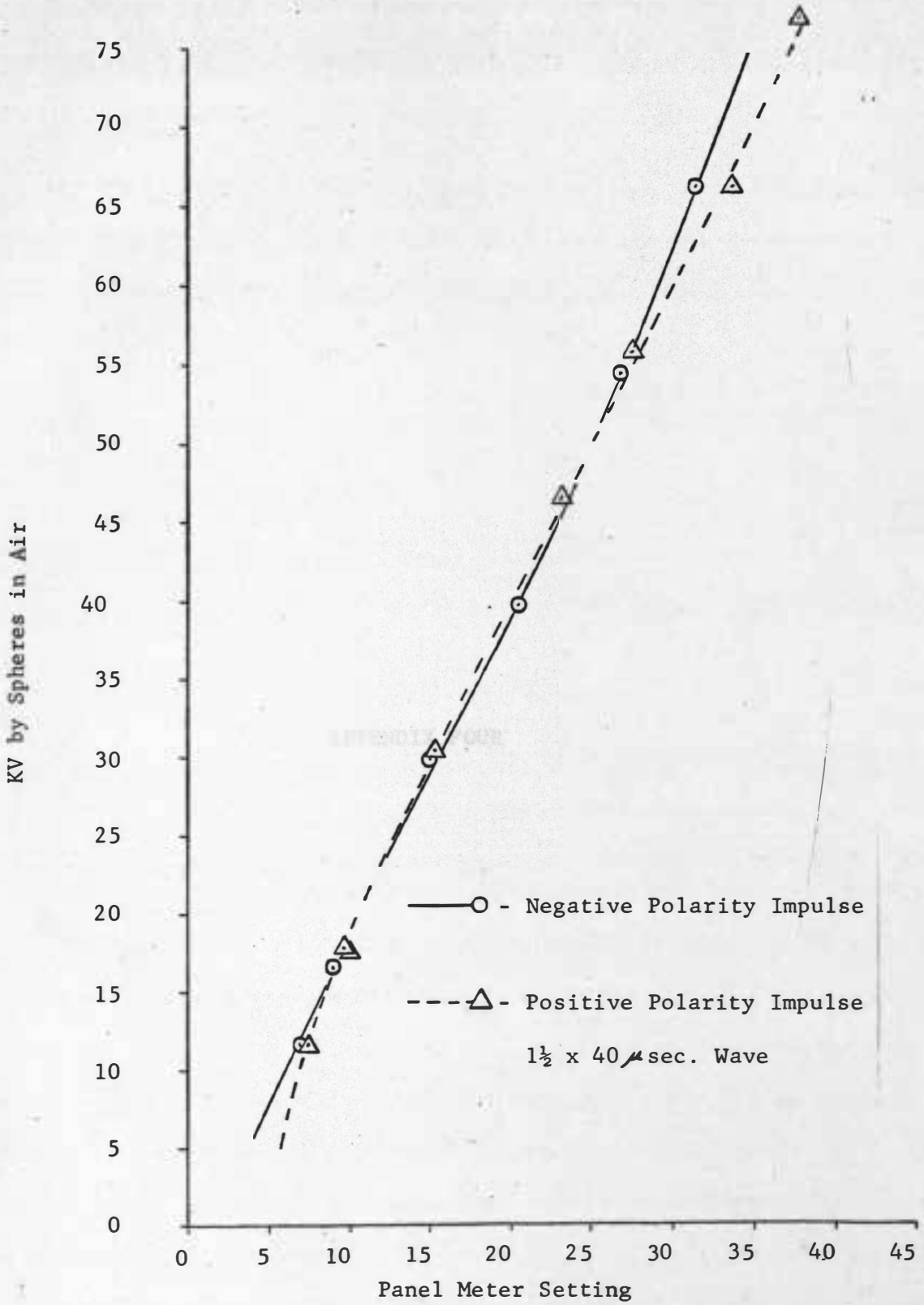

Fig. 49. Calibration Curves for Impulse Generator.

APPENDIX FOUR

DETERMINATION OF THE 1½ X 40 MICROSECONDS WAVE SHAPING CIRCUIT EXPERIMENTALLY AND THEORETICALLY

1. Experimentally

The wave most generally specified for use in testing electrical apparatus is the 1½ x 40μsec. wave, which reaches its crest value in 1½μsec. and reaches half crest value in 40μsec. This wave is shown in the following Figure where t_1 is 1½μsec. and t_2 is 40μsec.

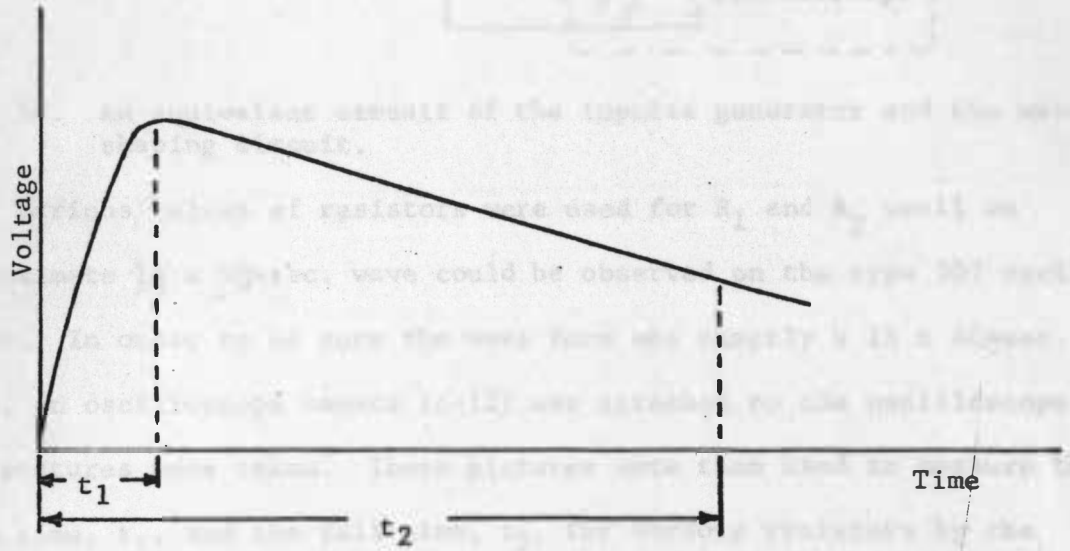

There are various types of wave shaping circuits that can be used to obtain this wave form such as an RL or an RC circuit. An RC wave shaping circuit was used in this thesis to obtain the 1½x40μsec. wave. The equivalent circuit representing the impulse generator and the wave shaping circuit is shown in Figure 50, where C_1 is the series capacitance of all three of the capacitors in the impulse generator, V_o is the voltage across C_1 when fully charged, R_4 is the input resistance of the oscilloscope having a value of 72.8 ohms, R_3 is a 75.6 ohm resistor, C_2 is a 0.00337 fd high voltage capacitor, and e(t) is the output voltage.

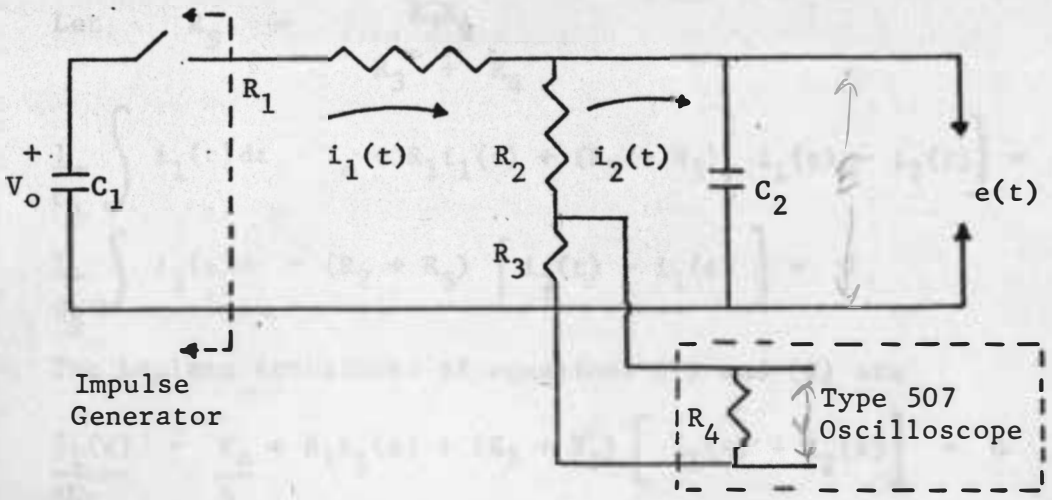

Fig. 50. An equivalent circuit of the impulse generator and the wave shaping circuit.

Various values of resistors were used for R_1 and R_2 until an approximate 1½ x 40μsec. wave could be observed on the type 507 oscilloscope. In order to be sure the wave form was exactly a 1½ x 40μsec. wave, an oscilloscope camera (c-12) was attached to the oscilloscope and pictures were taken. These pictures were then used to measure the rise time, t_1, and the fall time, t_2, for various resistors by the method suggested in the AIEE Proposed Guide for Transformer Impulse Tests, No. 93, 1962.[30] The final values selected for R_1 and R_2 were 160 ohms and 2900 ohms, respectively. The value of resistors used by Keith E. Crouch in his Thesis titled, The Effect of Wave Shape on the Electrical Breakdown of Nitrogen Gas, and the theoretical determined values were used as a starting point.[16]

2. Theorical Determination of R_1 and R_2

A. Determination of t_1 and t_2

From Figure 50 two loop equations can be written.

Let $R_5 = \dfrac{R_3R_4}{R_3 + R_4}$

$$\frac{1}{C_1}\int i_1(t)dt - V_o + R_1 i_1(t) + (R_2 + R_5)\left[i_1(t) - i_2(t)\right] = 0 \qquad (1)$$

$$\frac{1}{C_2}\int i_2(t)dt + (R_2 + R_5)\left[i_2(t) - i_1(t) \right] = 0 \qquad (2)$$

The Laplace transforms of equations (1) and (2) are

$$\frac{I_1(s)}{sC_1} - \frac{V_o}{s} + R_1 I_1(s) + (R_2 + R_5)\left[I_1(s) - I_2(s)\right] = 0 \qquad (3)$$

$$\frac{I_2(s)}{sC_1} + (R_2 + R_5)\left[I_2(s) - I_1(s)\right] = 0 \qquad (4)$$

Solving for I_2:

Let $R_2 + R_5 = R$

$$I_2(s) = \frac{V_oR}{(s)\left(\frac{1}{sC_2} + R\right)\left(\frac{1}{sC_1} + R_1 + R\right) - sR^2} \qquad (5)$$

The output voltage is:

$$e(t) = \frac{1}{C_2}\int i_2(t)dt \qquad (6)$$

Laplace transform of equation (6) is:

$$E(s) = \frac{I_2(s)}{sC_2} \qquad (7)$$

Substituting equation (5) into equation (7), than

$$E(s) = \frac{C_1RV_o}{s^2(C_1C_2RR_1) + s(C_1R_1 + C_1R + C_2R) + 1} \qquad (8)$$

Now let:

$$A = C_1C_2RR_1 \qquad B = C_1(R_1 + R) + C_2R \qquad D = C_1RV_o$$

equation (8) becomes

$$E(s) = \frac{D/A}{(s + B/2A)^2 + (1/A - B^2/4A^2)} \tag{9}$$

The inverse transform of equation (9) is:

$$e(t) = D/2AB\left[\varepsilon^{-(\alpha-\beta)t} - \varepsilon^{-(\alpha+\beta)t}\right] \tag{10}$$

where $\alpha = B/2A$ and $\beta = \sqrt{B^2/4A^2 - 1/A}$

Since t_1 is defined as the time for the voltage to reach crest or maximum value, then by taking the derivative of e(t) in equation (10) and setting it equal to zero, a value for t_1 can be found in terms of the wave shaping circuit parameters. The derivative of equation (10) is

$$\frac{d\,e(t)}{dt} = -(\alpha-\beta)\,\varepsilon^{-(\alpha-\beta)t} + (\alpha+\beta)\,\varepsilon^{-(\alpha+\beta)t}$$

Now by setting the above equation equal to zero and taking the natural log of the equation, the value for the time to crest becomes:

$$t_1 = \frac{\ln(\alpha+\beta)/(\alpha-\beta)}{2\beta} \tag{11}$$

The solution for the time, t_2, for which the voltage falls to half crest value is found in the following manner.

By definition:

$$e(t_1) = 2\,e(t_2) \tag{12}$$

therefore from equation (10)

$$e(t_1) = D/2AB\left[\varepsilon^{-(\alpha-\beta)t_1} - \varepsilon^{-(\alpha+\beta)t_1}\right] \tag{13}$$

and

$$e(t_2) = D/2AB\left[\varepsilon^{-(\alpha-\beta)t_2} - \varepsilon^{-(\alpha+\beta)t_2}\right] \tag{14}$$

$\varepsilon^{-(\alpha-\beta)t_1}$ is large compared to $\varepsilon^{-(\alpha+\beta)t_1}$

and $\varepsilon^{-(\alpha-\beta)t_2}$ is large compared to $\varepsilon^{-(\alpha+\beta)t_2}$

The above comparisons are found to be true for times t_1 and t_2 greater then 1μsec. or for a 1½x40μsec. wave. This can be proven numerically; therefore

$$e(t_1) = D/2AB \; \varepsilon^{-(\alpha-\beta)t_1} \tag{15}$$

$$e(t_2) = D/2AB \; \varepsilon^{-(\alpha-\beta)t_2} \tag{16}$$

Now substituting equations (15) and (16) into equation (12) and simplifing, equation (12) becomes:

$$\varepsilon^{-(\alpha-\beta)t_1} = 2\,\varepsilon^{-(\alpha-\beta)t_2} \tag{17}$$

Taking the natural log of equation (17) and solving for t_2, the fall time to half crest value can be found.

$$t_2 = 0.694/(\alpha - \beta) + t_1 \tag{18}$$

B. Calculation of R_1 and R_2

Known Parameters are:

$t_1 = 1.5\mu\text{sec.}$ $\quad R_5 = 37.1$ ohms
$t_2 = 40\mu\text{sec.}$ $\quad A = 5.62 \times 10^{-17} RR_1$
$C_1 = 0.05/3$ Fd
$C_2 = 0.00337$ Fd $\quad B = 2.005 \times 10^{-8} R + 1.668 \times 10^{-8} R_1$

Using equations (11) and (18) and eliminating all variables except R_1 and R, than the following equations are derived.

$$(1.668R_1 + 2.005R)/(1.124 \times 10^{-8} RR_1) = 0 \tag{19}$$

$$\frac{(2.01)(R^2 + 1.102RR_1 + 0.692R_1^2)}{(1.124 \times 10^{-8} RR_1)} = 0 \tag{20}$$

The series resistor R_1 in Figure 50 determines how fast C_2 will charge up and R_2 and R_3 will determine how fast C_2 will discharge; therefore R_1 must be much smaller then the sum of the two resistors R_2 and R_3 in order for the wave to have a short wave front.

Solving equations (11) and (18), the values for α and β were found to be 1.776×10^6 and 1.758×10^6, respectively. Equations (19) and (20) were derived in terms of R and R_1 from the relations for α and β given on page 110 with the known parameters. Solving equations (19) and (20) the values for R and R_1 were calculated to be approximately 1550 ohms and 106 ohms, respectively; therefore the resistor R_2 would be a 1512.9 ohm resistor. Resistors R_1 and R_2 are non-inductive wire wound resistors.

The above calculated values for R_1 and R_2 and the values in which Keith Crouch calculated for the same resistors were used as a starting point in determining the actual experimental values needed for a 1½x40 μ sec. wave.

The reason for the difference between the experimental values and the theorical values for R_1 and R_2 may be due to stray capacitance and inductance in the circuit, which are not being accounted for mathematically.

APPENDIX FIVE

DETERMINATION OF RELATIVE AIR DENSITY CORRECTION FACTORS

The breakdown voltage of any gas at a certain gap setting and for a certain electrode system varies with relative air density. In order to convert ambient breakdown voltages to breakdown voltages at standard conditions, relative air density correction factors must be obtained. Generally, sparkover voltages for most electrode systems increase with increasing air density and decrease with decreasing air density. For tests made in this thesis relative air density correction factors could not be obtained from the AIEE Standard #43, 1953, because different electrode configurations were used than those in the standards. The following method was used to determine relative air density correction factors for the 1" sphere to plane and the point to plane electrode systems. Only the correction factor for the 1" sphere to plane with rapidly applied, 60 cycle, voltages will be discussed in this Appendix. The other correction factors were determined by this same method.

The 2" diameter test cell with the 1" sphere to plane at a gap of 200 mils was filled with dry air with the gas filling apparatus. The leveler tubes of the gas filling apparatus were used to increase the pressure of air in the cell above the ambient barometric pressure by 13 inches of silicone oil. An increase of one inch of silicone oil in level tube L_1 is equivalent to increasing the pressure in the cell by 0.0641 inches of mercury. By increasing the pressure in the cell the relative air density is increased in the cell. Rapidly applied 60 cycle voltages were then applied for ten trials and breakdown voltages

were recorded. Breakdown voltages were also obtained for dry air at ambient conditions and at a pressure decreased below ambient barometric pressure by 12.5 inches of silicone oil. The following Figure shows how the breakdown voltage varied with the change in air density in the cell.

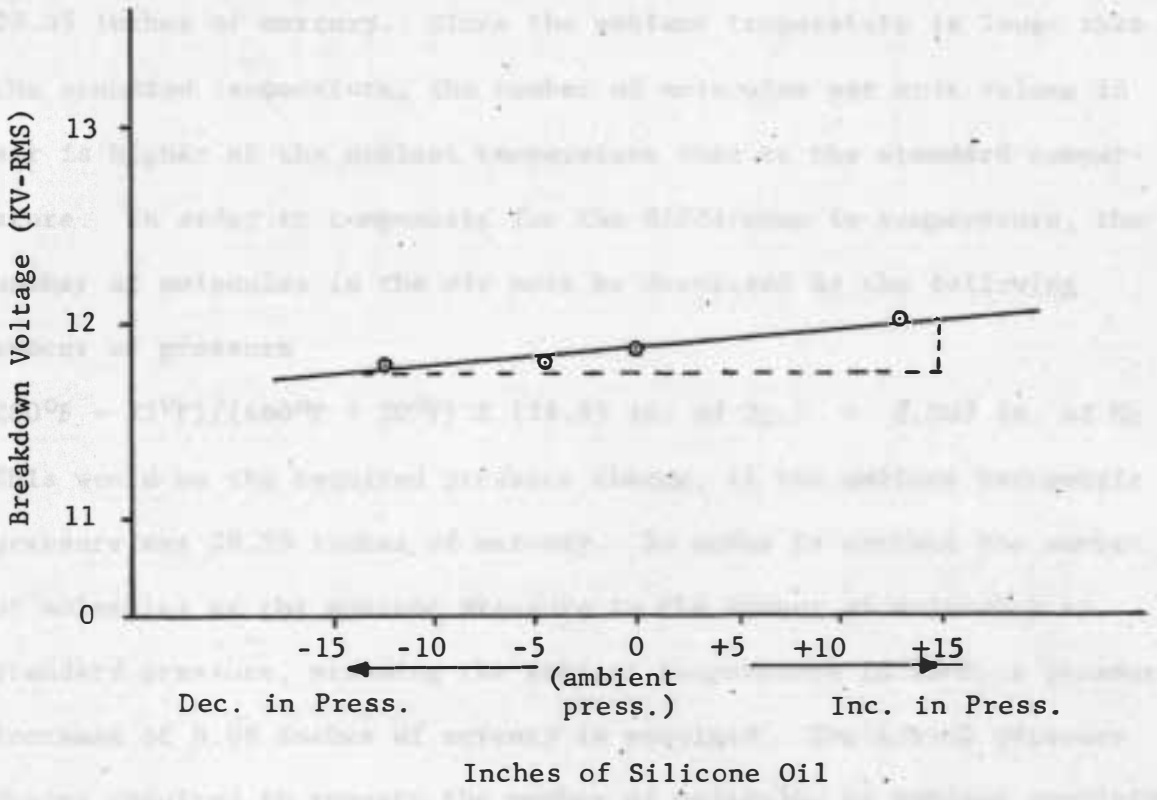

Fig. 51. Rapidly applied 60 cycle breakdown voltage (500 volts/sec.) in KV vs. Inches of silicone oil above and below ambient pressure for dry air, 1" sphere to plane, gap spacing of 200 mils, and in the 4" dia. test cell

From the above Figure breakdown voltage increases linearly with an increase in air density. The correction factor for this particular electrode system and voltage source is calculated by taking the ratio of the change in breakdown voltage to the change in the pressure in the cell in inches of silicone oil. The correction factor is calculated to be 0.00987 KV/inch of silicone oil.

Example:

The rapidly applied 60 cycle breakdown voltage for a 1" sphere to plane in air at a gap of 200 mils is 24.90 KV. The ambient temperature and barometric pressure were 73°F and 28.27 inches of mercury, respectively. The standard temperature and barometric pressure are 80°F and 28.35 inches of mercury. Since the ambient temperature is lower than the standard temperature, the number of molecules per unit volume in air is higher at the ambient temperature then at the standard temperature. In order to compensate for the difference in temperature, the number of molecules in the air must be decreased by the following amount of pressure

$(80^{o}F - 73^{o}F)/(460^{o}F + 80^{o}F)$ X (28.35 in. of Hg.) = 0.367 in. of Hg.

This would be the required pressure change, if the ambient barometric pressure was 28.35 inches of mercury. In order to correct the number of molecules at the ambient pressure to the number of molecules at standard pressure, assuming the ambient temperature is 80°F, a pressure increase of 0.08 inches of mercury is required. The actual pressure change required to convert the number of molecules at ambient conditions to the number of molecules at standard conditions is the sum of the pressure changes required by the ambient temperature and pressure individually. The actual pressure change is then 0.287 inches of mercury decrease. The actual breakdown voltage at standard conditions is

24.90 KV - (0.00987 KV/in. of silicone oil)(0.287 in. of Hg.) X

(15.6 in. of silicone oil/in. of Hg.) = 24.86 KV.

The correction factors for relative air density for all tests in this thesis are shown in the following table.

Voltage Source	Electrode System	Breakdown Voltage Inc. or Dec. with Relative Air	Correction Factors $\frac{\cdot \text{ KV}}{\text{in. of Silicone oil}}$
Rapidly Applied 60 cycle Voltages	1" Sphere to Plane	increase	0.00987
	Point to Plane	decrease	0.0542
Impulse Voltages Neg. Pol	1" Sphere to Plane	increase	0.029
	Point to Plane	increase	0.017
Impulse Voltages Pos. Pol.	1" Sphere to Plane	increase	0.071
	Point to Plane	decrease	0.073

Fig. 52. Relative Air Density Correction Factors.

APPENDIX SIX

DETERMINATION OF VAPOR PRESSURE CORRECTION FACTORS

Vapor pressure correction factors were determined for the 1" sphere and point to plane electrode systems for all tests where the breakdown strength of open air was being obtained. The correction factors suggested by the AIEE Standard #4, 1953, were not used, because the electrode systems used in this thesis were of different configuration. The method for obtaining the vapor pressure correction factors for various types of tests will be explained by the following procedure. Only the vapor pressure correction factor for the negative polarity impulse breakdown voltages of open air for the point to plane electrode system will be determined as an example. The open cell was adjusted to a gap setting of 600 mils for each test. A series of five tests was made in which the 50% breakdown voltages were obtained for each test and the relative humidity, temperature, and the barometric pressure were recorded. With the exception of two of the tests for which the vapor pressure was the same, each test was run at a different ambient vapor pressure. The appropriate relative air density correction factor was applied to the 50% breakdown voltages. These corrected breakdown voltages were then plotted against vapor pressure which is calculated from the ambient relative humidity, temperature, and barometric pressure at the time the test was run. The relative humidity for each test was determined by a sling psychrometer and a psychrometric chart. Figure 53 shows how the 50% breakdown voltages varied with vapor pressure for the point to plane electrode system in air and for a $1\frac{1}{2} \times 40\ \mu$sec. negative polarity wave.

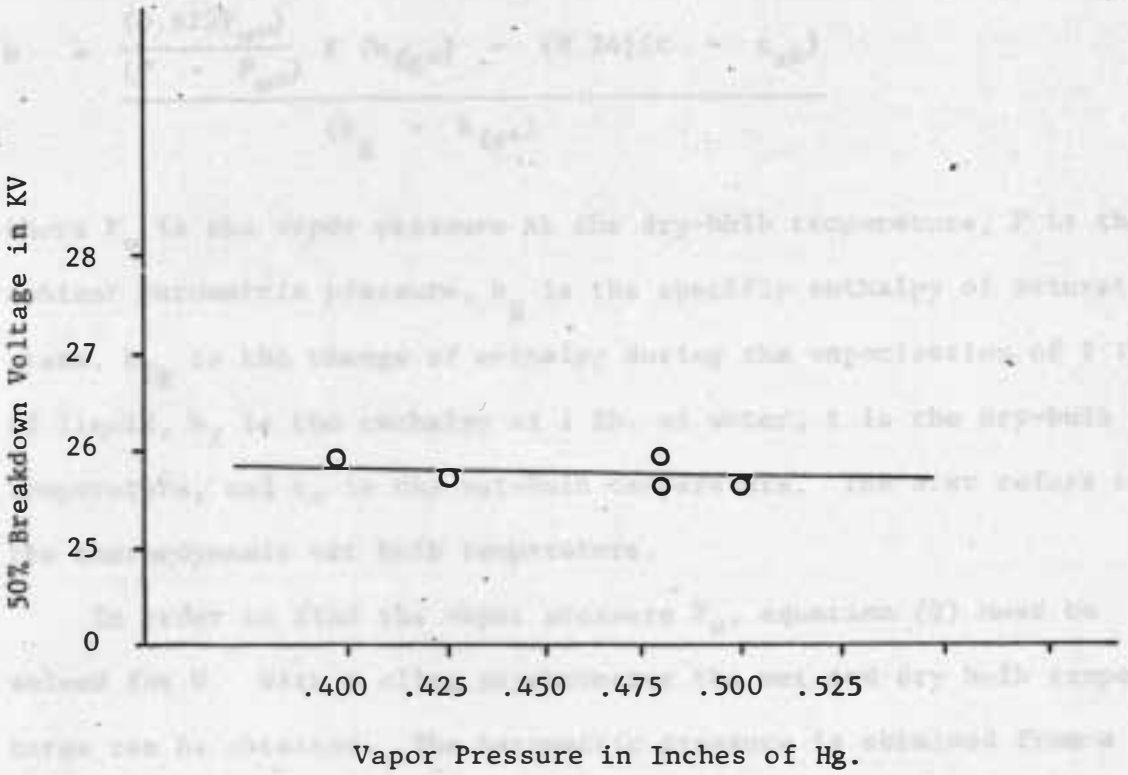

Fig. 53. 50% breakdown voltage in KV vs. vapor pressure in inches of Hg. for open air, point to plane, 1½x40μsec. wave-negative polarity, 600 mils gap, and with the open cell.

From Figure 53 vapor pressure is found to have an insignificant effect on breakdown voltage for negative polarity impulse waves and for a point to plane electrode systems. The same results were found for open air with point and 1" sphere to plane electrode systems under rapidly applied 60 cycle voltages. Also positive polarity impulse breakdown voltages were not affected by vapor pressure for the same electrode systems; therefore, there were no corrections made for vapor pressure in any of the tests in this thesis.

Vapor pressure can be calculated from known ambient conditions as follows. (The following equations are taken from reference 19.)

$$P_w = W \times P/(0.622 + W) \quad (1)$$

$$W = \frac{(0.622P_{w*})}{(P - P_{w*})} \times \frac{(h_{fg*}) - (0.24)(t - t_{s*})}{(h_g - h_{fs*})} \quad (2)$$

where P_w is the vapor pressure at the dry-bulb temperature, P is the ambient barometric pressure, h_g is the specific enthalpy of saturated steam, h_{fg} is the change of enthalpy during the vaporization of 1 lb. of liquid, h_f is the enthalpy of 1 lb. of water, t is the dry-bulb temperature, and t_* is the wet-bulb temperature. The star refers to the thermodynamic wet bulb temperature.

In order to find the vapor pressure P_w, equation (2) must be solved for W. With a sling psychrometer the wet and dry bulb temperatures can be obtained. The barometric pressure is obtained from a barometer. All of the other unknown terms in equation (2) can be found in Table A.1 of reference 19.

The above method was used to obtain the ambient vapor pressure in this thesis.